Abstract

Metwally, Walid Abdel Mohsen, "Investigation of Coincidence Techniques in Prompt Gamma Neutron Activation Analysis". (under the supervision of Prof. Robin P. Gardner)

After configuring the proper electronic system to be used, the initial observations of the gamma-gamma coincidence approach were presented. These observations included hydrogen peak elimination, background and sum peak elimination, pulse pile up reduction, and two dimensional spectra.

Three practical applications of the coincidence counting approach were presented in this work. The first application was performing elemental analysis for a mixture of radioisotopes using Library Least Squares (LLS). The LLS was applied to the coincidence data as well as the normal single detector data. The coincidence results showed to be much closer to the original activity values of the radioisotopes than the singles. In addition, the coincidence approach greatly reduced the background, summing, and pulse pile up effects.

The second application was the two dimensional diagonal summing. The main advantages from this application were improving the peak resolution and greatly reducing the background (Compton Continuum). In addition, it was shown that different diagonal sums can be examined by use of the same set of data from the current electronic system (and software). The two dimensional diagonal summing was used for identifying coincidence schemes and for elemental analysis. The obtained spectra showed to be very promising and could be effectively used for these purposes.

The third practical application was using a new NaI detector arrangement. The arrangement was designed to deal with the problem of the low detection probability of the high energy gamma rays of interest in the oil well logging industry. This arrangement consisted of two NaI detectors, one of which was a well type. The detectors were designed to fit in each other. Coincidence data were collected using this new arrangement. The results show that this new arrangement enhances the count rate in the coincidence data, thus increasing the Signal to Noise Ratio, as opposed to two separate detector setups.

Finally, a Monte Carlo simulation attempt was made to try to predict the coincidence spectra. The attempt did not yield satisfactory results. It is our intent to continue pursuing coincidence simulation.

Investigation of Coincidence Techniques in Prompt Gamma Neutron Activation Analysis

by

Walid A. Metwally

A dissertation submitted to the graduate faculty of
North Carolina State University
in partial fulfillment of the
requirements for the Degree of
Doctor of Philosophy

Nuclear Engineering

Raleigh, North Carolina

March 31, 2003

Approved By:

Robin P. Gardner

Prof. Robin P. Gardner, Chair

Charles W Mayo

Prof. Charles Mayo

D. Anistratov

Dr. Dmitriy Anistratov

Richard Lindstrom

Dr. Richard Lindstrom

Biography

Walid Abdel Mohsen Metwally was born in Cairo, Egypt in October 1969. He grew up in Alexandria, Egypt, where he attended most of his school years. After his successful completion of the high school at Victoria College in Alexandria, Egypt, he joined the College of Engineering at Alexandria University where he obtained his Bachelor of Science from the Department of Nuclear Engineering in 1992. He later obtained his Master of Science from the same department in 1997. In 1994 he joined the Reactor Operations Group at the Atomic Energy Authority in Egypt. He stayed there until 1998, where he joined the Department of Nuclear Engineering at North Carolina State University as a Ph.D. Student. He remained there until the completion of his doctorate in 2003. During that period, he obtained a Master of Science degree in Operations Research at North Carolina State University in 2002.

The author got married to Reem Abdalla in August 1995. The couple was blessed with a baby boy, Yousouf, in March 2002.

Acknowledgement

I praise thee, ALLAH, for whatever thou hast taught me and whatever thou hast inspired me with throughout this work.

I am deeply indebted to my teacher and advisor, Prof. Robin P. Gardner, for his continued guidance and support. His style of advising is an example to be followed. I am also grateful to Prof. Charles W. Mayo for his invaluable help throughout this work. I would like to express my appreciation to Dr. Richard M. Lindstrom for his technical discussions and editorial advice. I would also like to thank Prof. Dmitriy Y. Anistratov for serving on my committee.

Special thanks to all the NCSU PULSTAR reactor staff, especially Gerald Wicks and Scott Lassell, for facilitating the experimental part of this work. I am grateful to El-Sayyed S. El-Sayyed for familiarizing me with the old electronic setup used in this work and to my colleagues Ashraf Shehata and Weijun Guo for their help in the thesis preparation.

I am very appreciative to my family and friends for their continuous encouragement and support. They are the shelter that provides me with safety and comfort. In particular, my gratitude goes to:

My Father - for your love, wisdom, and guidance.
My Mother - for your love, care, and sacrifice.
My wife - for your love, support, patience, more patience, and being my harbor.
My Son - for being the light of my life.
Mofreh Zaghloul - for being there when I needed a friend.

بسم الله الرحمن الرحيم

In the Name of ALLAH (God), Most Gracious, Most Merciful

Contents

List of Figures

List of Tables

1. INTRODUCTION

All nuclear techniques of chemical analysis involve the interaction of an incoming projectile (neutron, charged particle, or gamma photon) and a target nucleus. As a consequence of this interaction, there is usually a formation of two products – the light one and a heavier product. In the case of Prompt Gamma-Ray Neutron Activation Analysis (PGNAA), the projectile is a neutron and the light product is a gamma-ray photon. PGNAA offers a non-destructive, relatively rapid method for determination of trace and major elements that cannot be determined by conventional activation analysis.

In PGNAA, when a nucleus captures a neutron, it gains energy which results in excited nuclear states. These states de-excite quickly (in less than 10^{-14} seconds) by prompt gamma ray emission. The gamma rays are detected and used analytically. In general, a neutron of any energy may be used for PGNAA, but thermal neutrons are more commonly used because of their large capture cross section and thus wide range of available data.

Because of the short half life of the nuclear excited states, PGNAA analyzers must be designed so that irradiation and counting can be done simultaneously. This necessitates placing the counting equipment very close to the neutron source. This is normally an environment with a very high background of gamma rays and neutrons. The sources of this background can be listed as follows:

a. Gamma rays emitted by the neutron source (or with the neutron beam),
b. Gamma rays produced by neutron interactions from the source within the detector, and
c. Gamma rays produced from non sample materials of construction around or within the PGNAA analyzer.

In addition to the background sources listed above, there are also sources of natural background resulting from:

a. Potassium – 40,
b. Natural uranium and thorium chains, and
c. Cosmic radiation.

Hydrogen (from sample and/or non-sample materials) is a particulary common element and causes problems in many typical cases of PGNAA. When activated, hydrogen de-excites by emitting a single prompt gamma ray with energy of 2.223 MeV. The magnitude of this peak from a normal sample spectrum is often one or two orders of magnitude larger than other elements of interest. This adds a source of complexity to the spectrum and causes sensitivity problems.

Other sources of complexity in PGNAA are *summing* and *pulse pile up* effects. The *summing effect* is basically explained as follows. If two (or more) gamma rays are emitted in coincidence from the sample, they may interact simultaneously in the detector. The resulting pulse will not lie within the full energy peak corresponding to either one. The problem is particularly severe where many cascade gamma rays are involved. This can lead to errors when analyzing the spectrum.

The fact that pulses from a radiation detector are randomly spaced in time can lead to interfering effects between pulses when counting rates are not low. These effects are generally called *pulse pile up*. This leads to distortions in the recorded spectrum, including an occasional sum peak.

Both of these effects, summing and pulse pile up, add a source of complexity to the spectrum and cause interferences with quantitative measurements. For example, they may lead to false amounts when elemental analysis is performed using full energy peaks or Library Least Squares (LLS).

Most of the prompt gammas from the same element are emitted in coincidence. The Coincidence Prompt Gamma ray Neutron Activation Analysis (CPGNAA) is thus introduced as a method to try to eliminate the background, summing, and pulse pile up effects. In the past ten years, new electronic devices have been provided that allow fast coincidence measurements to be performed. Utilizing these devices, as well as computer software, also introduced the concept of multiparameter data acquisition which adds more flexibility in data analysis.

There are three main advantages of using the coincidence technique in PGNAA. The first is the elimination of most of the interfering background. The second is decreasing the effect of summing and pulse pile up.

The third advantage of coincidence techniques in PGNAA stems from the fact that prompt gamma-ray spectra from individual elements typically consist of more than 100 gamma rays (see Figure 1.1 with data from Brookhaven National Laboratory) with photon energies from almost zero up to about 11.5 MeV. A sample material consisting of a few elements can generate gamma-ray spectra with several hundred individual lines while a complex matrix can generate spectra with several thousand. With such spectra, even high resolution detectors must contend with overlapping peaks. The commonality of many nuclear levels also leads to an even higher overlap potential. Since the use of coincidence techniques should identify the gamma rays emitted at the same time from the same element ("true coincidences"), this should simplify spectra and make elements easier to identify and quantify.

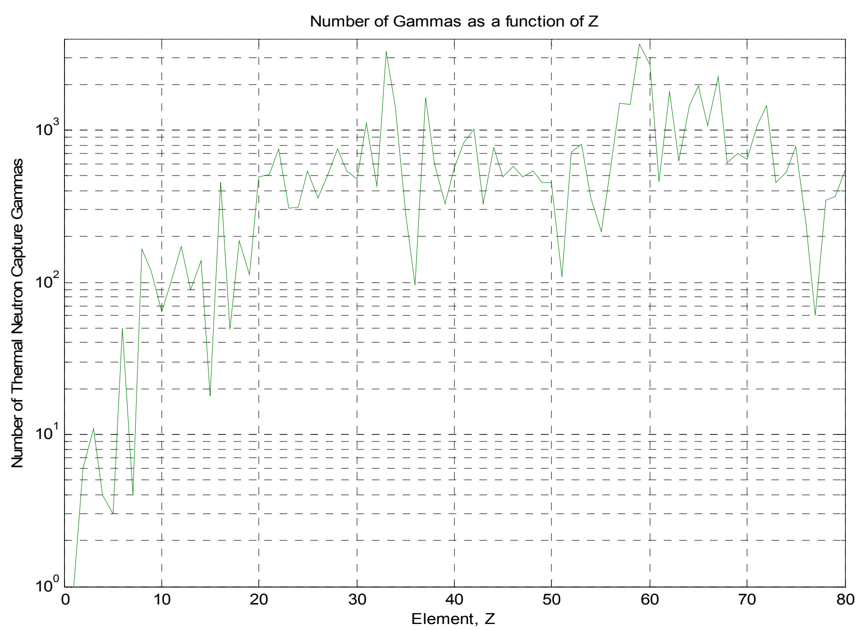

Figure 1-1: Thermal Prompt Gamma Ray Lines Per Element

Ref.: Brookhaven National Laboratory

Unfortunately, the use of coincidence techniques is expected to reduce the output signal somewhat and also complicates the detection system. The hope is that the S/N improvement from background (noise) reduction more than offsets the degradation of the S/N by signal reduction. To improve the sensitivity of the coincidence system, one can impose an energy selection criterion, i.e. energy window or gate, on one detector. This type of analysis is done offline using the multiparameter acquisition data. This idea can be used to look for the coincidence schemes of different elements by setting a window around one of the peaks and observing the resulting coincidence spectrum. The resulting spectra should consist of just those gamma rays that are in coincidence with the triggering gamma ray.

A new NaI detector arrangement was introduced in this work, Section 4.4. The arrangement consists of two NaI detectors, one of which is a well type. The detectors were designed to fit in to each other. Coincidence data were collected using this new arrangement. The results show that this new arrangement enhances the count rate in the coincidence data as opposed to two separate detector setups.

It is also possible to apply the coincidence counting approach to standard Neutron Activation Analysis (NAA) where the measurements are made after the end of the irradiation. Using the coincidence counting technique in this case has the same advantages as PGNAA, except that the background due to the neutron source will no longer be a relevant issue.

To the best of our knowledge, no Monte Carlo simulation has been made yet for prompt gamma-gamma coincidence. A patch was written for MCNP (Watson, 1999) that dealt with annihilation photons only. An attempt to simulate the coincidence spectrum was made during this work. It is our intent to continue pursuing this simulation in the near future.

The remainder of this work is organized as follows: Chapter two contains the literature review for the previously published works in gamma- gamma coincidence measurements. In Chapter 3, a brief introduction is given on the different standards used in the coincidence hardware. Then, a description of the old and new electronic setups is given, as well as a result comparison between them.

The initial observations of the gamma-gamma coincidence approach are presented at the beginning of Chapter four. The chapter goes on to introduce three applications of the coincidence approach. They are as follows:

1. Elemental analysis using Library Least Squares (LLS);
2. Diagonal summing in two dimensional spectra and its applications; and
3. The new NaI detector arrangement.

The Monte Carlo simulation attempt is then discussed in chapter five. Chapter six includes the discussions and conclusions regarding this work. Finally, Chapter seven contains the suggested future work to be pursued using the gamma-gamma coincidence counting approach..

2. LITERATURE SURVEY

One of the early experimental works that used gamma-gamma coincidence measurements were done by Kim, Speecke, and Hoste (1965) and Kim and Hoste (1965). They were interested in determining Copper, Silver, and Antimony in Bismuth. They used two 3 by 3 inch detectors and a coincidence unit having a resolving time of 0.58 microseconds. Based on their knowledge of the decay schemes (at that time) and the gamma yields, they gated their system on the high percentile occurring gammas of the elements of interest. Their analysis was based on scalar counts and yielded results with considerable errors.

Some of the gamma-gamma coincidence measurements was devoted to the determination of Se and Ir in geological samples (Vobeczky, Pavlik, and Benes, 1977; Wangen, Gladney, and Hensley, 1980; Meyer, 1987; Meyer et al, 1993). Their main goal was to improve the sensitivity in determining these elements. They achieved this by eliminating the background and spectral interferences. They showed that coincidence counting improved the detection limits for Se and Ir and spared them from performing radiochemical separation. All of these works were done for Instrumental Neutron Activation Analysis (INAA). Koeberl and Huber (2000) latter applied multiparameter coincidence measurements using two Ge detectors to optimize the external factors affecting the determination of Ir in geological samples. These factors included the sample size, irradiation time, flux, shaping time, and coincidence time. Recently Hatsukawa et al (2002) tested the feasibility of multiparameter coincidence spectrometry using a Ge detectors array. They applied it to neutron activation analysis with two reference igneous rock samples. Twenty four elements were identified in the samples and the quantitative results were consistent with previous data derived from other methods.

An important use of the gamma-gamma coincidence measurements is the determination of the excited states of elements. This in turn leads to the identification of the decay schemes. All the references cited implementing these types of measurements are dedicated to heavy elements. Demanins and Raicich (1992) studied the excited states of

^{93}Nb by using two Ge detectors and a neutron source. Coincident data was stored event by event, and then offline data reconstruction was made. They later (1994) repeated the same procedure for ^{141}Pr. Jungclaus et al(1994) studied the excited levels in ^{168}Er above 2 MeV using reactor thermal neutrons and three Ge detectors. Offline data analysis and spectrum reconstruction was made. New levels were found. Recently, the level structure of ^{120}Cs (Moon et al, 2001) and ^{72}Ge (Medeiros et al, 2001) were studied. In ^{120}Cs, 11 HPGe detectors were used and data were taken for events in which two or more detectors registered in prompt coincidence. The level structure of ^{72}Ge was studied following the β^- decay of ^{72}Ga and new transitions were found.

An interesting use of coincidence measurements was introduced by Falciglia et al (1995). They accurately measured the speed of gamma rays using their fast timing coincidence system. Their main goal was to test the long term stability of the system after eliminating most of the instrumental errors. The source used was ^{22}Na which is a positron emitter that causes annihilation photons to appear. The source was moved in constant increments along the line connecting the two detectors. By knowing the distances, the speed of the gamma rays was calculated.

McGrath et al (1999) made gamma-gamma coincidence measurements following inelastic neutron scattering. They used accelerator produced monoenergetic neutrons (10 MeV) and three HPGe detectors. Conventional NIM and CAMAC modular electronics were used with 100 nanosecond resolving time. The aim of the paper was to show the capability of doing such measurements. The elemental analysis was not reported.

Jakubek et al (1998) used two HPGe detectors and performed the gamma-gamma coincidence measurements for INAA. They used NIM modules in connection with CAMAC data acquisition systems. The goal of this work was to describe the system and show some preliminary results. A continuation of this work was made by Vobecky et al (1999) where the same system was used. They irradiated reference samples to look for concentrations of Scandium, Cobalt, and Cesium. Their analysis was performed offline where they set different resolving time windows to obtain optimum results. The results were acceptable when compared to the published ones.

Gardner et al (2000) did a feasibility study of the coincidence counting approach. Their main concern was applying this approach for PGAA applications. They used NIM modules, NaI detectors, and neutron sources from reactor beam and Cf-252. They efficiently reduced the background (such as the Hydrogen 2.223 MeV gamma) and showed an increase in the signal to noise ratio. Monte Carlo simulation was also performed to predict the coincidence spectrum.

A recent work by Ember, Belgya, and Molnar (2002) suggested a method called the "γ-γ regional coincidence method" that improves the capabilities of PGAA. The main idea of this method it to construct the coincidence spectrum (via offline analysis) that is in coincidence with a range of energies. Using this method they eliminated the Hydrogen 2.223 MeV Gamma from the spectrum and showed an increase in the signal to noise ratio. It is noted that previous work (Gardner et al, 2000) accomplished the same goal of this work when using the whole range of energies in coincidence.

A useful application of the gamma –gamma coincidence counting approach was introduced by Metwally, Gardner, and Mayo (In press). Elemental analysis was performed for a mixture of radioisotopes using the Library Least Squares method (LLS). The LLS was applied to the coincidence data as well as the normal single detector data. The coincidence results showed to be much closer to the original activity values of the radioisotopes than the singles. In addition, the coincidence approach greatly reduced the background, summing, and pulse pile up effects. Another useful application was introduced by Ember, Belgya, Weil., and Molnar (In press). They studied the applicability of γ-γ coincidence for the determination of concentrations with PGAA method.

The latest work in gamma-gamma coincidence measurements was introduced by Gardner and Metwally (In press) where a new NaI detector arrangement was introduced. The objective was to try to detect high energy gamma rays with high efficiency. They showed that this arrangement does in fact increase the signal to noise ratio without a great decrease in the total count rate.

3. COINCIDENCE ELECTRONICS:

Initially, this study started with a set of electronics that produced acceptable results to demonstrate the feasibility of the coincidence counting approach. These results were previously published (Gardner et al, 2000). To obtain better and accurate timing and pulse height information, a new set of electronics was used. This chapter starts by defining the different standards used in modular electronics and introduces the concept of multiparameter data acquisition. Then a description of the old and new coincidence electronic setups is given, along with a brief description of the computer software used with the new coincidence electronics. Finally, a comparison of results obtained by both electronic setups is presented.

3.1. Modular Electronics:

Most of the nuclear electronic instrumentation is designed in accordance with either the Nuclear Instrument Module (NIM) standard or Computer Automated Measurement and Control (CAMAC) standard for modular instrumentation. Two of the most important advantages of the NIM and CAMAC concepts are flexibility and interchangeability. Both NIM and CAMAC standards incorporate modular instruments that plug into a "bin" or "crate", and derive their power from a standard power supply attached to the rear of the bin or crate. In the next sections, a brief description of both these standards we be given.

3.1.1. NIM Instrumentation Standard:

To a large extent, the NIM based modules are still widely used (and more popular) than the CAMAC ones. The NIM bin is subdivided across its width and can take up to 12 individual single width modules. Each of the 12 bin locations is provided with a 42 pin connector that mates with a corresponding connector at the back of each module. Pin assignments and functions are illustrated in Figure (3.1). The dc supply voltages provided by the bin are $\pm$ 6 V, $\pm$ 12 V, and $\pm$ 24 V.

NIM modules are capable of handling either linear or logic signals. The primary means of transmitting linear and logic pulses between NIM modules is by coaxial cables connected to the appropriate jacks on either the front or the back panel of the module. BNC and SHV connectors are specified for single jacks and high voltage connections respectively. Detailed specifications for the NIM standard are contained in USAEC Report TID-20893 initially published in 1964.

One of the major problems with the NIM modules is that they do not perform well in situations which involve large volumes of digital data. Another problem is that they do not have a standard interface with digital computers. These problems have led to the development of the CAMAC instrumentation standard described next.

3.1.2. CAMAC Instrumentation Standard:

The basis of the CAMAC system is the *crate* that houses the interfacing modules. The crate can house up to 25 single width modules (stations), or 12 for *mini-crates*. The crate contains a backplane which buses common signals to all the modules in the crate through a printed circuit board edge connector having 86 contacts. The CAMAC standard is defined by the ANSI/IEEE Std 583-1982.

The backplane of the CAMAC crate is called the *dataway*. The dataway provides a digital pathway that:

1. Interconnects the modules within a crate;
2. Provides control signals to the modules; and
3. Provides power to the modules (±6 V and ± 24 V).

All signals on the dataway have standard TTL levels (low logic level 0 to 0.8 V and high logic level 2 to 5 V). Table (3.1) gives a description of the available signals on the dataway and Figure (3.2) shows a diagram of the dataway.

The extreme right-hand station in the CAMAC crate is a special station, called the *control station*, and is reserved for the *crate controller*. The crate controller is the instrument in the crate that speaks the common dataway language and serves as the interface between the crate and any external hardware.

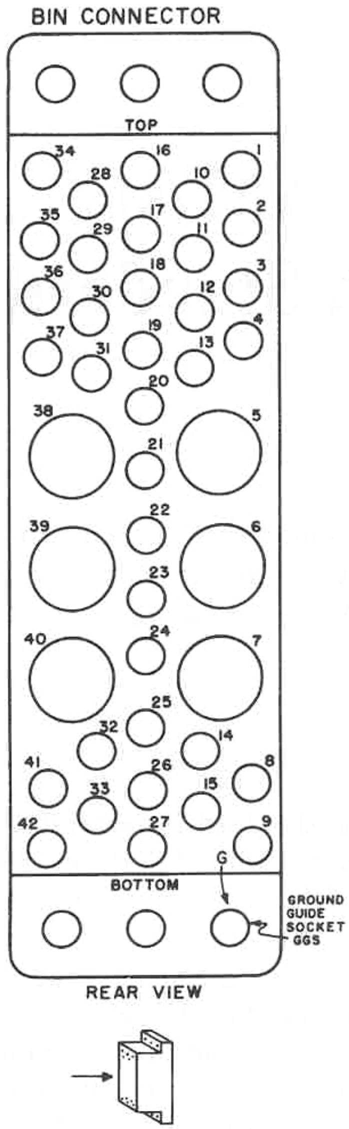

PIN	FUNCTION
1	RESERVED
2	RESERVED
3	SPARE
4	RESERVED
5	COAXIAL
6	COAXIAL
7	COAXIAL
8	+200 VOLTS D.C.
9	SPARE
* 10	+6 VOLTS
* 11	-6 VOLTS
12	RESERVED
13	SPARE
14	SPARE
15	RESERVED
* 16	+12 VOLTS
* 17	-12 VOLTS
18	SPARE
19	RESERVED
20	SPARE
21	SPARE
22	RESERVED
23	RESERVED
24	RESERVED
25	RESERVED
26	SPARE
27	SPARE
* 28	+24 VOLTS
* 29	-24 VOLTS
30	SPARE
31	SPARE
32	SPARE
* 33	117 VOLTS A.C. (HOT)
* 34	POWER RETURN GND
35	RESET
36	GATE
37	SPARE
38	COAXIAL
39	COAXIAL
40	COAXIAL
* 41	117 VOLTS A.C.(NEUTRAL)
* 42	HIGH QUALITY GND
G	GROUND GUIDE PIN

* MUST BE BUSSED TO ALL BIN CONNECTORS PG1B THROUGH PG12B

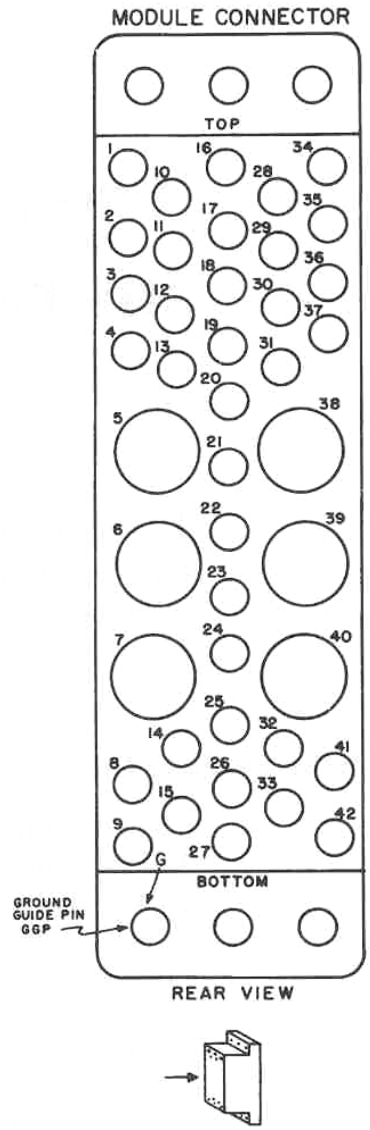

NOTES:-

A. CONNECTORS ARE IN ACCORDANCE WITH DRAWING NO. ND-519.

B. RESERVED PINS ARE FOR FUTURE ASSIGNMENT BY THE COMMITTEE AND SHALL NOT BE USED UNTIL SUCH ASSIGNMENTS ARE MADE.

C. GP-1 = GUIDE PIN
GGP = GROUND GUIDE PIN
GS-1 = GUIDE SOCKET
GGS = GROUND GUIDE SOCKET
} PER ND-519

D. SEE ALSO SECTION F OF THIS REPORT

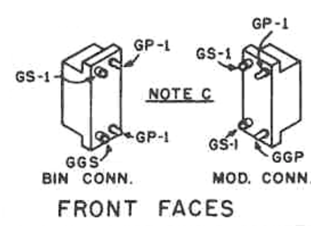

Figure 3-1: PIN Assignments for the NIM standard connector between bin and module. (Adapted from National Bureau of Standards Photo 74-08-4044.)

Table 3-1: Description of the available signals on the CAMAC dataway

Title	Designation	Contacts	Use at a Module
Command			
Station Number	N	1	*Selects the module (individual line from control station)*
Subaddress	A1,2,4,8	4	*Selects a section of the module*
Function	F1,2,4,8,16	5	*Defines the function to be performed in the module*
Timing			
Strobe 1	S1	1	*Controls first phase of operation (Dataway signals must not change)*
Strobe 2	S2	1	*Controls second phase (Dataway signals may change)*
Data			
Write	W1-W24	24	*Bring information to the module*
Read	R1-R24	24	*Take information from the module*
Status			
Look-at-Me	L	1	*Indicates request for service (individual line to control station)*
Busy	B	1	*Indicates that a Dataway operation is in progress*
Response	Q	1	*Indicates status of feature selected by command*
Command Accepted	X	1	*Indicates that module is able to perform action required by the command*
Common Controls			*Operate on all features connected to them, no command required*
Initialize	Z	1	*Sets module to a defined state (Accompanied by S2 and B*
Inhibit	I	1	*Disables features for duration of signal*
Clear	C	1	*Clears registers (Accompanied by S2 and B)*
Nonstandard Connections			
Free bus lines	P1,P2	2	*For unspecified uses*
Patch contacts	P3-P5	3	*For unspecified interconnections. No Dataway lines*
Mandatory Power Lines			*The crate is wired for mandatory and additional lines*
+24 V dc	+ 24	1	
+6 V dc	+ 6	1	
- 6 V dc	- 6	1	
- 24 V dc	- 24	1	
0 V	0	2	*Power return*
Additional Power Lines			
+ 12 V dc	+ 12	1	
- 12 V dc	- 12	1	
Clean Earth	E	1	
Supplementary -6 V	Y1	1	
Supplementary +6 V	Y2	1	
Reserved undesignated		3	
Total		**86**	

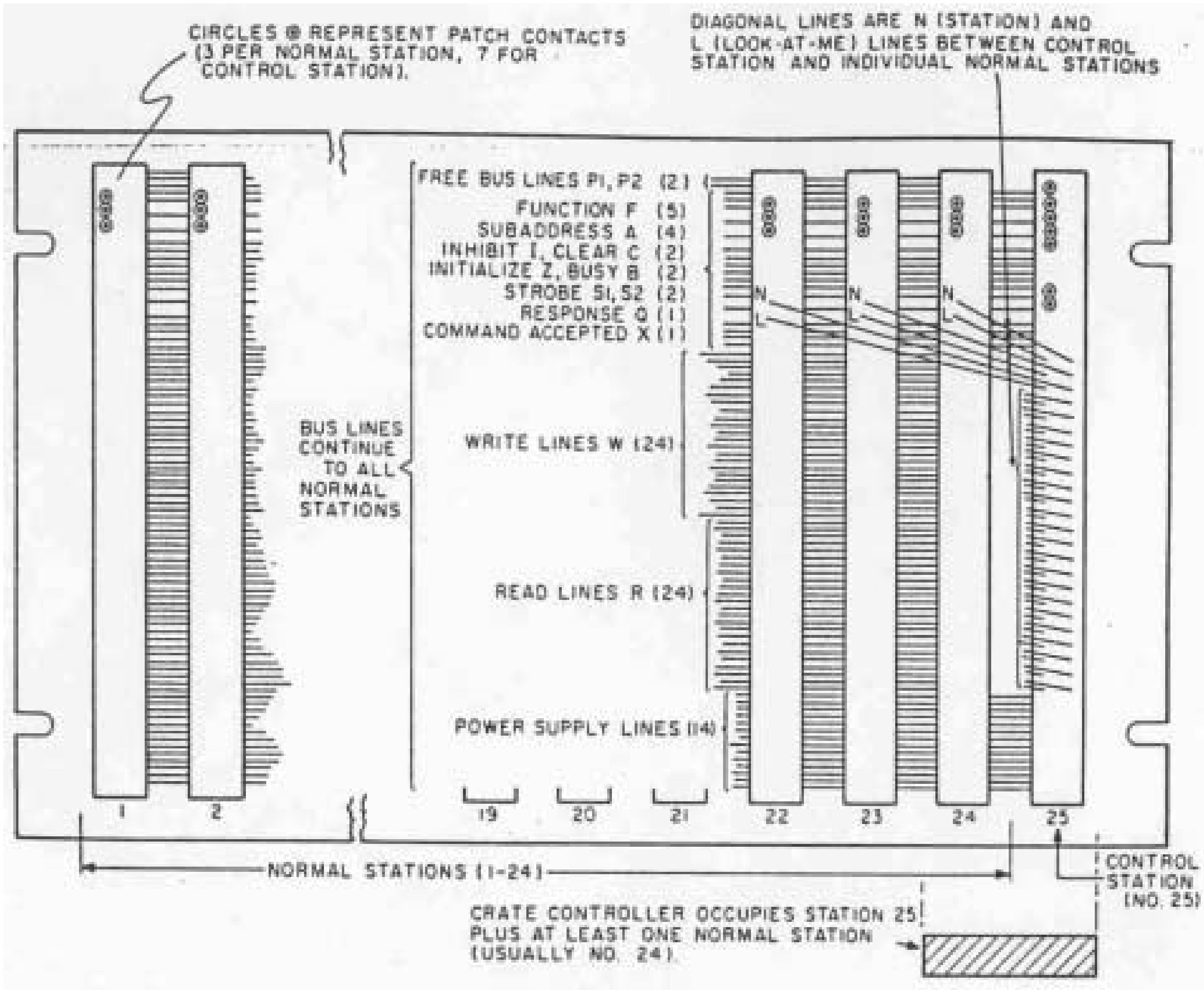

Figure 3-2: CAMAC Dataway Wiring for a 25 Station Crate

(Ref.: ANSI/IEEE Std 583-1982)

Except for the control station, all normal stations are interconnected by 24 parallel *read* lines and 24 *write* lines. These lines can be used to transmit 24 parallel bits of data from a module along the read lines and to a module along the write lines. The control station is connected to each of the normal stations by separate private lines. Twenty four of these are *station* lines (N lines), one of which corresponds to each normal station and must be activated to communicate with that specific station. An additional 24 are *look-at-me* lines (L lines), one for each station, by means of which each individual normal station may signal to the control station that it requires attention.

Each normal station has four *subaddress* lines (A lines) and five *function* lines (F lines). The subaddress lines are standard for all modules. They are used to select different sections in the module. The function lines are used to define the function to be performed by the module. The functions differ from one module to another. Two *strobe* lines (S1 and S2) are also fully bussed to all stations and must be activated to initiate operations or to transfer data.

To control and manage modules within the CAMAC crate, the controller issues *CAMAC Commands* to the modules via the dataway. A command is a set of dataway signals that tell a particular module to perform a particular operation. The command syntax is as follows:

$$(N(i),A(j),F(k))$$

Where:

N: Station number in the crate ($1 \le i \le 24$)

A: Subaddress within the module at the station number ($0 \le j \le 15$)

F: Function to be executed ($0 \le k \le 31$)

Notes:

- Commands are written in binary codes
- In software format, an additional number is added in the command syntax which corresponds to the crate number.

3.2. Multiparameter Data Acquisition:

One major improvement to recent coincidence counting approaches is faster and more complex data acquisition. This improvement is mainly due to the advances in computer technology which led to faster computer speeds and increased memory. This also led to more usage of CAMAC based modules. Also, the computer technology advances dramatically lowered the cost of computers, which in turn led to the increased popularity of CAMAC based modules.

An example of a complex data acquisition is multiparameter data acquisition. As opposed to single parameter data acquisition, multiparameter data acquisition generally means acquiring two or more correlated parameters initiated by a common trigger. These parameters are usually correlated in time and, thus, the time signal serves as the trigger for recording these parameters. The trigger may originate in external logic hardware or in a timer.

In any unit designed for multiparameter data acquisition, at least two separate inputs with dedicated Analog to Digital Converters (ADC) must be provided, together with an associated coincidence circuit. The coincidence circuit is responsible for producing the common trigger between the inputs. The memory consists of a two (or more) dimensional array in which each axis corresponds to one of the inputs. When the inputs are in coincidence, the memory location corresponding to the intersection of the digitized addresses is incremented. As data accumulate, the intensity distribution then takes the form of a two dimensional surface with peaks representing intense areas.

For gamma gamma coincidence measurements, two or more detectors are setup with specific settings. The parameters of interest are the pulse height, which is correlated to the deposited gamma ray energy, resulting in each detector at the same time instant. In this case, the parameters, and thus their resulting signal, are correlated in time. The trigger signal must be derived from these signals and their relation in time, so as to be simultaneous with the occurrence of the signals themselves.

When the trigger occurs, the raw data signals are converted in the data acquisition electronics and read into the host computer. At this point, the data exist as a correlated set of raw parameters. The data is stored in two dimensional arrays and then sorted into histograms to be analyzed either in an online or offline mode.

An alternative method to recording the data in arrays is storing in an event data file Here, the digitized ADC outputs are quickly written to the memory along with the time difference between them. The time difference is usually derived from an external hardware called the Time to Analog Converter (TAC). The data is then sorted off-line based on arbitrary criteria.

3.3. Old Electronic Setup:

Figure (3.3) shows a block diagram of the coincidence electronics setup previously used at NCSU, Gardner et al (2000). The outputs of the detector's preamplifier are passed the Single Channel Analyzers (SCA). The timing of the two SCA signals is compared in the coincidence unit. If they arrive within the resolving time of the coincidence unit, a logic signal is produced. The logic signal then operates the linear gate and the delayed linear pulse from the detector is accepted. Upon acceptance, the linear pulse is processed by the Multi Channel Analyzer (MCA). Depending on the pulse height of the linear pulse, the MCA positions it in the appropriate channel.

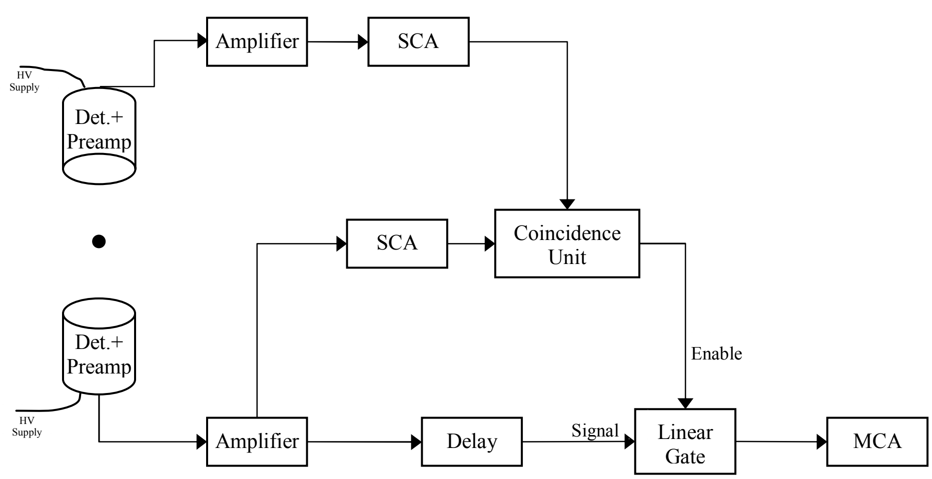

Figure 3-3: Block Diagram of the Old Coincidence Electronics

There are several sources of lack of accuracy of the results obtained using this electronic system. To start off, this electronic system is classified as a "slow-slow" coincidence system. The reason being is that the timing information required to drive the SCA's is picked off after the linear amplifiers. Thus the inaccuracy is resulting from the slow (long rising time) pulses generated by the linear amplifiers.

Other sources of lack of accuracy are the coincidence unit and the SCA. The coincidence unit used originally had a resolving time of about one microsecond. This resolving time was too large for gamma coincidence measurements. Modifications were made to this unit in our electronics shop and the resolving time was reduced to 80 $\pm$ 25 nanoseconds. The imprecise resolving time produced a source of inaccuracy to the experiment.

To understand why the SCA causes inaccuracy, a description of how it functions will be given. The SCA produces a logic output pulse only if the linear input pulse amplitude falls between a lower level discriminator (LLD) and an upper level discriminator (ULD). The time appearance of the logic signal is not closely coupled to the actual event timing. The reason for this is that the logic pulse is generated at a time dependent on when the linear pulse crossed the trigger level. To illustrate this further, Figure (3.4) shows two pulses that have identical true time of origin but give rise to output logic pulses that differ substantially in their timing. It is thus not precise in situations where accurate timing is needed, as in coincidence measurements.

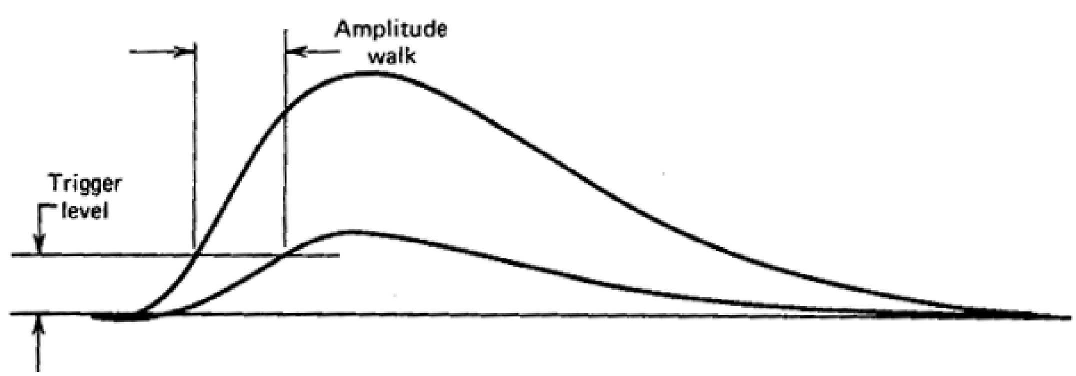

Figure 3-4: Single Channel Analyzer Triggering

Ref.[knoll, G.F., 2000]

3.4. New Electronic Setup:

Two major improvements were added to the coincidence electronics. These improvements allowed us to:

i. Obtain accurate timing information;

ii. Perform multiparameter data acquisition.

Figures (3.5) and (3.6) show a block diagram of the new coincidence electronic setup. Note that the electronics in Figure (3.5) (as well as Figure (3.4)) are based on Nuclear Instrument Module (NIM) instrumentation standards, while those in Figure (3.6) are based on Computer Automated Measurement and Control (CAMAC) instrumentation standards.

3.4.1. Accurate Timing Information:

This was obtained by (Figure (3.5)):

a. Replacing the SCA by a Timing Filter Amplifier and a Constant Fraction Discriminator (CFD);

b. Replacing the coincidence unit by a new one.

The timing filter amplifiers offer some amplitude gain and adjustable differentiation and integration time constants that are typically much shorter (a few hundred nanoseconds or less) than those common in linear amplifiers. The resulting pulses generally have faster rise times and smaller widths than from linear amplifiers.

The Constant Fraction Discriminator produces an output (logic) signal a fixed time after the leading edge of the input pulse has reached a constant fraction of the peak pulse amplitude. This point (where the output is generated) is then independent of pulse amplitude for all pulses of constant rising time. The fraction of the peak pulse amplitude is determined by adjusting the external delay cable length.

The combination of the timing filter amplifier and the CFD offer precise timing signals to be compared by the coincidence unit. Finally, it is worth noting that the timing information is extracted without passing through the linear amplifiers. It is extracted from the preamplifiers, thus making this a “fast-fast” coincidence system.

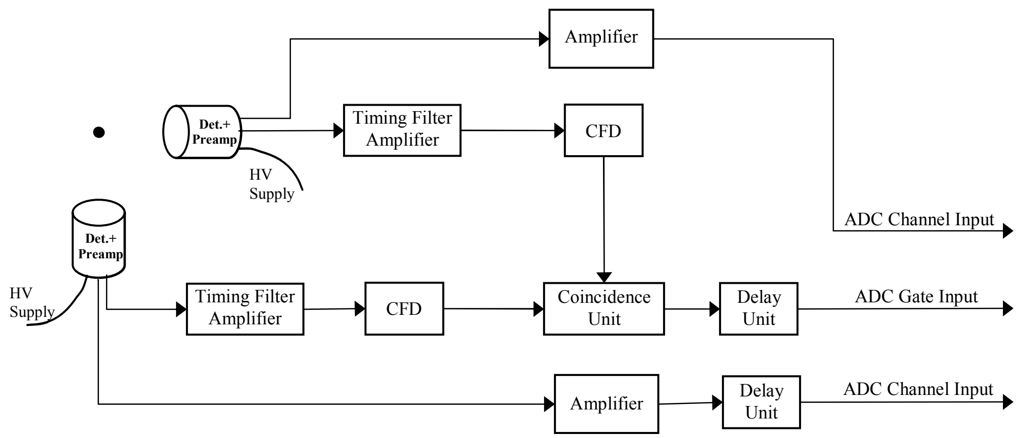

Figure 3-5: Block Diagram of New Coincidence Electronics (NIM Standards)

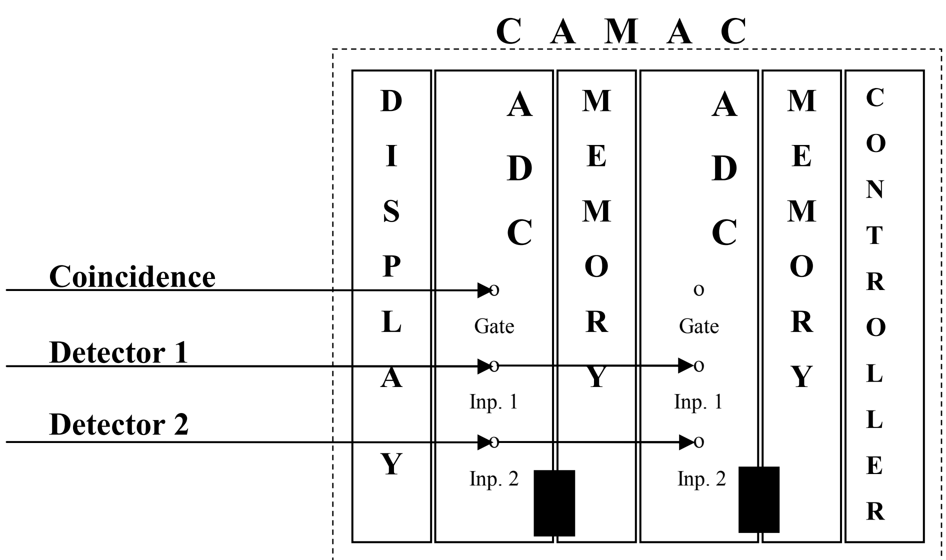

Figure 3-6: Block Diagram of New Coincidence Electronics (CAMAC Standards)

The new coincidence unit operates in the same manner as the old one but has an accurate resolving time. The resolving time is adjustable from ten nanoseconds to one microsecond. The coincidence unit has three coincidence inputs and one anticoincidence input.

3.4.2. Multiparameter Data Acquisition Capability:

Multiparameter data acquisition was achieved using an additional set of six modules (Figure (3.6)) that are based on CAMAC standards. The six modules were used in the CAMAC crate, they were;

a. Two Analog to digital Converters (ADC);
b. Two Memory Units;
c. CAMAC controller; and
d. Dataway display module.

The linear pulse output from the NIM bin amplifiers is duplicated and passed to the ADC's in the CAMAC crate. Each ADC processes one set of linear pulses. Each ADC can take up to four inputs, with 8192 channels for each input.

The logic signal from the coincidence unit on the NIM crate serves as a gate signal for one of the ADCs'. Thus this ADC acquires coincidence data. The other ADC (without a gate signal input) acquires the singles data.

Finally, the computer software used to manage the CAMAC modules and analyze the acquired data was KMAX NT. A brief description of this software is given in the next section.

3.5. Computer Software (KmaxNT)

KmaxNT is a complete Windows environment for data acquisition, data analysis and instrument control with advanced features for visualization, data management, and report generation. KmaxNT also provides both low and high level support for interfacing to external hardware and for building virtual instrumentation toolsheets. KmaxNT has its own built-in script language (Command Sequence Language or CSL) for developing data acquisition and process control tasks.

For our application, KmaxNT is used to manage the CAMAC crate modules and analyze the acquired data. Through KmaxNT we can process and plot the coincidence and singles data at the same time. Two dimensional data (and plots) are also obtained through KmaxNT. These two dimensional data give us the ability to perform offline coincidence data analysis. This ability is gained because the data is stored in a two dimensional matrix where the row indices represent the channels in one detector and the column indices represent the channels in the other detector. The coincidence data analysis will be shown in Chapter four. For example, we can (offline) set an energy window on one of the detectors and observe the coincidence spectrum in the other detector. This is one of the main advantages of Multiparameter data acquisition.

3.6. Result Comparison of Both Electronic Setups:

To compare the results of the old and new electronics, a specific experimental setup was used for both of them. The experimental setup is shown in Figure (3.7). A Cf-252 neutron source was placed in the center of a lead cube to attenuate the source gamma rays. The cube was placed over a layer of wax to thermalize the fast neutrons from the source before interacting with the sample box containing sulfur. Finally, the detectors were mounted on wooden table side by side. A lithium sheet was placed on the face of the detectors and the sides were wrapped with lead. Results for this experimental setup, and using the old electronics, were previously published [Gardner et al, 2000]. For sulfur, the spectra are shown in Figure (3.8).

To observe the improvement in results, the same experiment was performed again using the new electronics. Again for sulfur, the spectra are shown in Figure (3.9).

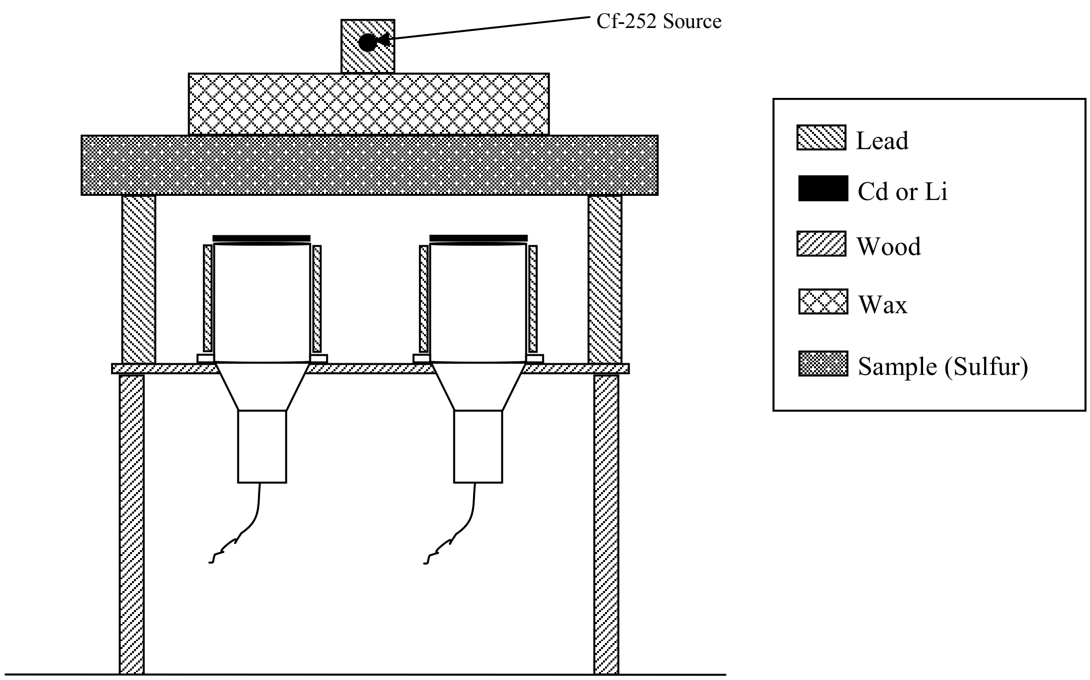

Figure 3-7: Experimental Setup for Electronics Comparison

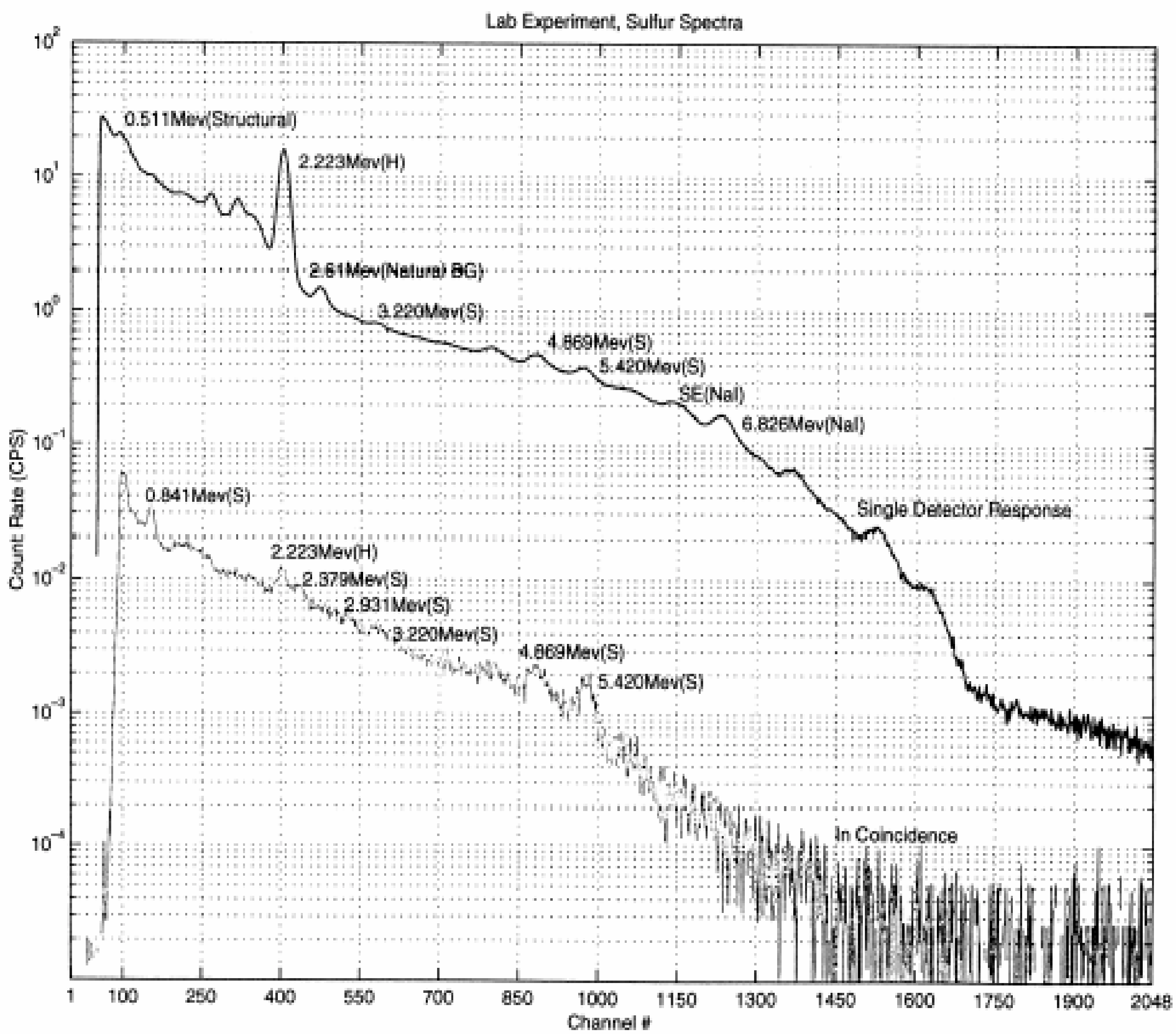

Figure 3-8: 5″*5″ NaI Sulfur Spectra, Old Electronics

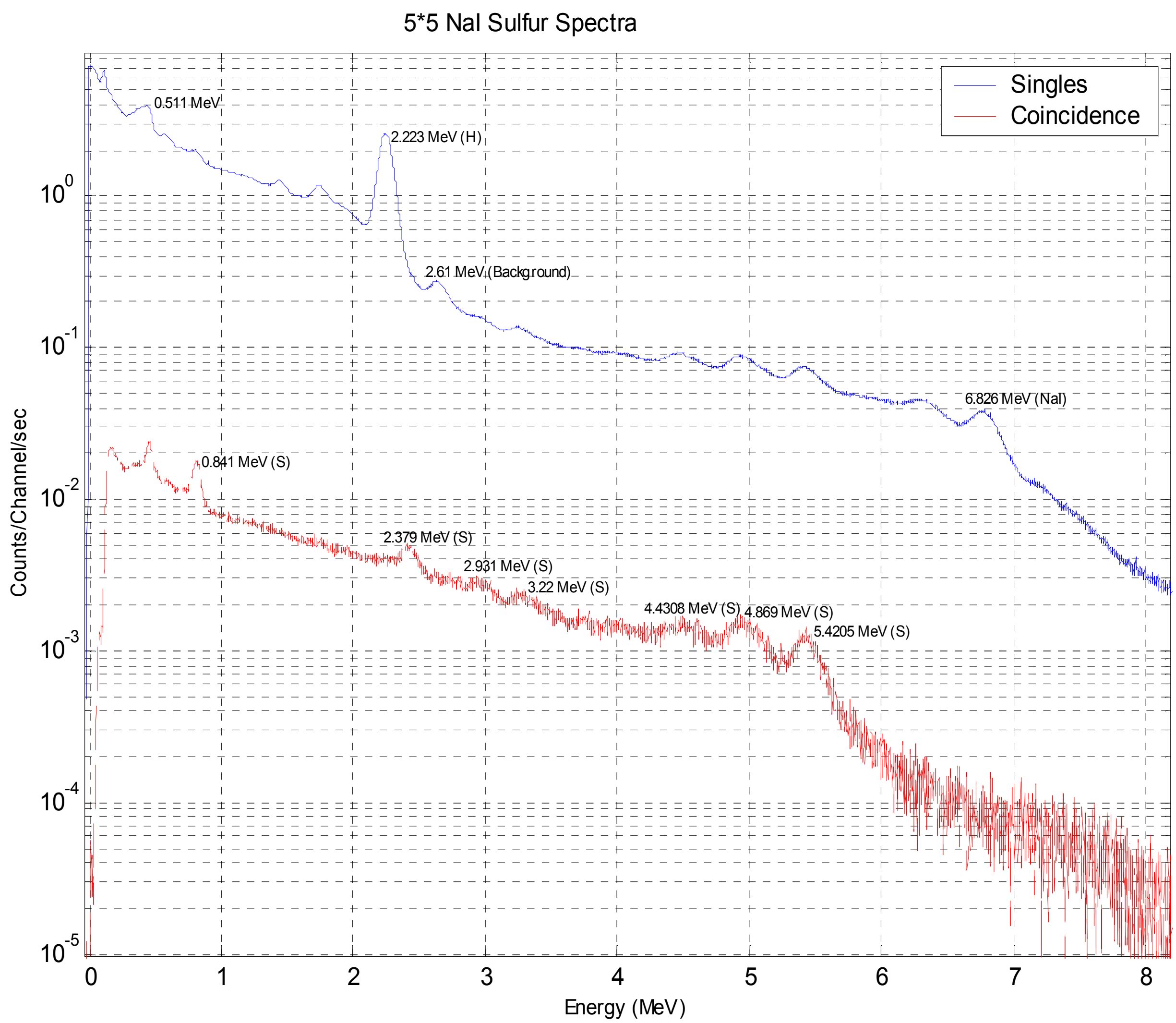

Figure 3-9: 5″*5″ NaI Sulfur Spectra, New Electronics

Comparing the coincidence spectrum in Figures (3.8) and (3.9), improvements are noticed and can be summarized as follows:

1. Complete elimination of the Hydrogen 2.223 MeV peak;
2. The 2.379 MeV sulfur peak is now more defined; and
3. The rest of the sulfur peaks are more obvious (e.g. 2.931 MeV, 3.22 MeV, etc.)

All the improvements listed above lead to an increase in signal-to-noise ratio. Thus, major improvements and new capabilities were achieved due to the new coincidence system.

4. EXPERIMENTAL RESULTS AND ANALYSIS

The first part of this chapter is devoted to the feasibility studies for the gamma-gamma coincidence counting approach. The studies deal with the problematic effects observed in normal single detector spectrum. In the remaining part of this chapter, three practical applications of the gamma-gamma coincidence apparoach are introduced. Note that all the spectra presented in this chapter were acquired with the new coincidence electronics described in section 3.4.

4.1. Initial Observations:

To demonstrate the feasibility of the gamma-gamma coincidence counting approach, the problematic effects observed in normal single detector spectra were addressed. Namely, the effects are the background (including hydrogen), summing, and pulse pile up. In addition, examples of two dimensional spectra are given at the end of this section. These types of spectra may be used for decay scheme analysis.

4.1.1. Hydrogen Peak Elimination:

When activated by thermal neutrons, hydrogen de-excites by emitting a single prompt gamma ray with energy 2.223 MeV. The magnitude of this peak in a normal spectrum is often one or more orders of magnitude larger than other elements of interest. Not only does hydrogen dominate the 2.223 MeV energy range, but also the energy range below that. This is due to the Compton continuum of that gamma ray. This poses a difficulty in analyzing the spectrum at and below 2.223 MeV.

As the hydrogen gamma ray is a single one, coincidence counting should eliminate it, and its continuum, from the spectrum. An example of this was given in section 3.3 for a NaI detector. Here, a similar example will be given. Two HPGe detectors (59 % and 72 % efficiency) were placed at 180 degrees angle with respect to each other. The distance between the two detectors was approximately 23 cm and the sample was placed in between them at an angle of 45 degrees. The sample used was silicon and was placed in the thermal neutron beam of the NCSU PULSTAR reactor.

Figure (4.1) shows the singles and coincidence spectra of the silicon sample from the 59 % HPGe detector. The energy range 0 – 2.5 MeV is shown. It can bee seen from the coincidence spectrum that the hydrogen peak (and thus its continuum) was completely eliminated.

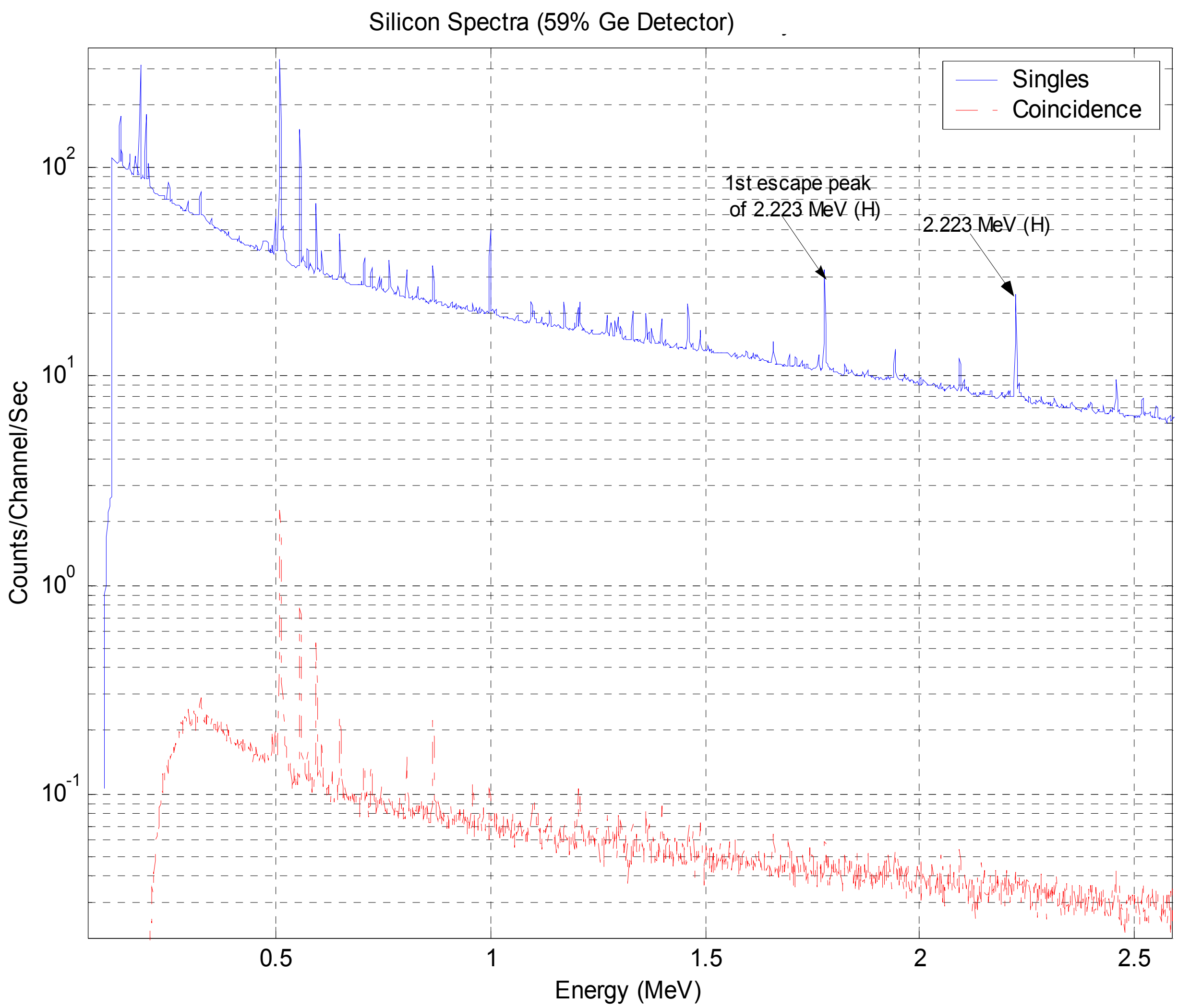

Figure 4-1: Feasibility, Hydrogen Peak Elimination

4.1.2. Background and Sum Peak Elimination:

A cobalt-60 radioisotope was used for this experiment and two HPGe detectors (59% and 72% efficiency). The experiment was conducted in the NCSU PULSTAR reactor bay while the reactor was in operation. The resulting spectra are shown in Figure (4.2). Because the reactor was operating at the time of the experiment, there was a high background level in the singles spectrum. Observing the coincidence spectrum, we notice that the 2.505 MeV cobalt sum peak was eliminated. We also notice that the background (1.462 MeV, 2.614 MeV, and surrounding structural material) is negligible.

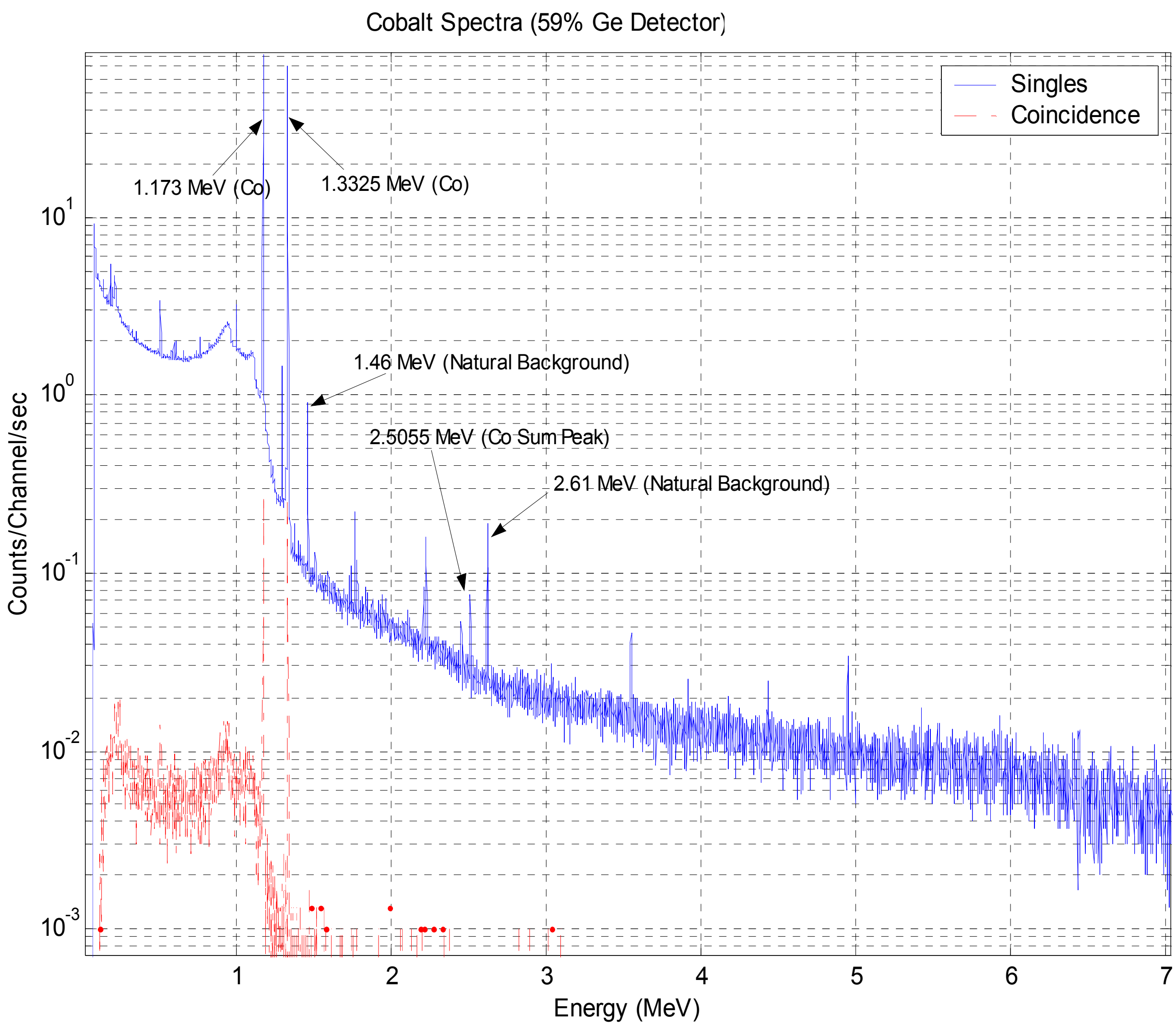

Figure 4-2: Feasibility, Background and Sum Peak Elimination

4.1.3. Pulse Pile Up Reduction:

A cesium-134 radioisotope was used for this experiment and two HPGe detectors (59% and 72% efficiency). The highest energy gamma for Cs-134 is 1.365 MeV. The experiment was conducted in the lab where the background level was low. Thus, any peaks or continuum above the 1.365 MeV was due to summing and pulse pile up effects respectively, Figure (4.3). Observing the coincidence spectrum above 1.365 MeV, we notice no peaks and negligible continuum. It must be noted that this observation is a function of the count rate. As the count rate increases, the Pulse Pile Up effects become more observable in the obtained spectrum, singles and coincidence.

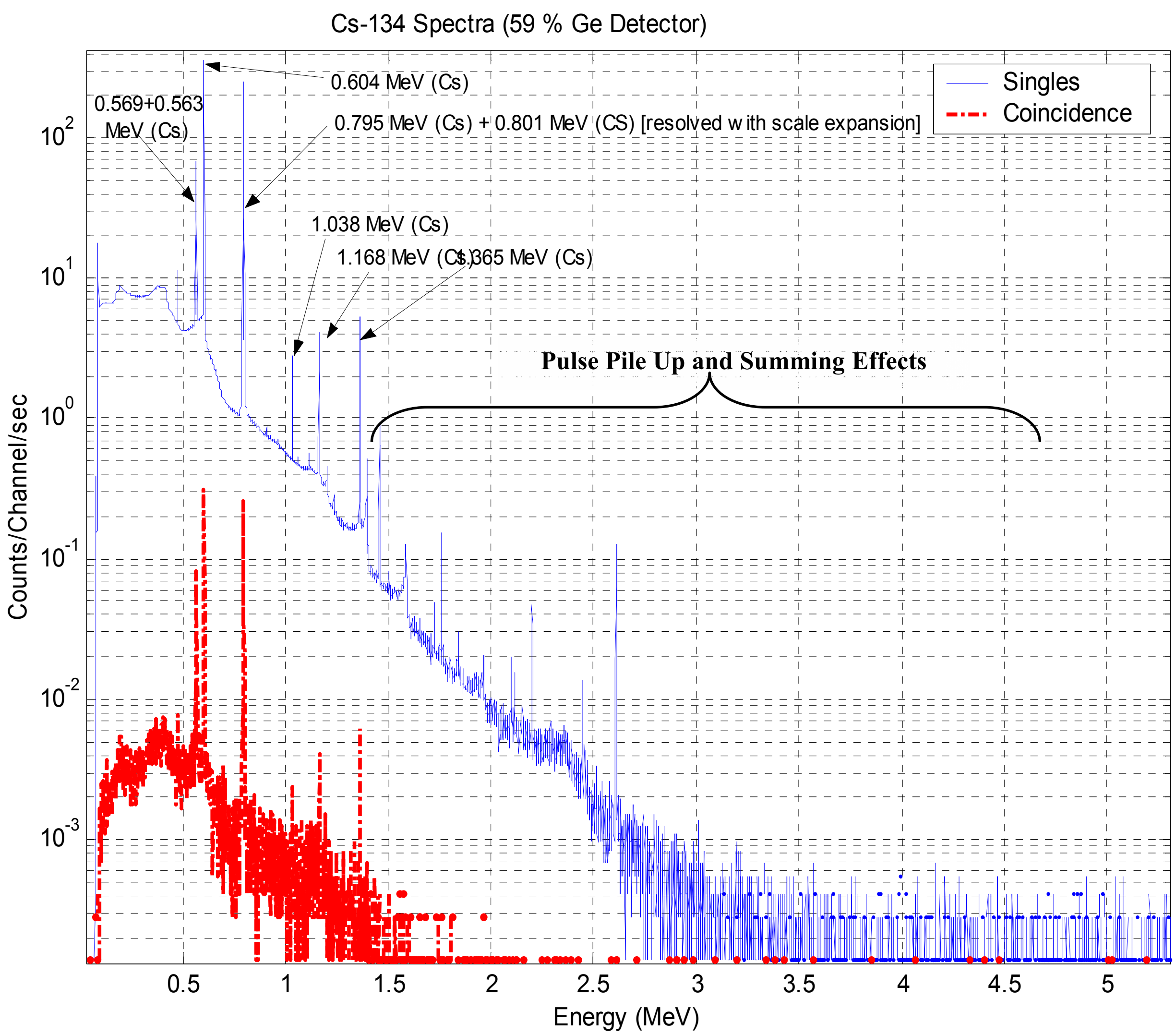

Figure 4-3: Feasibility, Pulse Pile Up Elimination

4.1.4. Two Dimensional Spectra:

This section includes two examples of two dimensional spectra obtained via the multiparameter data acquisition capability. By two dimensional spectra, we are referring to the array obtained when a detector pair is used for coincidence measurements. If more than two detectors are used, the number of obtained arrays would correspond to the different number of detector combinations. In general, two dimensional spectra provide us with more information than the one dimensional ones and may be used, as an example, for decay scheme analysis.

The two dimensional spectra are usually presented on three dimensional plots where each of the X and Y axis represent a detector in the detector pair used. The Z axis represents the obtained counts. The plots thus take the form of a three dimensional surface where the peaks represent intense coincidence areas.

To illustrate the two dimensional spectra, two Ge detectors were used- One had 72% efficiency and the other was 59% . The detectors were set in a horizontal position with a 90 degrees angle with respect to each other. The sample was placed at the intersection of the centerlines on both detectors, 15 cm away.

Two examples are presented. The first example, Figure (4.4), shows the two dimensional spectrum of cobalt-60. Two features of this spectrum are noted on the figure. The second example, Figure (4.5), is for Na-24, which is a more complicated spectrum than Co-60. The features of Figure (4.5) are explained in Table (4.1). Note that the detectors were placed at 90 degrees with respect to each other and that is why the 135° edge is appearing in both figures instead of the Compton edge.

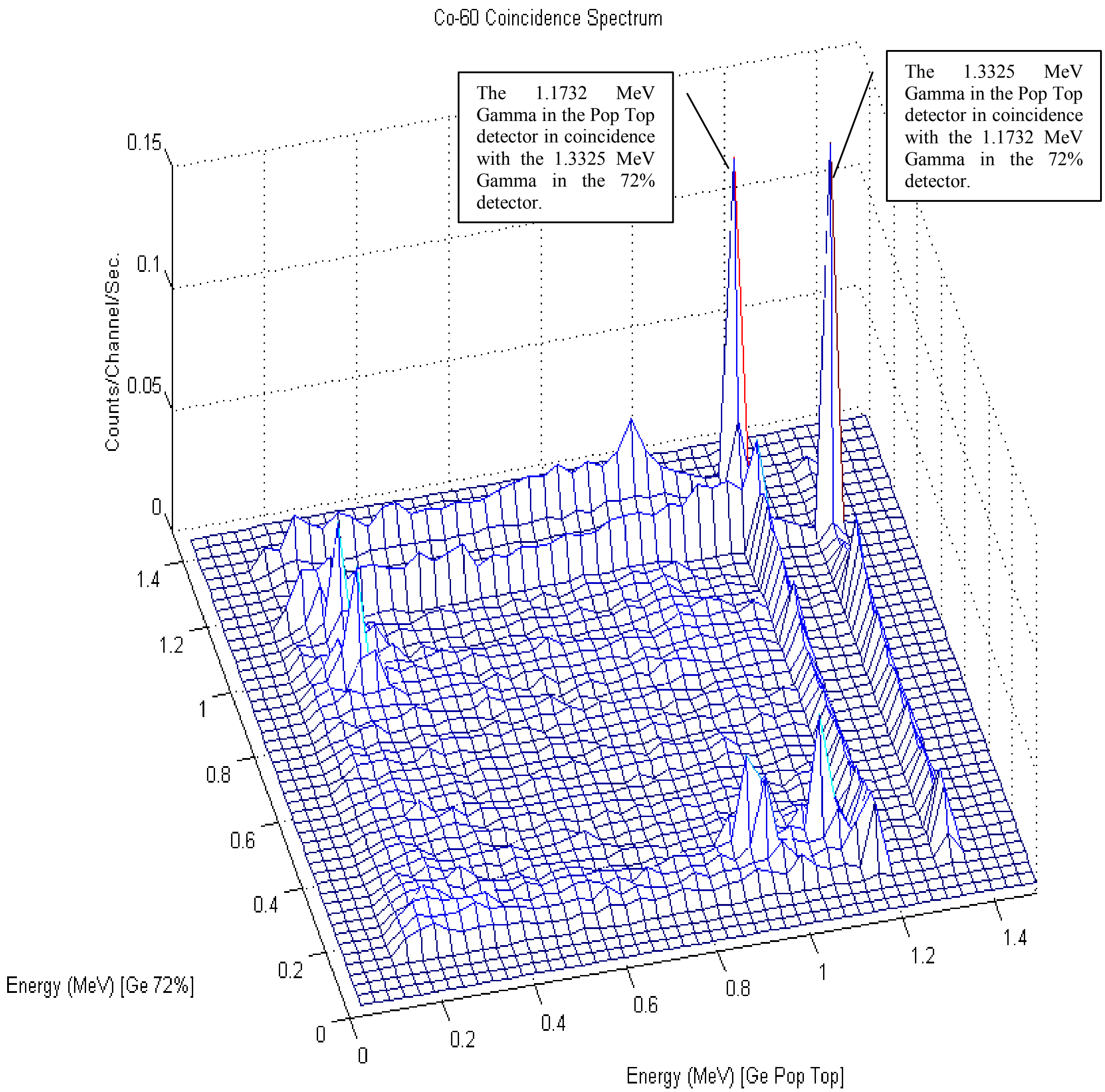

Figure 4-4: Feasibility, Co-60 Two Dimensional Spectrum

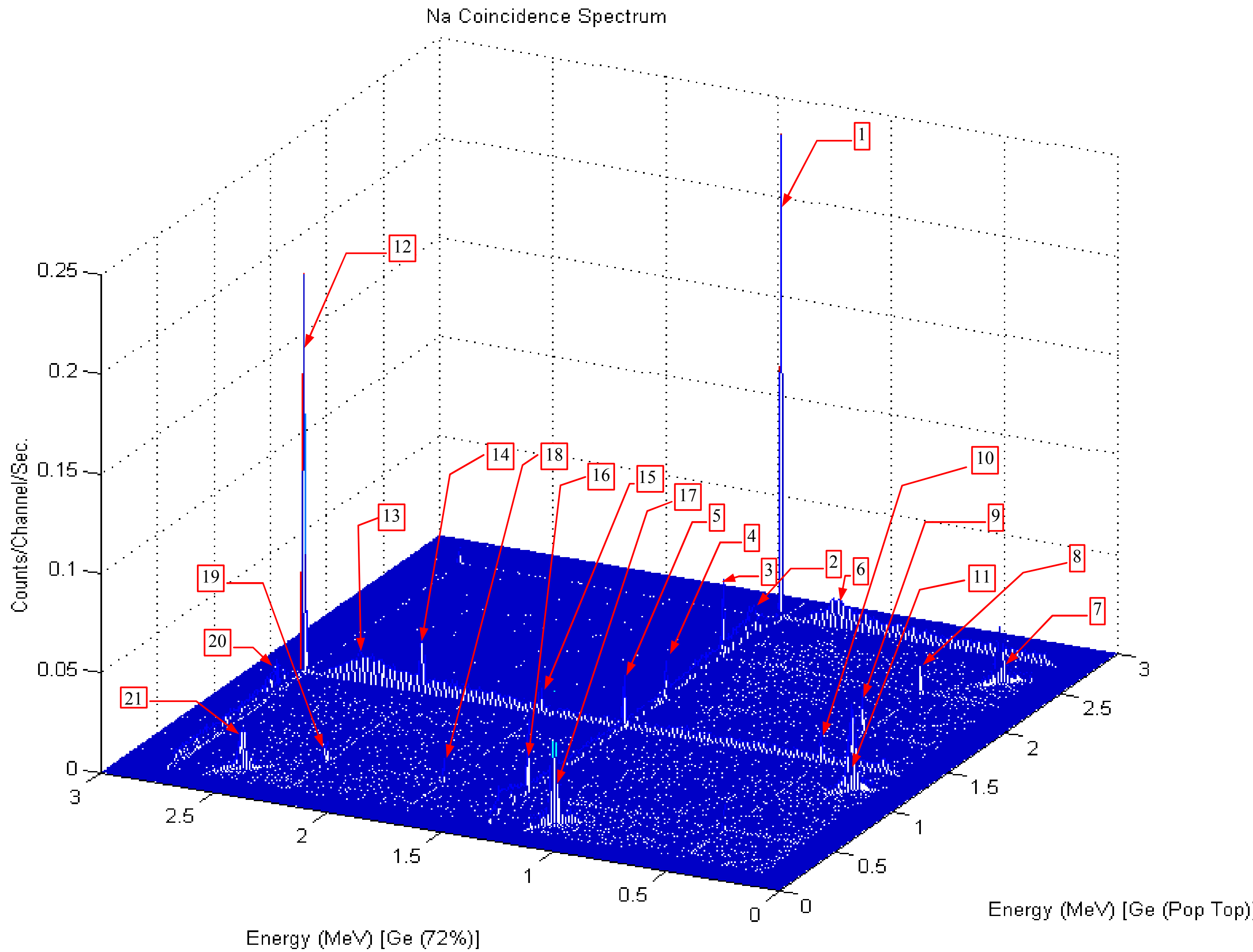

Figure 4-5: Feasibility, Na-24 Two Dimensional Spectrum

Table 4-1: Na-24 Two Dimensional Spectrum Features

#	Peaks Correspond to in the	
	Pop Top Ge Detector	**72% Ge Detector**
[1]	2.754 MeV Na-24 γ	1.368 MeV Na-24 γ
[2]	135° edge of the 2.754 MeV Na-24 γ	1.368 MeV Na-24 γ
[3]	1^{st} escape of the 2.754 MeV Na-24 γ	1.368 MeV Na-24 γ
[4]	2^{nd} escape of the 2.754 MeV Na-24 γ	1.368 MeV Na-24 γ
[5]	1.368 MeV Na-24 γ Chance Coincidence	1.368 MeV Na-24 γ
[6]	2.754 MeV Na-24 γ	135° edge of the 1.368 MeV Na-24 γ
[7]	135° edge of the 2.754 MeV Na-24 γ	Backscatter γ the 2.754 MeV Na-24 γ
[8]	1^{st} escape of the 2.754 MeV Na-24 γ	0.511 MeV Annihilation γ
[9]	2^{nd} escape of the 2.754 MeV Na-24 γ	0.511 MeV Annihilation γ
[10]	1.368 MeV Na-24 γ	0.511 MeV Annihilation γ
[11]	135° edge of the 1.368 MeV Na-24 γ	Backscatter γ the 1.368 MeV Na-24 γ
[12]	1.368 MeV Na-24 γ	2.754 MeV Na-24 γ
[13]	1.368 MeV Na-24 γ	135° edge of the 2.754 MeV Na-24 γ
[14]	1.368 MeV Na-24 γ	1^{st} escape of the 2.754 MeV Na-24 γ
[15]	1.368 MeV Na-24 γ	2^{nd} escape of the 2.754 MeV Na-24 γ
[16]	0.511 MeV Annihilation γ	1.368 MeV Na-24 γ
[17]	Backscatter γ the 1.368 MeV Na-24 γ	135° edge of the 1.368 MeV Na-24 γ
[18]	0.511 MeV Annihilation γ	2^{nd} escape of the 2.754 MeV Na-24 γ
[19]	0.511 MeV Annihilation γ	1^{st} escape of the 2.754 MeV Na-24 γ
[20]	135° edge of the 1.368 MeV Na-24 γ	2.754 MeV Na-24 γ
[21]	135° edge of the 2.754 MeV Na-24 γ	Backscatter γ the 2.754 MeV Na-24 γ

4.2. Library Least Squares (LLS) Analysis:

4.2.1. Introduction:

The library least-squares (LLS) approach is very useful for inverse spectral problems such as determining radioisotope amounts from gamma-ray spectra and determining elemental amounts from X-ray or prompt gamma-ray spectra. While other methods make use of only the peaks and/or regions (Vobecky et al, 1999 and Ember et al, 2002) to perform elemental analysis, the LLS method has the advantage of using the entire spectrum (peaks and continuum). The LLS method was used for both scintillator and HPGE spectra and has shown to be about 2.5 times better than the single peak analysis method (Gardner et al, 1997). More details on the LLS approach will be given in Chapter 5.

An accurate method for determining elemental analysis is presented. The method combines the precision of the LLS approach and the advantages of gamma-gamma coincidence counting. To demonstrate this method, a known mixture of three radioisotopes was used and data was deliberately collected at high counting rates to determine the effect of pulse pile-up distortion. The results obtained, with the library least-squares (LLS) analysis, of both the normal and coincidence counting are presented and compared to the known amounts. The coincidence results are shown to give much better accuracy. It appears that in addition to the expected advantage of reduced background, the coincidence approach is considerably more resistant to pulse pile-up distortion.

4.2.2. Setup and Experimental Procedures:

To demonstrate the coincidence LLS approach, as compared to the normal singles approach, activity measurements were made for a mixture of radioisotopes. Two HPGe detectors (59% and 72% efficiency) were used. The detectors were placed at 90 degrees with respect to each other with lead shielding in between to reduce the cross talk between them. An additional tungsten shield was placed around the 59% detector. Because of this additional shielding, the 59% detector spectra were used for the LLS analysis.

A system of three radioisotopes (Na-24, Co-60, and Cs-134) that emit coincident gamma rays was used. The radioisotopes were made, in liquid form, using the NCSU PULSTAR reactor. Table (4.2) lists the energies of the gamma rays emitted from each radioisotope and their corresponding intensity. Using the two HPGe detectors, the singles (for each detector) and coincidence spectra of each radioisotope were collected simultaneously and later used as libraries. Then, a known mixture of the three radioisotopes was made and its singles and coincidence spectra were collected. The experiment was carried at relatively high counting rates so that pulse pile up distortion of the spectra was a significant problem. The samples were placed 20 cm from each detector and the collection duration for each spectrum was 2 hours. The resolving time of the coincidence unit was set 80 nanoseconds.

Table 4-2: Na^{24}, Co^{60}, and Cs^{134} Gamma-Ray Energies and Intensities

Na-24		**Cs-134**	
E_γ(MeV	**I_γ(%)**	**E_γ(MeV**	**I_γ(%)**
1.368	99.99	0.475	1.57
2.754	99.87	0.563	8.35
3.867	0.056	0.569	15.3
		0.604	97.62
Co-60		0.796	87.0
E_γ(MeV	**I_γ(%)**	0.802	8.7
0.347	0.0076	1.038	1.0
1.173	99.97	1.168	1.79
1.332	99.98	1.365	3.1

4.2.3. Results:

Figures (4.6) and (4.7) show the single detector and coincidence spectra collected for the 59% detector, respectively. It appears that in addition to the expected advantage of coincidence counting of reducing the background, one also has the additional advantage that the coincidence approach is considerably more resistant to pulse pile-up effects.

Using the libraries obtained for Co-60, Cs-134, and Na-24, the LLS analysis was performed to determine the amount of activity of each radioisotope in the mixture. A FORTRAN program, CURLLS, was used for this purpose. To implement the LLS approach, the program uses the multiple linear regression (Bevington, 1969) method which minimizes the reduced χ^2 value. More information on the LLS approach can be found in Section 5.1.

The LLS analysis was performed for both the singles and coincidence spectra. The singles and coincidence mixture spectra and the LLS fitting are shown in Figures (4.8) and (4.9) respectively. A summary of the obtained results can be found in Table (4.3).

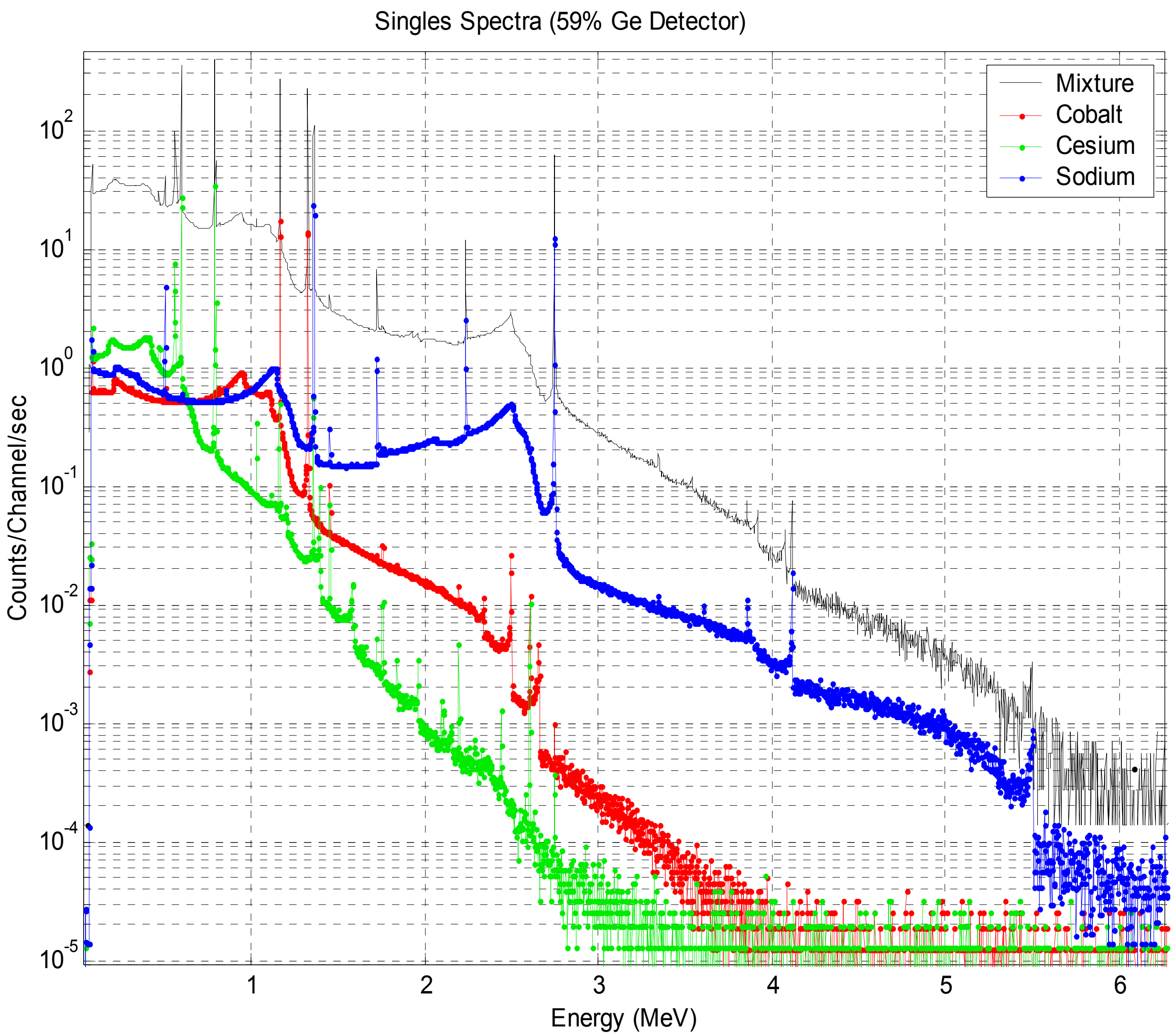

Figure 4-6: Single Detector Spectra of the Mixture and Libraries

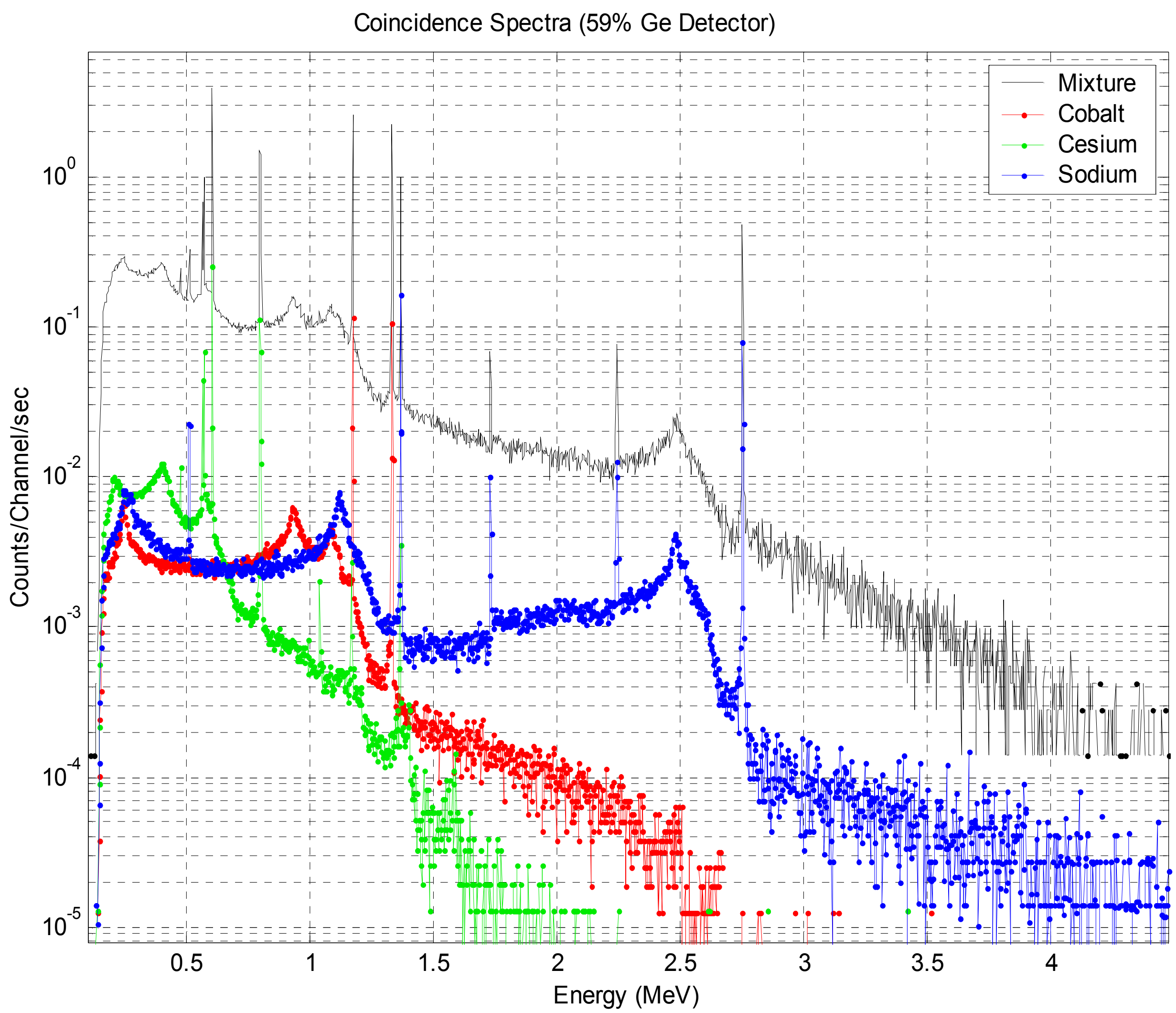

Figure 4-7: Coincidence Spectra of the Mixture and Libraries

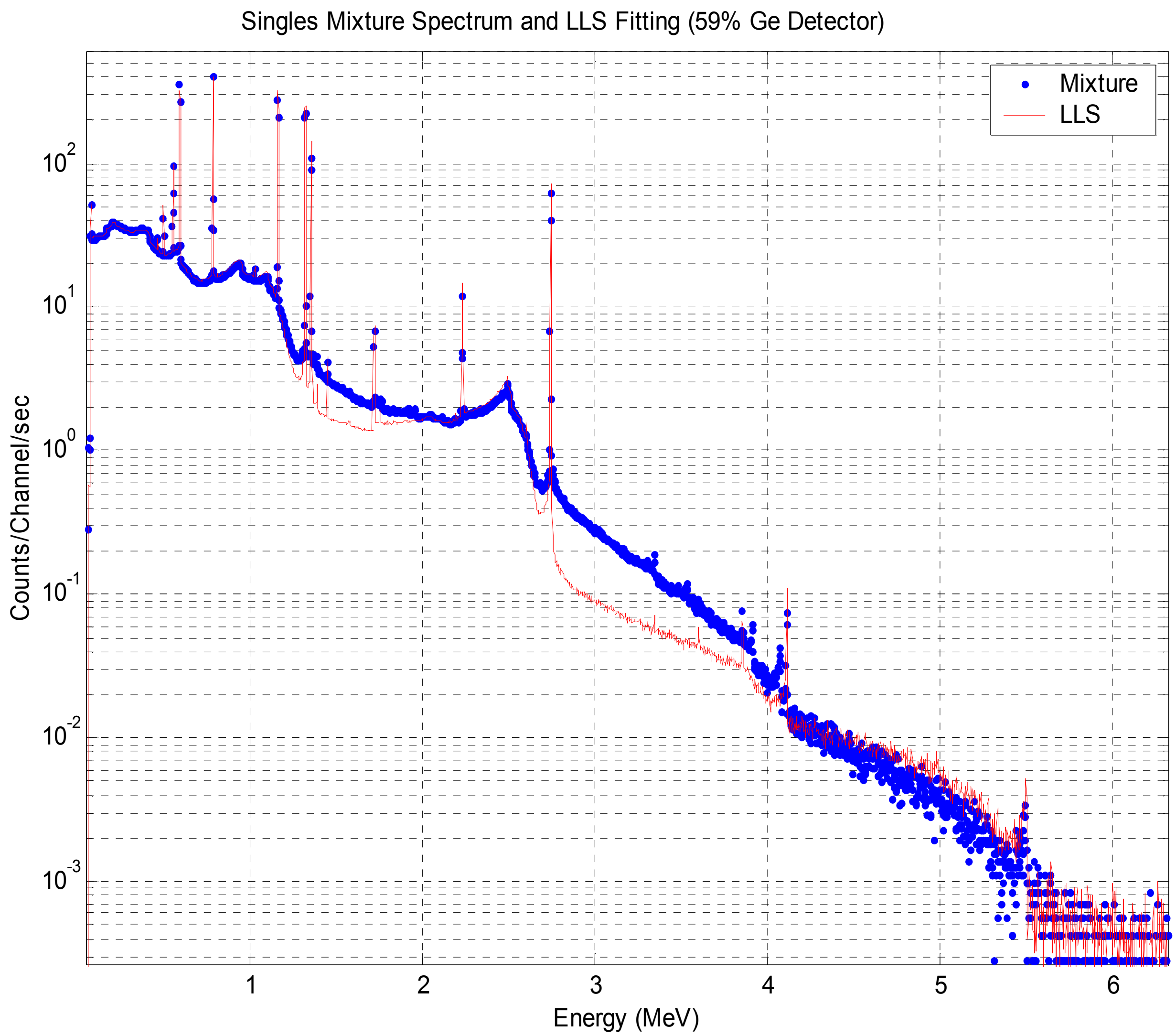

Figure 4-8: Singles Mixture Spectrum and LLS Fitting

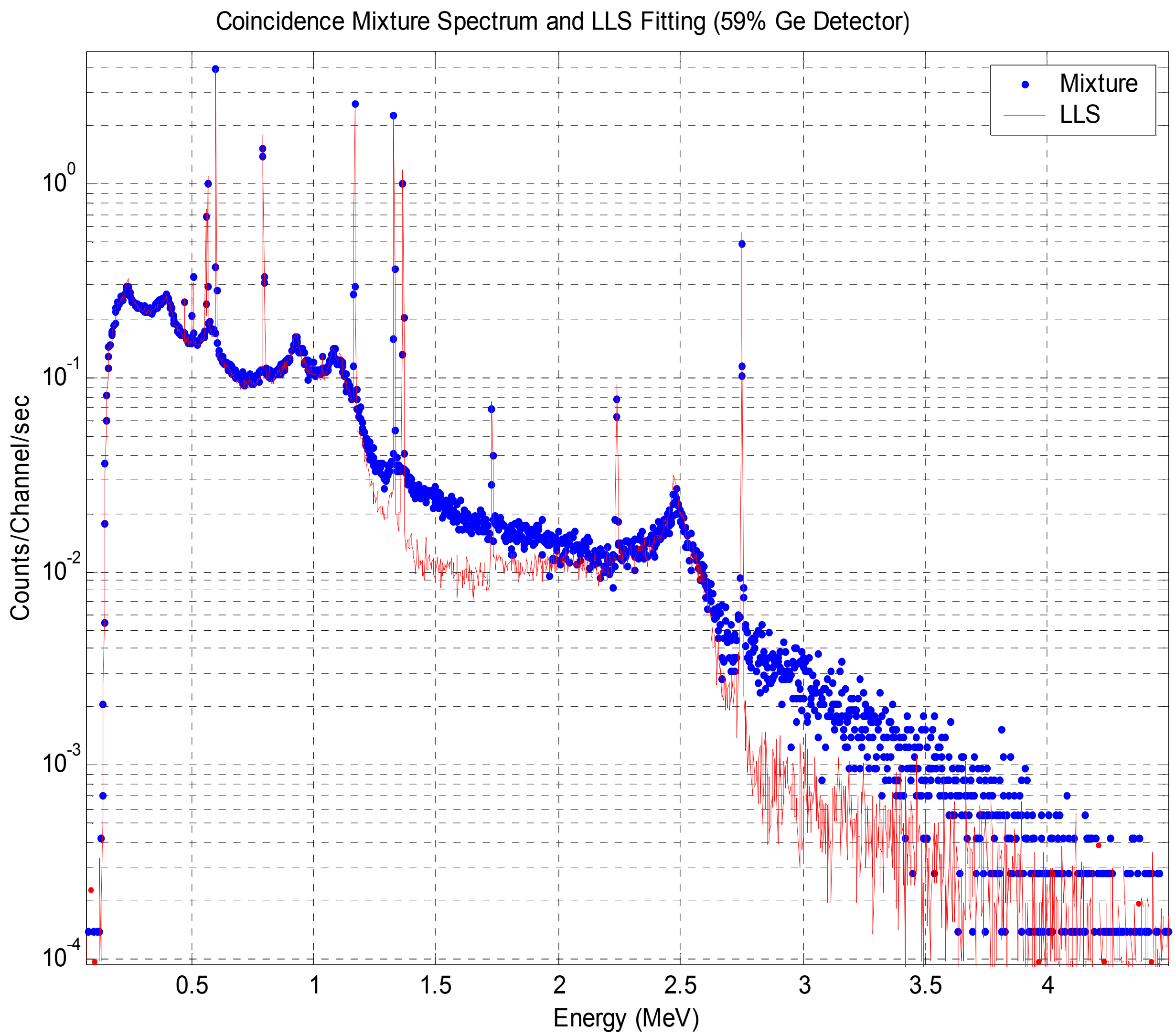

Figure 4-9: Coincidence Mixture Spectrum and LLS Fitting

Table 4-3: Results of LLS Analysis

	Activities (µCi)		
	Singles	**Coincidence**	**Actual**
Co-60	18.350 ± 0.021	21.641 ± 0.075	22.035
Cs-134	11.287 ± 0.019	15.072 ± 0.049	15.644
Na-24	5.868 ± 0.0038	7.147 ± 0.033	7.157
Reduced χ^2	43.26	3.63	

Table (4.3) shows that the results obtained by applying the LLS method to the coincidence spectrum are much closer to the original values than the singles. This is attributed to background elimination in the coincidence spectrum as well as negligible pulse pile up effects. As a consequence, the reduced Chi square value from the coincidence fitting is much closer to 1 than that from the singles.

4.2.4. Pulse Pile Up Effect:

A Monte Carlo simulation code CEARPPU (R.P. Gardner and S.H. Lee, 1999) is used to study the pulse pile up effects. CEARPPU simulates pulse piled up spectra for high counting rates from given spectra. Forcing and other variance reduction techniques are used to accelerate the simulation process.

To generate the input spectrum for CEARPPU, a pseudo singles mixture spectrum was formed using the actual amounts of the radioisotopes. Specifically, the actual amounts of the radioisotopes were multiplied by the corresponding singles library of each radioisotope and the results were added together to form the pseudo mixture spectrum. It is assumed that the pulse pile up in the individual libraries is small and, consequently, also small in the pseudo mixture spectrum.

Next, the pseudo singles mixture spectrum was used as an input for CEARPPU. The output of CEARPPU thus represents the singles mixture spectrum at higher counting rates. Figure (4-10) shows a plot of the actual and pseudo (piled up) singles spectra. Furthermore, the LLS method was applied again to the mixture singles spectrum but with using the pseudo spectrum as the library. The reduced Chi square for this case was 0.975, thus showing that high Chi square value (Table 4.3) reported in the previous section is, to a large extent, due pulse pile up.

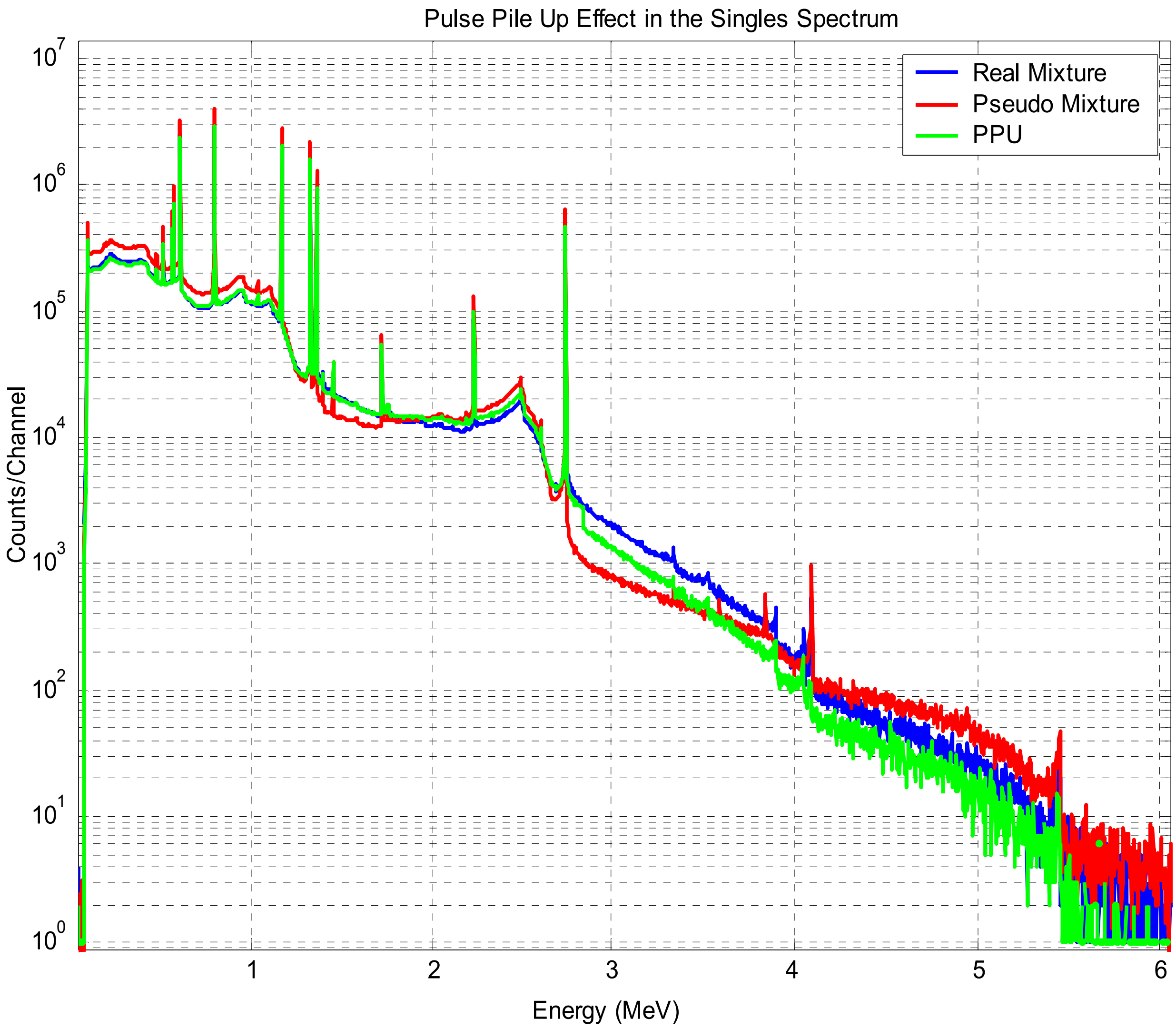

Figure 4-10: Pulse Pile Up Effect in the Mixture Singles Spectrum

4.3. Two Dimensional Diagonal Summing:

4.3.1. Introduction:

As previously stated, one of the characteristics of multiparameter data acquisition is obtaining two dimensional spectra. These types of spectra provide us with more detailed coincidence information than that from one dimensional spectra. Examples of two dimensional spectra were presented in section 4.1.4.

In this section we make use of the two dimensional spectra but in another way. The spectra are presented in a flat view where the intense coincident areas are now defined by the darker areas in the plot. Extracting part (or all) of the information from the flat view plots can transform them into normal two-dimensional plots. This is normally done by summing (projecting) a certain area in the two dimensional plot along one of the axes. This projection can be made in four different ways:

1. Projecting the whole spectrum area to one of the axes. This would yield the total coincidence spectrum in one of the detectors. This is the same as summing all the rows (or columns) in the coincidence data array. Examples of this were presented in the previous sections and an additional example will be presented in this section as well.
2. Projecting a horizontal (or vertical) range of the spectrum to one of the axes. This is called horizontal (or vertical) window summing. On one of the axes this would represent an energy range equivalent to the width of the window. On the other axis this would represent the spectrum that is in coincidence with this energy range. Examples of this will be presented in the next section.
3. Projecting a diagonal area of the spectrum to one of the axes. This is the main focus of this section and will be explained in further detail in the following. Several examples will be presented as well.
4. Projecting an irregular range of the spectrum to one of the axes. This type of projection depends on the type of physical problem being considered. Examples of this are not presented in this work.

Projecting a diagonal area in the two dimensional spectrum to one of the axes has a different interpretation. For gamma-gamma coincidence measurements, the spectrum obtained from this projection yields the gamma spectrum in one detector that corresponds to a specific total energy deposition in both detectors. The total energy deposited may be equal to the Q-value of the reaction studied or the sum of two individual gamma-ray energies, or other values of significant meaning.

The diagonal area is mainly defined by two diagonal lines (the window), as Figure (4-11). The slope of the diagonal lines depends on the calibrations of the two detectors. Two factors play a role in determining the window width. The first factor is the energy of interest. The energy can either be a single energy or a range of energies. A common energy of interest is the Q-value (total energy) of the reaction studied. If one of the decay schemes of the element of interest has only two gamma rays, we expect that these two gammas will show very clearly when making the diagonal projection.

The second factor that plays a role in determining the window width is the detector resolution. If the two detectors used have the same resolution, regardless of the detector type, the window should have a constant width along the diagonal. The reason for this constant window width is that, for diagonal summing, the low energy in one detector corresponds to a high energy in the other detector and vice versa. This width will thus be determined by the detector resolution at the highest energy of interest. If the detectors have different resolutions, the window will have a trapezoidal shape. The wide base of the trapezoidal shape will correspond to the high energy in the detector with poorest resolution.

4.3.2. Coincidence Scheme Application:

Two examples are presented for using the two dimensional diagonal summing for coincidence scheme application. The first example is for sulfur. The two detectors used were NaI with dimensions 5”×5” and 6”×6”. The experimental setup was similar to that shown in Figure (3-7). The resolution for these detectors was almost the same, thus a constant width window was used for the diagonal summing. Figure 4-11 shows the two dimensional plot (flat view) of the counts in both NaI detectors. Two windows are outlined,

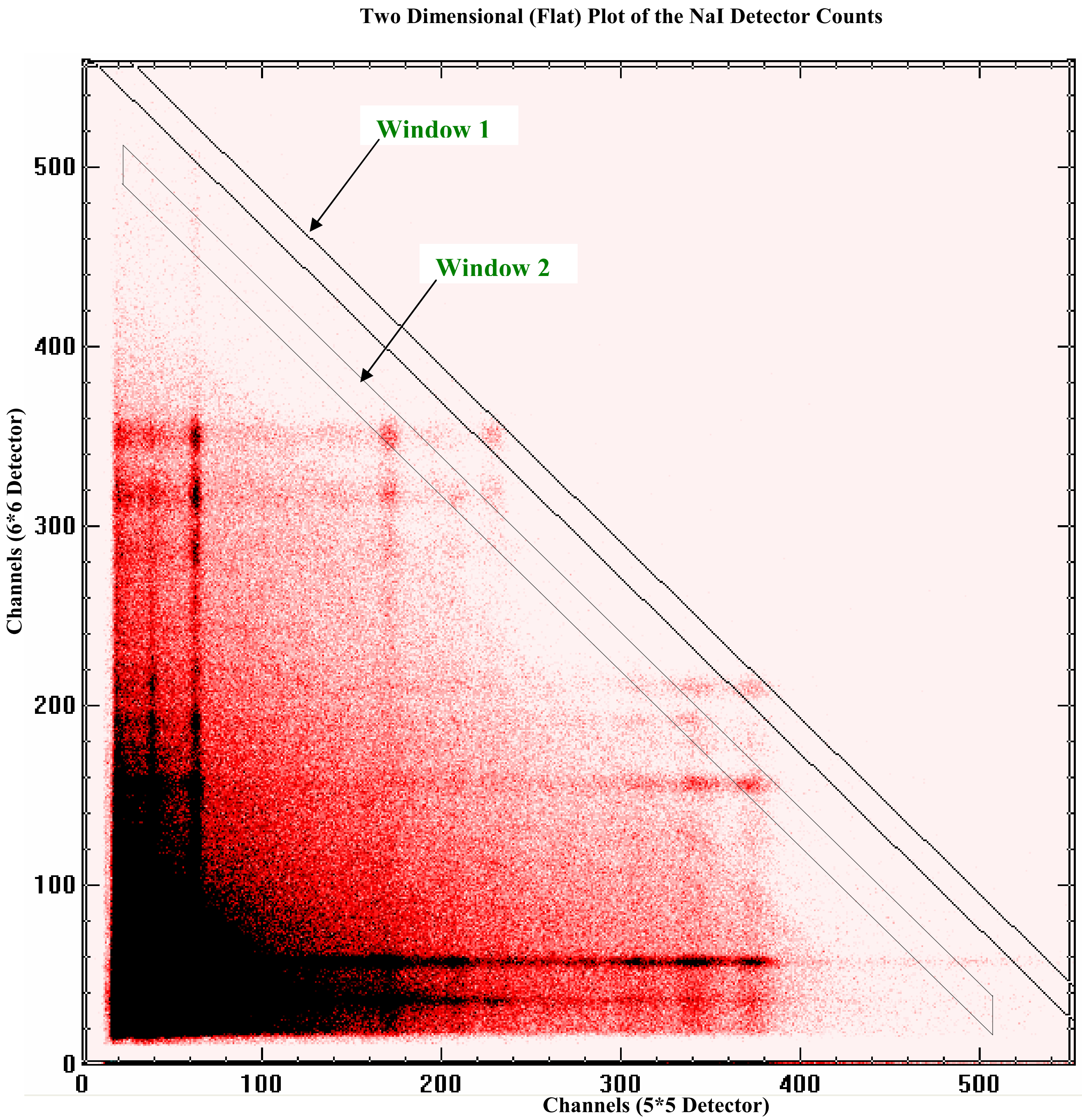

Figure 4-11: Two Dimensional Plot (Flat View) of the Counts in Both NaI Detectors, Sulfur Sample.

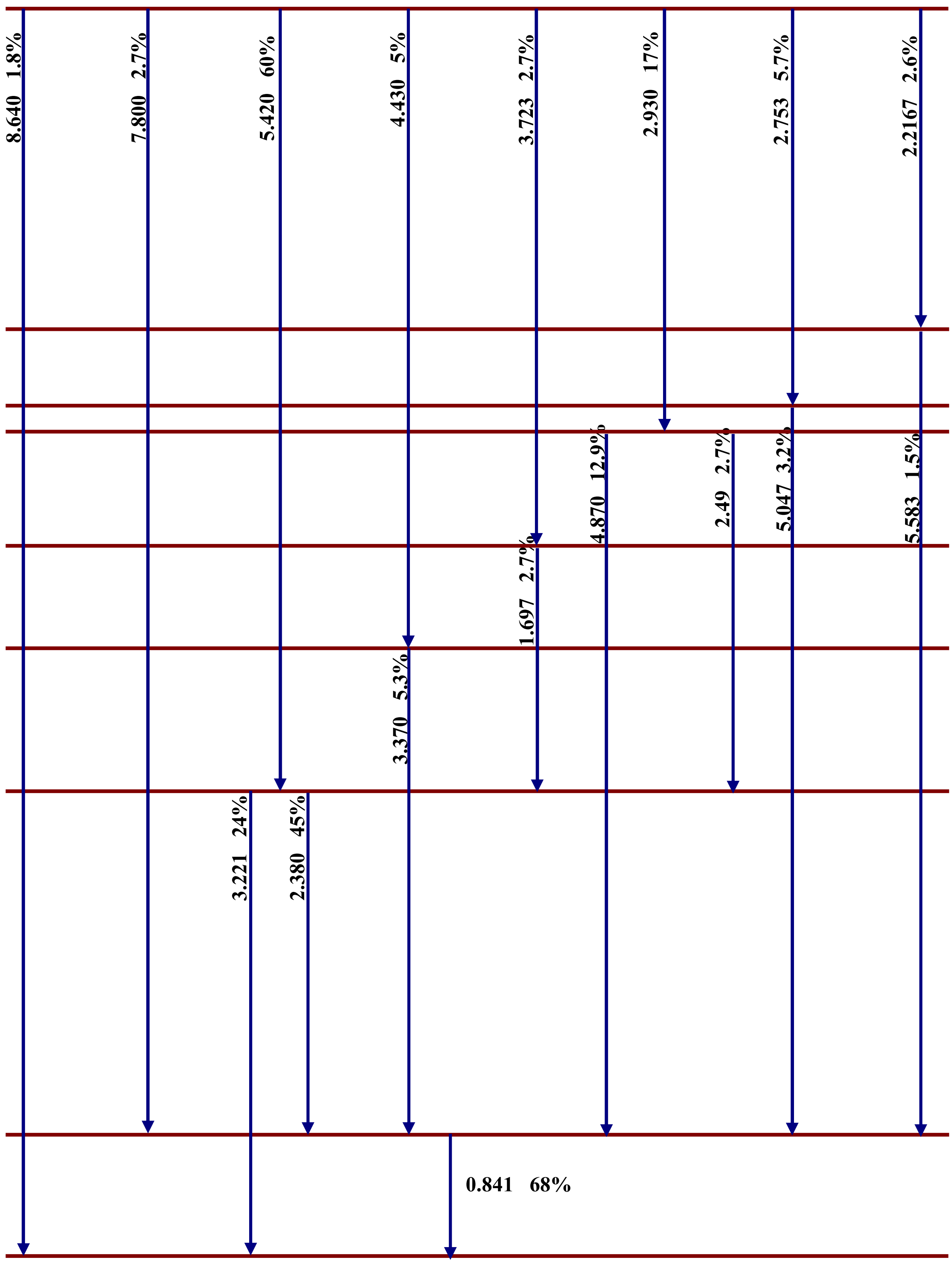

Figure 4-12: Sulfur-33 Gamma Ray Decay Scheme (Q-Value = 8.64165 MeV)

window 1 and window 2. The first window corresponds to the Q-value of the $^{32}S(n,\gamma)^{33}S$ reaction, while the second window corresponds to an energy of 7.800 MeV. The significance of the 7.800 MeV energy will be discussed shortly.

The level scheme that is used to analyze this data (Raman, Carlton, and Wells, 1985) is shown in Figure (4-12), along with the gamma intensities and energies (in MeV). This scheme shows 17 gamma rays out of a total of 103 for ^{33}S. The scheme probabilities deduced from this decay scheme are shown in Table (4-4), where it is shown that approximately 93 % of the transitions in the ^{33}S decay scheme are accounted for.

Table 4-4: Scheme Probabilities for ^{33}S

Scheme	Energies in Scheme (MeV)	Scheme Probability (%)
1	8.640	1.8
2	7.800 – 0.841	3.0
3	5.420 – 3.221	21
4	5.420 – 2.380 - 0.841	39
5	4.430 – 3.370 – 0.841	5.0
6	3.723 – 1.697 – 3.221	1.5
7	3.723 – 1.697 – 2.380 – 0.841	1.5
8	2.930 – 4.870 – 0.841	13
9	2.930 – 2.49 – 3.221	1.5
10	2.930 – 2.49 – 2.380 – 0.841	1.5
11	2.753 – 5.047 – 0.841	3
12	2.216 – 5.583 – 0.841	1.5
Total		**93.3 %**

Before presenting the results of the diagonal summing, the total coincidence spectrum in one of the detectors is shown. This can be obtained by performing the first type of projection (summing) stated earlier. Figure (4-13) shows the result of projecting the whole spectrum to the x-axis, i.e. the total coincidence spectrum in the 5”×5” NaI detector in coincidence with all events in the 6”×6” NaI detector .

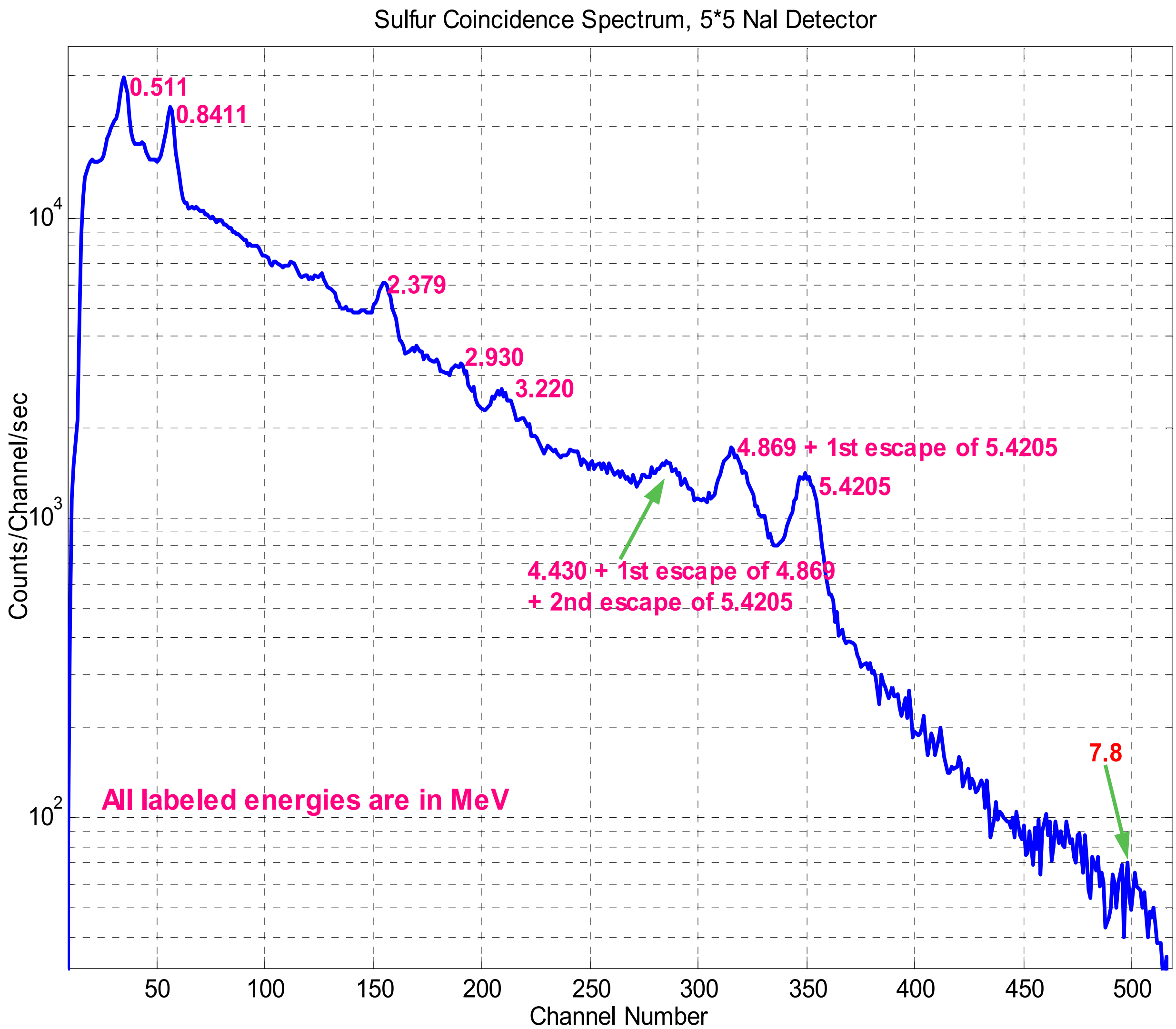

Figure 4-13: Two Dimensional Full Spectrum Projection for Sulfur

Next, we observe the resulting spectrum from performing a diagonal summing. Figure (4-14) shows the projection of "window 1" in Figure (4-11). The energy of that window corresponds to the Q-value of the $^{32}S(n,\gamma)^{33}S$, 8.64 MeV. From Table (4-4), the second and third schemes are the only schemes that contain two gamma rays in them. The energies of the second scheme are 7.800 and 0.841 MeV while those for the third scheme are 5.420 and 3.221 MeV. Thus we expect these four gamma rays to show up clearly when performing Q-value diagonal summing. Figure (4-14) confirms this fact. It also shows that the 5.420 - 3.221 MeV pair are much more intense than the 7.800 - 0.841 MeV pair. This is attributed to the difference in scheme probability.

An early paper by Hoogenboom (1958) demonstrated a hardware approach to obtain spectra that result from a specific sum of gamma ray energies. This approach was shown to greatly improve the peak resolutions over those obtained from a normal singles spectrum. The diagonal summing approach used here enables us to get the same type of spectrum but with much more accuracy and flexibility. Moreover, to examine another Q-value or sum one can simply interrogate the same data with the different diagonal sum by use of a single set of data from the current electronic system (and KmaxNT).

In addition to the improved peak resolution obtained from diagonal summing over the singles spectrum, there is also a noticeable improvement over the total coincidence spectrum. This improvement is enhanced as the energy increases. To illustrate this, Figure (4-15) shows a zoom of the two dimensional (flat) sulfur spectrum. The intense area corresponds to the 0.8411 MeV gamma ray in one detector and the 5.4205 MeV gamma ray in the other detector. Projecting in the vertical direction would yield the 0.8411 MeV peak while projecting in the horizontal direction would yield the 5.4305 MeV peak in the other detector. If the projections were performed on the area confined between the diagonal lines, peaks corresponding to the same energies would result but with improved resolution. The improved resolution is due to the elimination of the area between the horizontal (or vertical) lines and the diagonal lines. This area contributes to the tails of the peak and thus eliminating it results in narrower peak, i.e. better resolution. It also clear from the figure that higher energies are affected more than the lower energies.

Figure (4-16) shows the Q-value diagonal summing spectrum compared with the total coincidence spectrum. The peak resolution improvement is clearly shown.

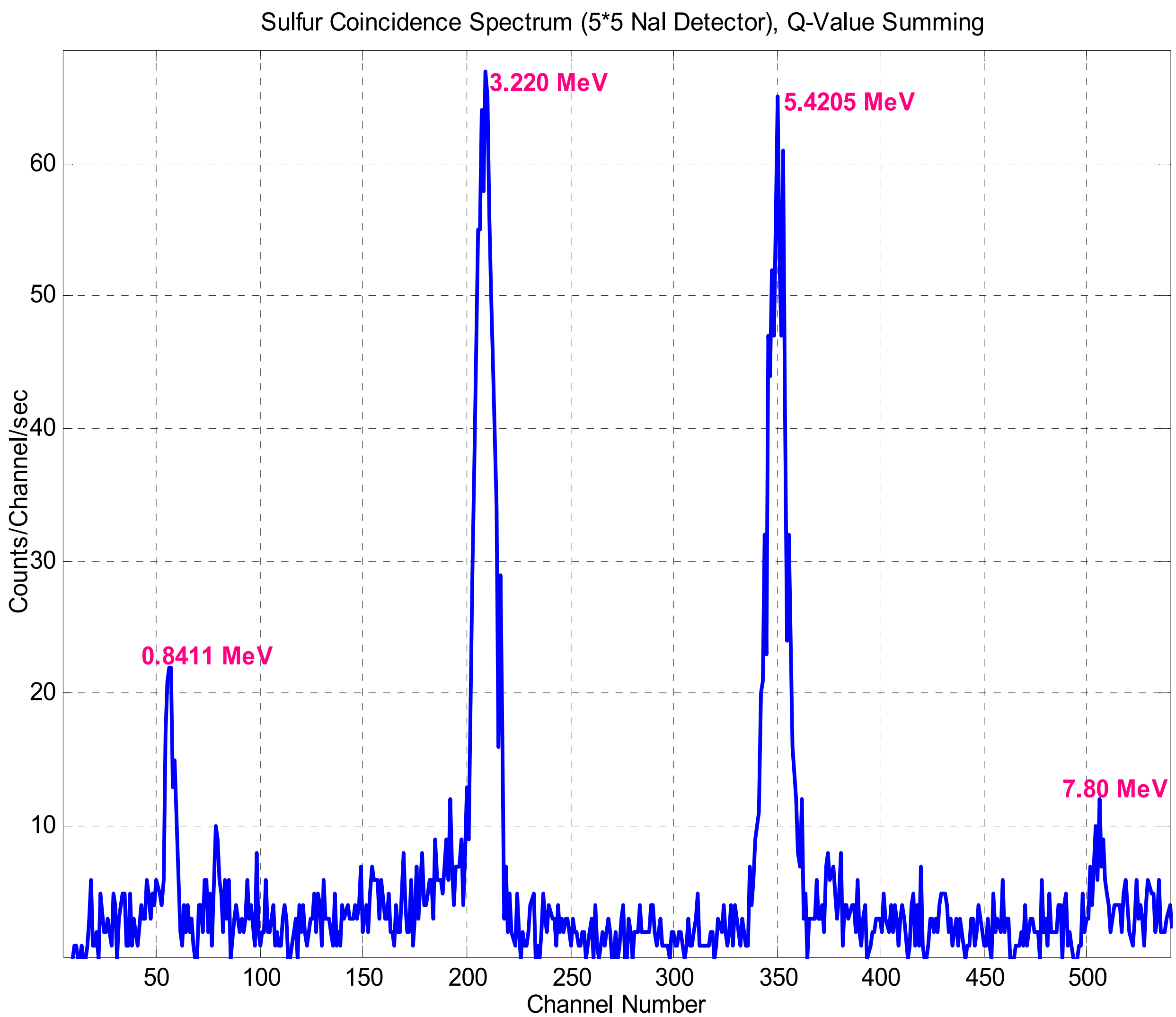

Figure 4-14: Q-Value Diagonal Summing for Sulfur

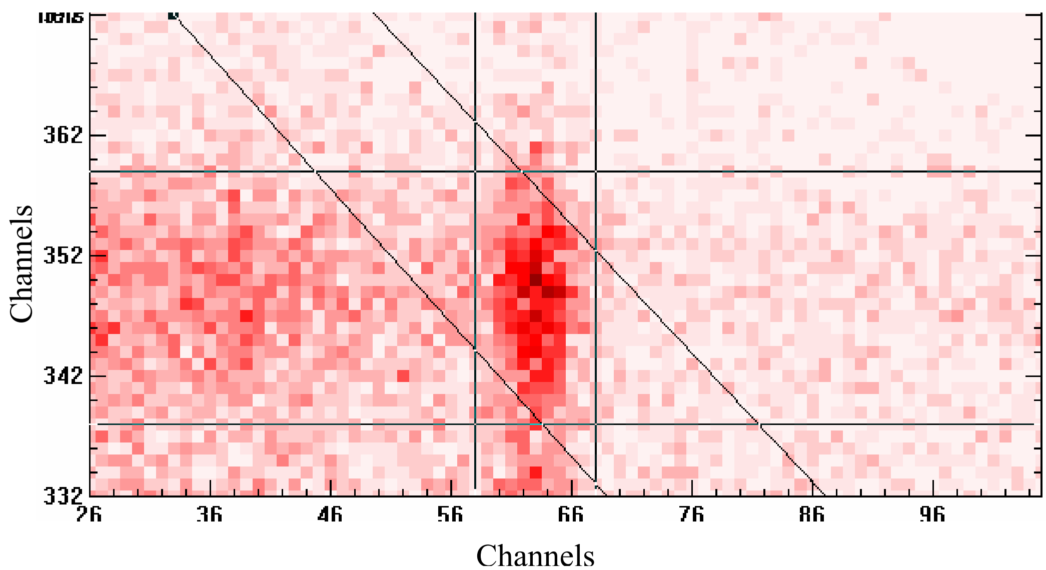

Figure 4-15: Resolution Improvement Due to Diagonal Summing

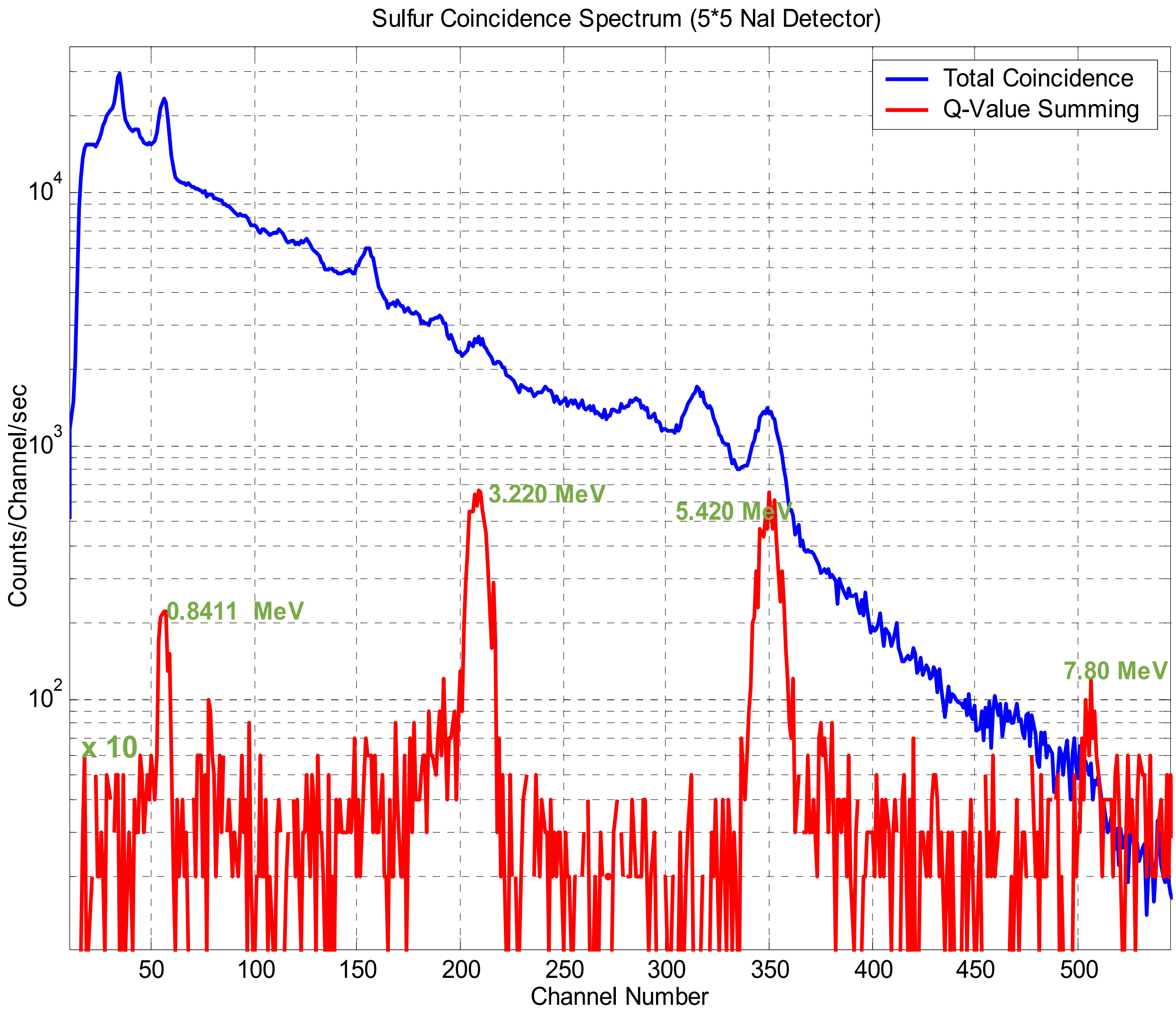

Figure 4-16: Comparison of Total and Diagonal Summing for Sulfur

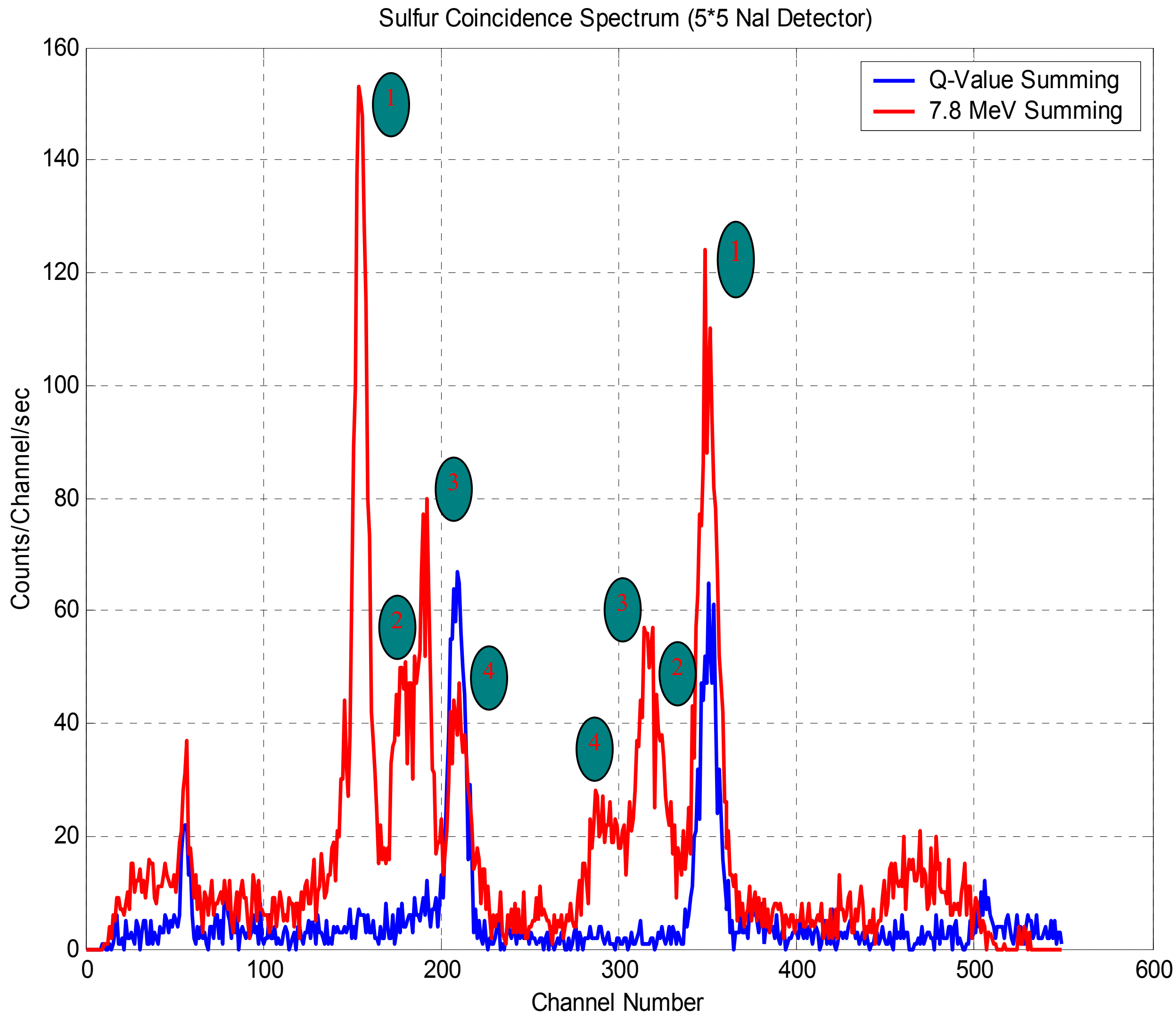

Figure 4-17: Diagonal Summing for Different Energies (Sulfur)

Finally, Figure (4-17) shows Diagonal summing spectra for the Q-value and 7.8 MeV. Observing the decay scheme of ^{33}S, Figure (4-12), one finds several energies that add up to 7.8 MeV. These energies are labeled on Figure (4-17) as pair numbers 1 through 4. The energies corresponding to these pairs are listed in Table (4-5).

Table 4-5: Energies Adding Up To 7.8 MeV in the ^{33}S Decay Scheme

Pair #	Energies in Coincidence (MeV)
1	5.4205 and 2.379
2	5.047 and 2.753
3	4.870 and 2.931
4	5.4205 Compton and 3.22

The second example presented for diagonal summing is for mercury. The PULSTAR thermal neutron beam was utilized in this experiment. The two NaI detectors (5"x5" and 6"x6") were setup facing each other with the sample in between. The sample to detector distance was 20 cm. The sample was natural mercury (12 gm).

Table (4-6) shows the naturally abundant isotopes in Mercury and their characteristics. The factor in the table corresponds to the product of the abundance and the (n,γ) cross section of each isotope. Using this factor, it can be shown that approximately 95% of the (n,γ) interactions will occur with ^{199}Hg isotope. The ^{199}Hg(n,γ)^{200}Hg has a Q-value of 8.028 MeV. This will be the energy used for the diagonal summing.

Figure 4-18 shows the two dimensional plot (flat view) of the counts in both NaI detectors. The outlined diagonal window corresponds to the Q-value of the reaction.

Table 4-6: Isotopes in Natural Mercury and their characteristics

Isotope	Abundance, %	σ_γ (b)	Factor*	Normalized Factor
Hg-196	0.15	3100	465	1.18%
Hg-198	10	1.9	19	4.83E-2%
Hg-199	16.9	2200	37180	94.55%
Hg-200	23.1	60	1386	3.5%
Hg-201	13.2	8	105.6	0.268%
Hg-202	29.8	4.9	146.02	0.371%
Hg-204	6.85	0.4	2.74	6.97E-3%

* **Factor = Abundance x σ**

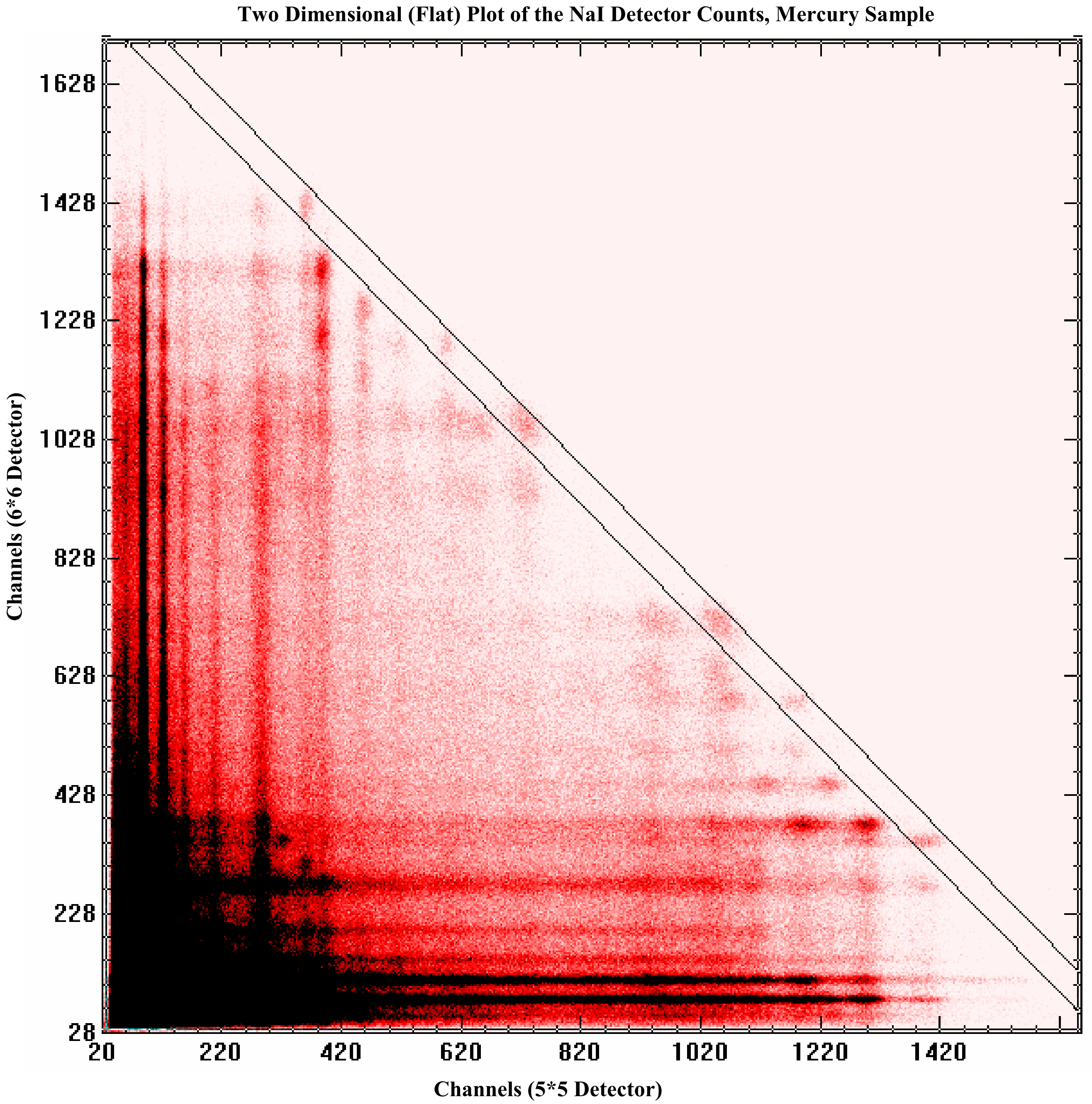

Figure 4-18: Two Dimensional Plot (Flat View) of the Counts in Both NaI Detectors, Mercury Sample

Figure (4-19) shows the Q-value diagonal summing for natural Mercury. The dominant coincidence pairs are labeled on the figure and their corresponding energies are listed in Table (4-6).

Table 4-7: Energies Adding Up To 8.02 MeV in the ^{200}Hg Decay Scheme

Pair #	Energies in Coincidence (MeV)
1	1.571 and 6.457
2	2.639 and 5.387
3	3.288 and 4.739; 3.185 and 4.841

Finally, a comparison between the Q-value diagonal summing spectrum and the total coincidence spectrum is shown in Figure (4-20). The peak resolution improvement is clearly shown.

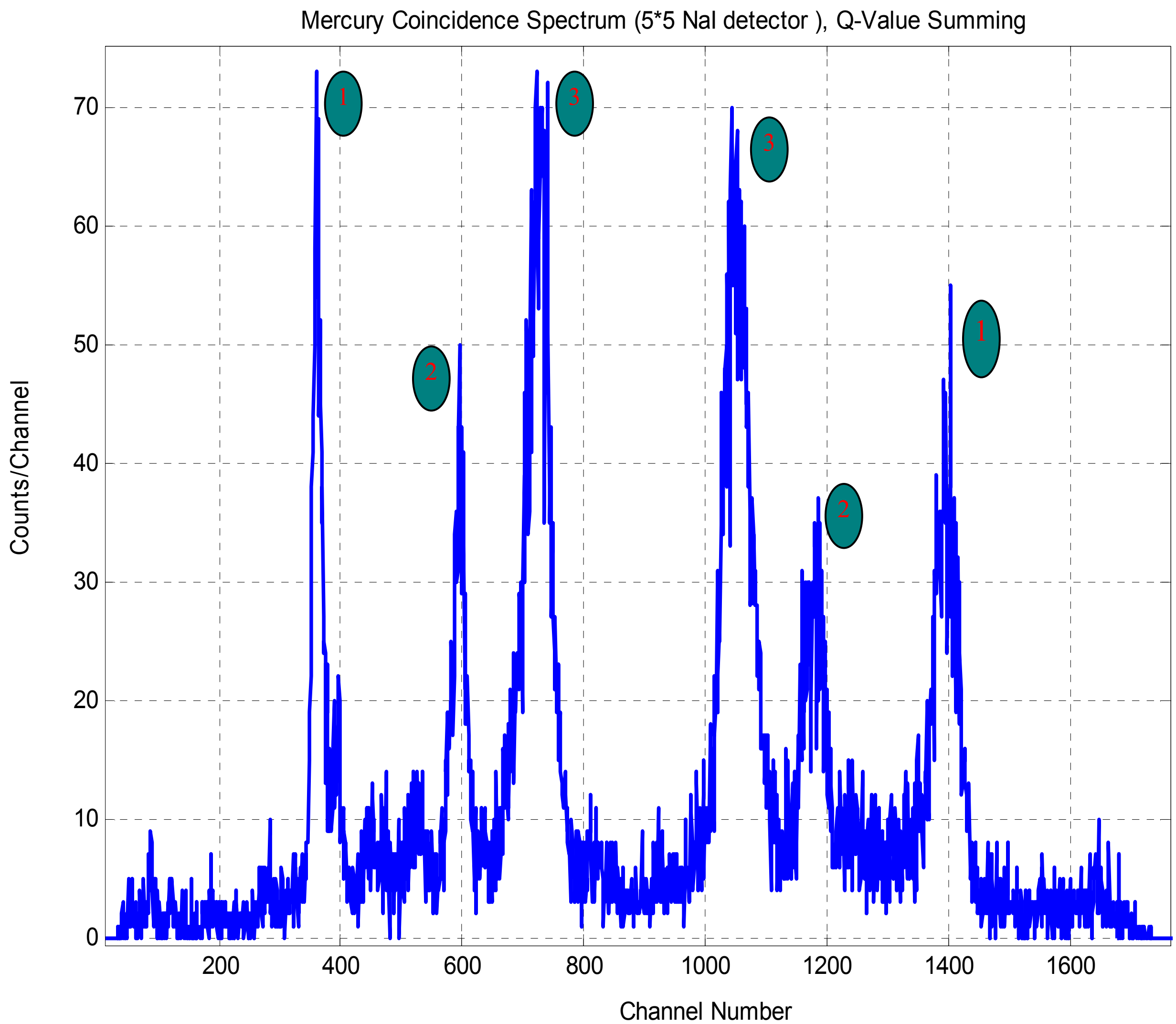

Figure 4-19: Q-value Diagonal Summing for Mercury

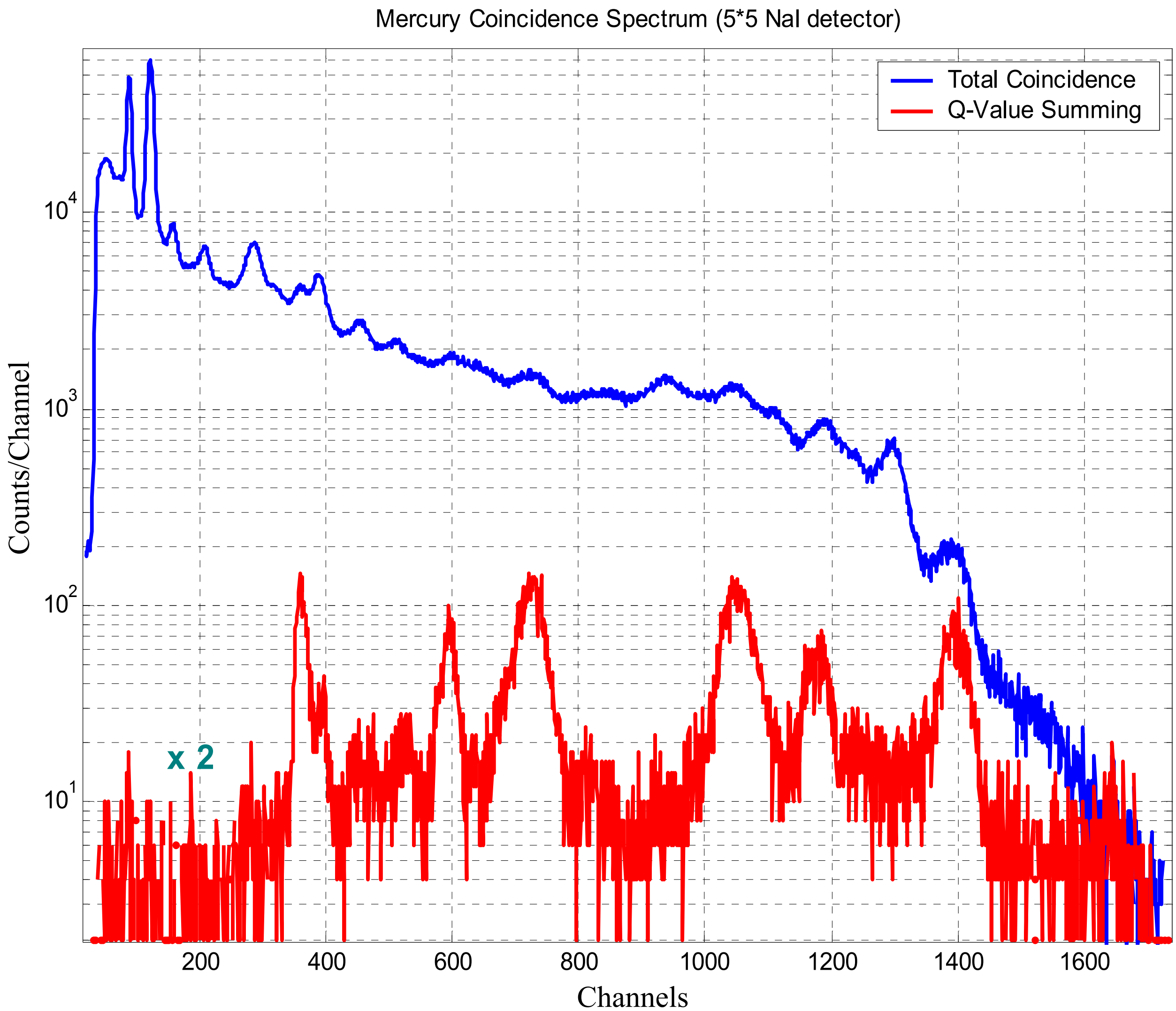

Figure 4-20: Comparison of Full and Diagonal Summing for Mercury

4.3.3. Elemental Analysis Application:

Another application where two dimensional diagonal summing can be used is elemental analysis. To illustrate this, an experimental setup similar to that shown in Figure (3-7) was used. The sample used was coal, approximately 22 Kg, with 100 grams of mercury (powder form) mixed in it. The objective was to try to identify the mercury in the sample.

Figure (4-21) shows the two dimensional plot (flat view) of the counts in both NaI detectors. The outlined diagonal window corresponds to the Q-value of the $^{199}Hg(n,\gamma)^{200}Hg$ reaction, 8.028 MeV.

Figure (4-22) shows the Q-value diagonal summing for outlined window in Figure (4-21). There is a strong resemblance between the obtained spectrum in Figure (4-22) and Figure (4-19), thus proving that mercury could be identified in the coal sample.

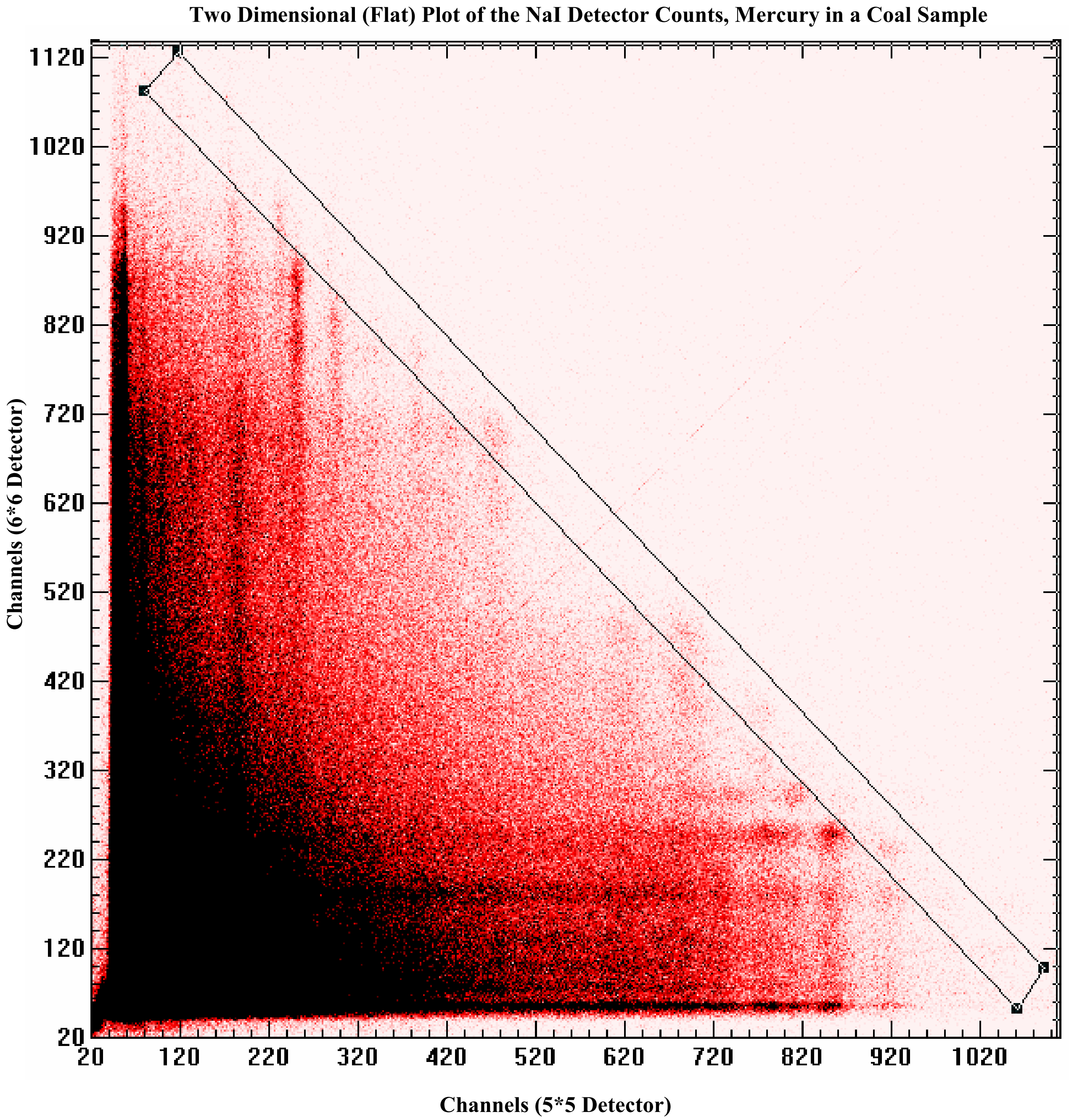

Figure 4-21: Two Dimensional Plot (Flat View) of the Counts in Both NaI Detectors, Mercury in a Coal Sample

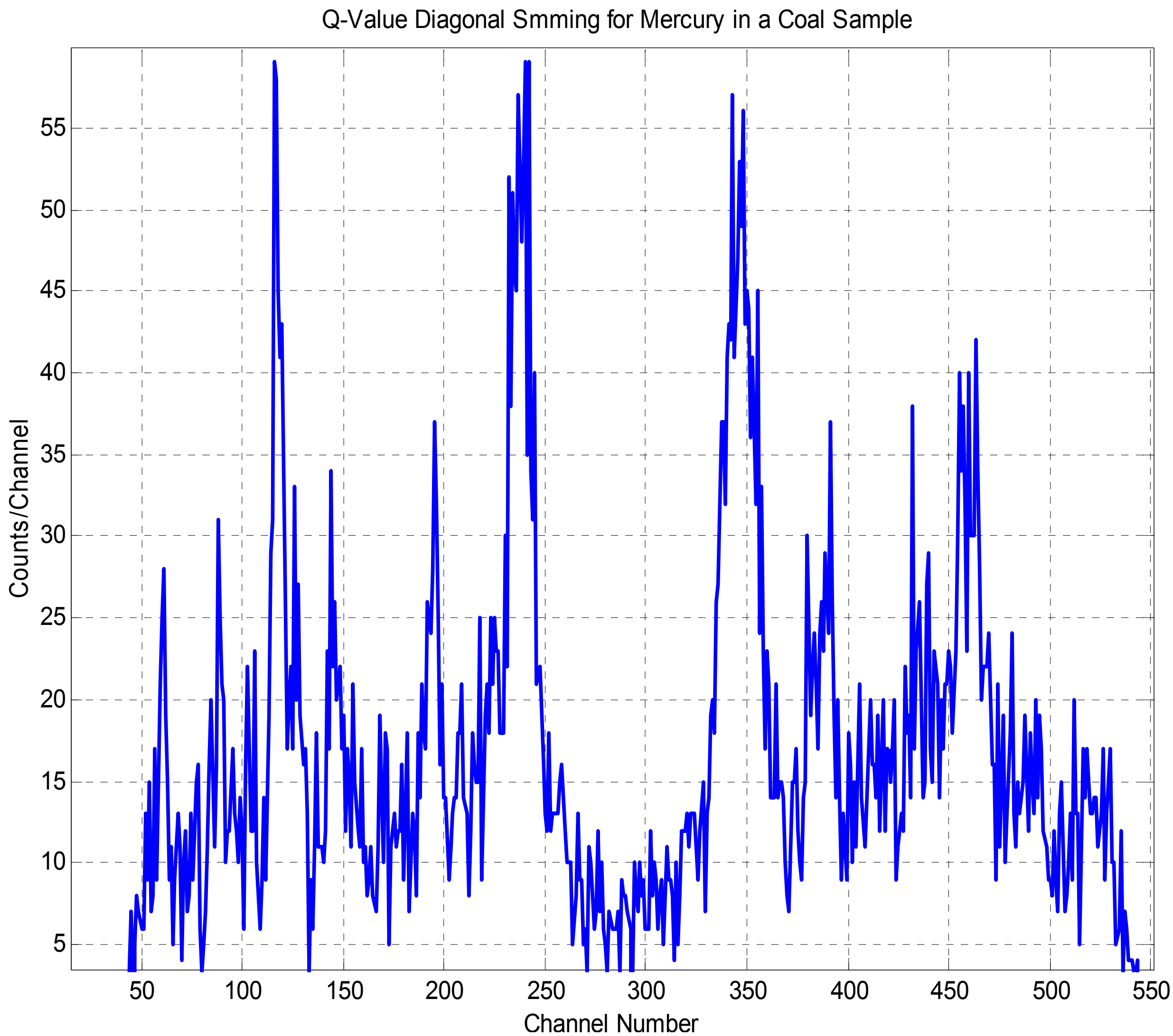

Figure 4-22: Q-value Diagonal Summing for Mercury in a Coal Sample

4.4. New NaI Detector Arrangement:

4.4.1. Introduction and Concept:

Prompt Gamma Neutron Activation Analysis (PGNAA) and Neutron Inelastic Scattering (NIS) techniques have been widely used for measuring elemental composition in bulk samples. They have the advantage of producing high energy (highly penetrating) gamma rays which allow the analysis of large sample volumes. The coal and oil well logging industries are two examples where these techniques are used.

In the oil well logging industry, the logging tool consists of a fast neutron source and one or more radiation detectors at different spacing from the source. The fast neutrons originating from the source undergo collisions with formation elements. These collisions usually result in the emission of inelastic gamma rays and subsequently the slowing down of the neutrons. Upon slowing down, the neutrons may be captured and another set of gamma rays may be emitted. The resulting gamma rays, either before or after neutron slowing down, are detected by the radiation detectors and the resulting spectra are analyzed to obtain information about the elemental amounts in the formation.

Carbon and oxygen are of particular interest in oil well logging. Practically, the most important gamma rays emitted from these elements range from 4.44 to 6.13 MeV. These gamma rays result from the interaction of fast neutrons with these elements. Gamma rays (ranging from 1.6—to 4.8—MeV) resulting from the capture of thermal neutrons by these elements are of lesser importance.

Because of the dimensions of the logging tool, there are limitations on the size of detectors that can be used. These limitations lead to a low detection probability of the high energy gamma rays of interest. A new NaI detector arrangement has been designed to deal with this problem (Gardner and Metwally, in press). The arrangement consists of two NaI detectors, one of which is a well type. The first detector is 1×5 inches and the second is a well type 5 inches long with a wall thickness of 0.35 inches, which gives a hole diameter of one inch. They are assembled together, as shown in Figure (4-23).

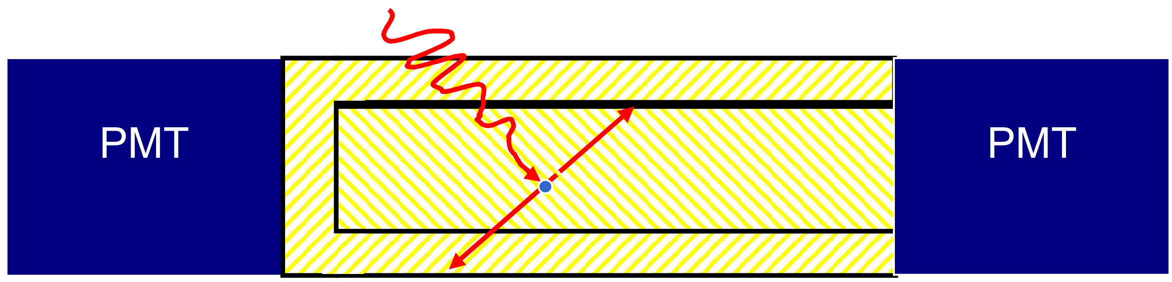

Figure 4-23: The New NaI Detector Arrangement.

The concept behind this arrangement is that an incident gamma ray undergoes an interaction in the inside detector. The probability that this a pair production interaction increases as the incidence gamma ray energy increases. As a consequence of pair production, two 0.511 MeV annihilation gamma rays are emitted in opposite directions. The detector arrangement thus provides approximate 4π geometry for detecting the annihilation gamma rays.

Measuring the coincidence spectrum in both detectors allows us to identify the original gamma ray and thus its source. After obtaining the coincidence spectrum, an offline analysis can be performed to extract different spectra from the two dimensional array. Specifically, we can extract the spectrum in the inside detector that is in coincidence with the 0.511 MeV energy in the well detector. This should result in two peaks in the spectrum, the first and second escape peaks, for every originally incident gamma ray. Feasibility studies are shown in the next section.

All the other coincidence measurements presented in previous sections were used to detect the coincidence spectrum resulting from two or more gamma rays. However, the NaI detector arrangement presented in this section is used to measure the coincidence spectrum resulting from one gamma ray only. This in turn results in numerous energy combinations that would sum up to the original gamma ray energy. The implications of this will be shown in the next section.

4.4.2. Feasibility Studies:

Feasibility studies were performed for the new NaI detector arrangement. The first study was made using radioactive sources. The second study was made using the PULSTAR thermal neutron beam and a sulfur sample.

4.4.2.1 Sodium-24 Study:

The first feasibility study was made using a ^{24}Na radioactive source. ^{24}Na decays by emitting two well separated gamma rays of energies 1.368 and 2.754 MeV. Both of these gamma ray energies are above the threshold (1.02 MeV) of the pair production effect and thus provide a good test for the detectors.

The source was placed approximately 10 cm away from the center of the detectors, along their sides. This is a normal source-detector setup for oil well logging applications where the gamma rays are incident on the side of the detector. Figure (4-24) shows obtained the singles and the total coincidence spectra. Two observations can be immediately made regarding the figure;

1. The total coincidence spectrum is approximately 2-3 times lower than the singles spectrum. This is a great improvement over the coincidence spectra obtained with two separated detectors where the coincidence spectrum was approximately 2-3 orders of magnitude lower than the singles spectrum. This improvement is due to the fact that only one gamma ray is being detected instead of multiple gamma rays. This provides a higher detection probability.
2. The total coincidence spectrum does not provide us with new information that can help in identifying the original gamma ray energies. On the contrary, we lose information. This again can be explained by the fact that we are detecting only one gamma ray in coincidence. Thus, we not only lose the full energy peak but also obtain numerous energy combinations that sum up to it.

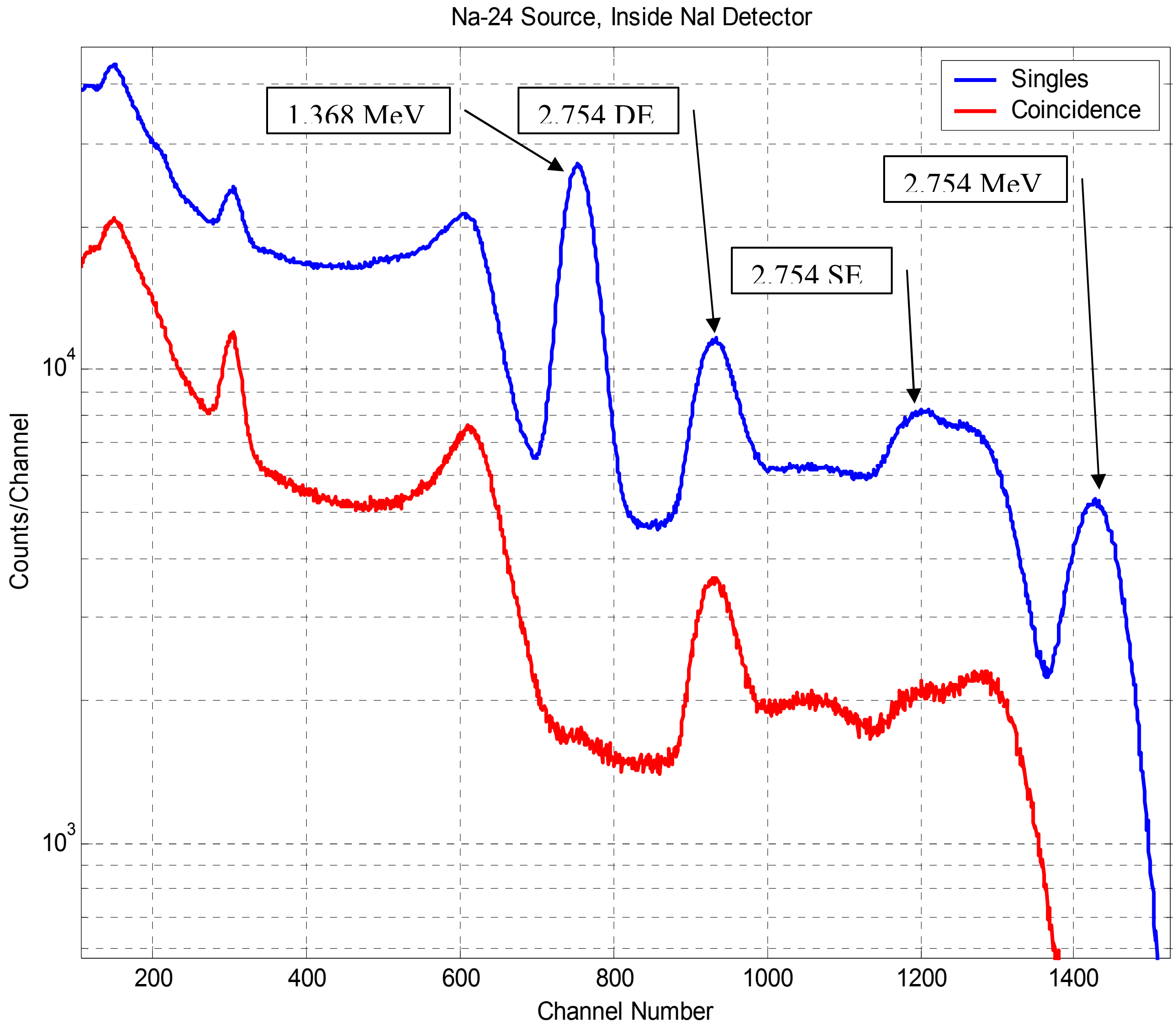

Figure 4-24: Singles and Coincidence Spectra in the Inside Detector, Na-24

Before proceeding further to show the benefits gained from this detector arrangement, it is important to show the two dimensional spectrum and explain the main features in it. Figure 4-25 shows the obtained two dimensional spectrum obtained when using the Na-24 source. The most important features are shown on the figure and explained in Table 4-8.

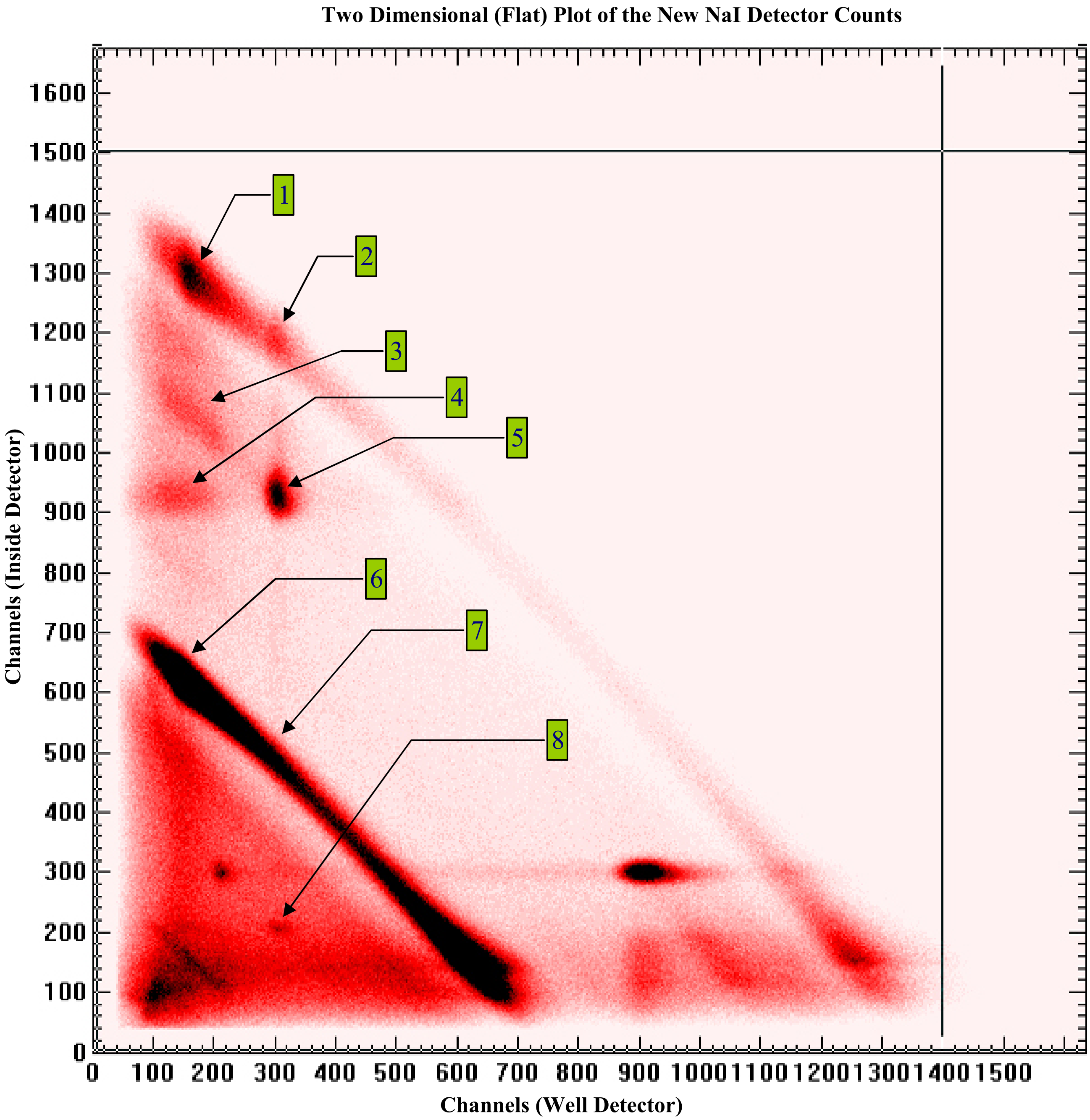

Figure 4-25: Two Dimensional Spectrum Using the New NaI Detector Arrangement, Na-24

Table 4-8: Na-24 Two Dimensional Spectrum Features Using the New NaI Detector Arrangement

#	Peaks Correspond to in the		Comment
	Well Detector	**Inside Detector**	
[1]	Backscatter gamma	Compton Edge of the 2.754 MeV gamma ray	The spread around the peak is caused by the wide range of angles that the gamma ray can scatter through, not just 180 degrees
[2]	0.511 MeV Annihilation gamma ray	Single escape of the 2.754 MeV gamma ray	Note how this feature and the first feature fall on the same diagonal line. This line corresponds to the 2.754 MeV sum.
[3]	Low energy gamma rays	High energy gamma rays, below the Compton Edge and above the double escape of the 2.754 MeV gamma ray	This feature lies on a diagonal line. This means that it corresponds to a certain energy sum, the double escape of the 2.754 MeV gamma ray. This feature is observed because of the partial energy deposition of the 0.511 MeV annihilation gamma ray in the inside detector before being completely detected by the Well detector
[4]	Low energy gamma rays	Double escape of the 2.754 MeV gamma ray	This feature is similar to the third feature except that there is no energy deposition in the inside detector by the 0.511 MeV annihilation gamma ray, only in the Well detector
[5]	0.511 MeV Annihilation gamma ray	Double escape of the 2.754 MeV gamma ray	The diagonal line joining this feature and the third feature corresponds to the Single escape energy sum of the 2.754 MeV gamma ray.
[6]	Backscatter gamma	Compton Edge of the 1.368 MeV gamma ray	Same comment as first feature.
[7]	0.511 MeV Annihilation gamma ray	Single escape of the 1.368 MeV gamma ray	Same comment as second feature, but for the 1.368 MeV gamma ray.
[8]	0.511 MeV Annihilation gamma ray	Double escape of the 1.368 MeV gamma ray	Same comment as fifth feature, but for the 1.368 MeV gamma ray.

After observing the different features in the two dimensional spectrum, we can perform different projections and observe the resulting spectra. The first projection is a vertical one corresponding to the 0.511 MeV energy range in the Well detector. This is shown in Figure 4-26. For comparison purposes, the singles and total coincidence spectra are shown on the same figure. It can be seen clearly that the escape peaks of the 2.754 MeV and the 1.368 MeV gamma rays appear with a high signal to noise ratio. Note that the 0.511 MeV coincidence spectrum is almost an order of magnitude less than the singles spectrum. This is still a big improvement over the two separated detector configuration. This is an example of a useful spectrum in practical applications.

Figure 4-27 shows the two diagonal summing spectra corresponding to the full energies of the 1.368 MeV and 2.754 MeV gamma rays. The shape of the spectra can be explained by the comments on the first and second features in Table 4-8. Although there are no distinct peaks in the spectra presented in Figure(4-27), one can still make use of this "V-shaped" data. This data would work very well in Library Least Squares (LLS) analysis as it has a definite shape to it that is unique. Also note that this type of data is almost the same intensity as the total coincidence on the right hand (high energy) side of the spectrum.

Figure 4-28 shows the two diagonal summing spectra corresponding to the single escapes of the 1.368 MeV and 2.754 MeV gamma rays. The shape of the spectra can be explained by the comments on the third and fifth features in Table 4-8. This is another example of a useful spectrum. For comparison purposes, the 0.511 MeV coincidence spectrum and the 2.754 SE diagonal summing spectrum are shown in Figure 4-29.

The spectra extracted from the Well detector are almost similar to those from the Inside detector for this energy range. Practically, we cannot use these spectra for the following reasons:

1) The Well detector has a NaI base. This base yields a higher light collection than the sides of the detector. This results in "Double Peaks" in the spectrum where each distinct gamma energy is represented by two peaks in the spectrum.
2) The detection efficiency of the Well detector is extremely low for high energy gamma rays. This is a typical consequence of the size of the Well detector.

Examples of the spectra obtained from the Well detector are shown in Figure 4-30. Two peaks that correspond to the 2.754 MeV gamma ray can be seen in the singles spectrum in approximately channels 1380 and 1510.

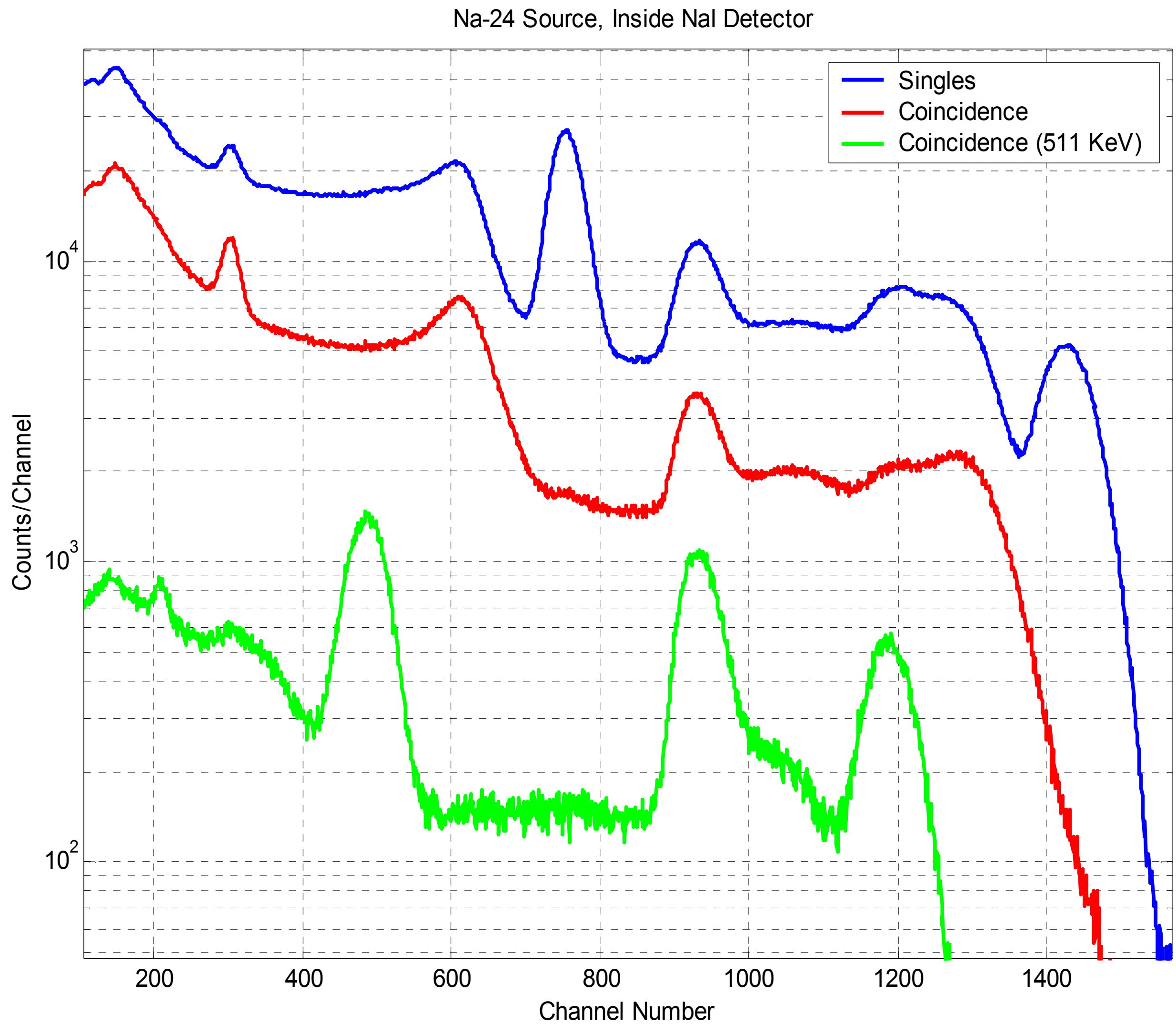

Figure 4-26: Singles, Total Coincidence, and 0.511 MeV Coincidence Spectra in the Inside Detector

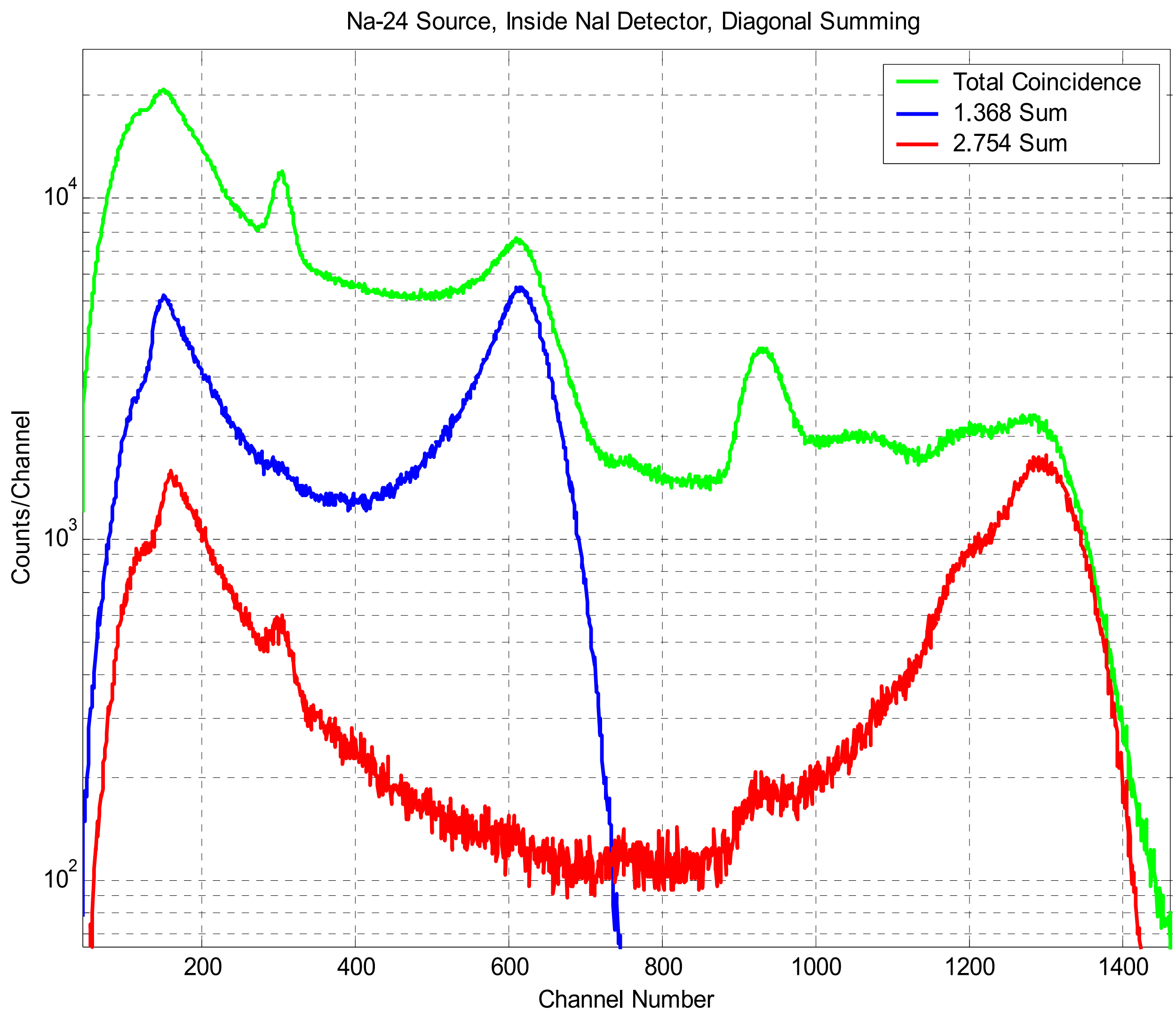

Figure 4-27: 1.368 MeV and 2.754 MeV Diagonal Summing in the Inside Detector.

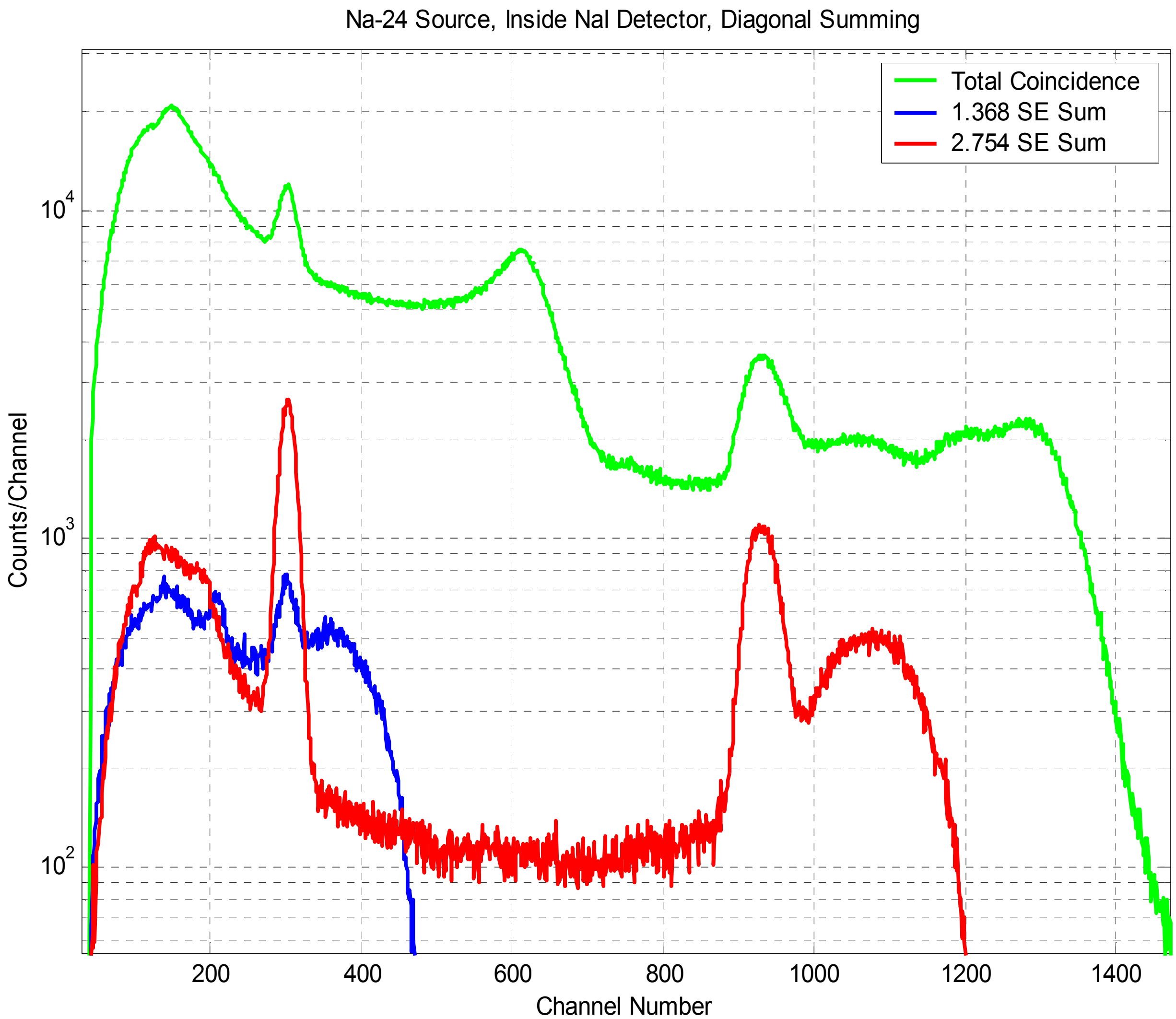

Figure 4-28: 1.368 SE MeV and 2.754 SE MeV Diagonal Summing in the Inside Detector.

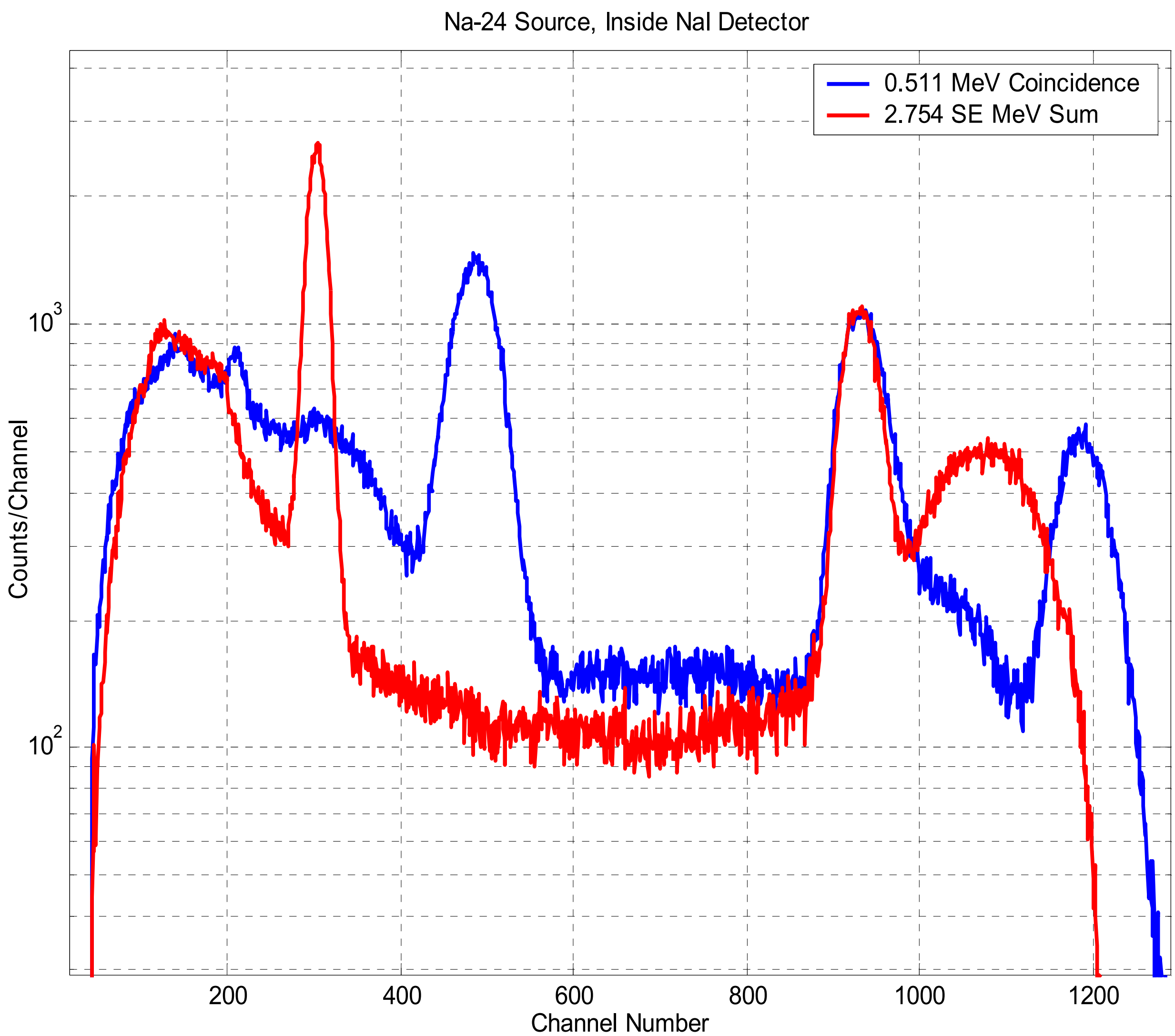

Figure 4-29: 0.511 MeV Coincidence and 2.754 SE MeV Sum Spectra

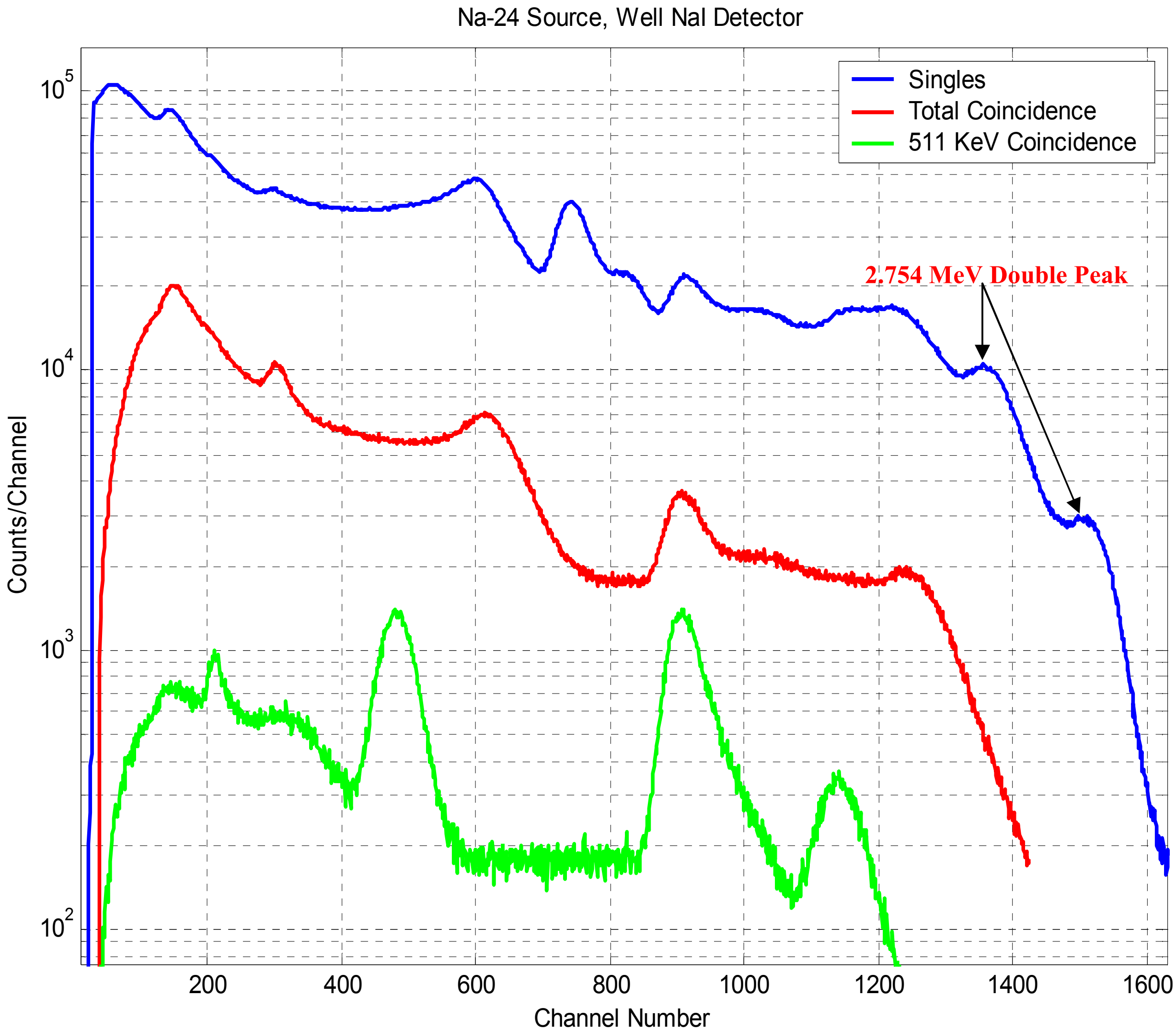

Figure 4-30: Singles, Total Coincidence, and 0.511 MeV Coincidence Spectra in the Well Detector

4.4.2.2 Sulfur Study:

The second feasibility study was made using a natural sulfur sample and the PULSTAR thermal neutron beam. The sample was placed approximately 25 cm away from the center of the detectors, along their side. The main isotope in natural sulfur is ^{32}S which, when activated by neutrons to $^{33*}S$, promptly decays by emitting gamma rays with a wide energy range (Figure 4-12).

In this application, we will concentrate on the 5.4205 MeV gamma ray resulting from the decay of $^{33*}S$. The reason is that the 5.4205 MeV gamma ray falls in the energy range of interest for oil well logging applications.

Figure 4-31 shows the singles, total coincidence, and 0.511 MeV coincidence spectra in the inside detector. Note how the escape peaks of the 5.4205 MeV gamma ray show up clearly in the 0.511 MeV coincidence spectrum. Note also that the escape peaks of the hydrogen 2.223 MeV gamma ray also show in the spectrum. This should not be a concern as this detector arrangement is intended to be used to detect higher energy gamma rays than the hydrogen gamma ray.

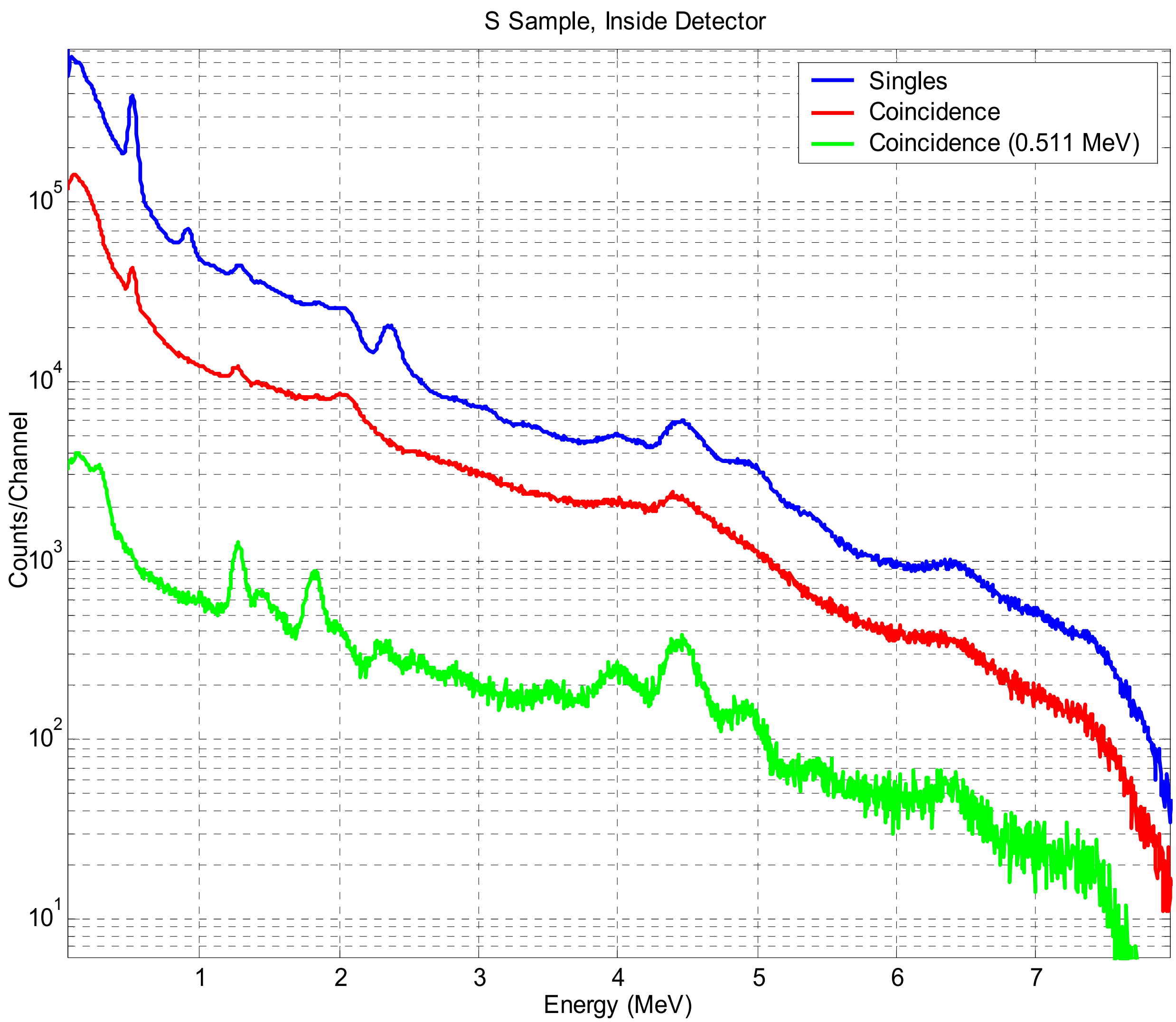

Figure 4-31: Singles, Total Coincidence, and 0.511 MeV Coincidence Spectra in the Inside Detector, Sulfur Sample.

5. Monte Carlo Simulation: The CEARPGA Code:

5.1. Introduction and History:

The CEARPGA is a specific purpose Monte Carlo code, developed at the Center for Engineering Applications of Radioisotopes (CEAR) of North Carolina State University, for modeling the spectral response of Prompt Gamma-Ray Neutron Activation Analysis (PGNAA) systems. Before explaining the features of this code, it is important to point out the motivation behind this code development and its different development stages.

In many situations, it is desirable to perform elemental analysis for bulk materials such as coal and concrete. A common mathematical approach to perform this analysis (in conjunction with PGNAA) is the Library Least Squares approach (LLS) (Marshall and Zumberge, 1989). The LLS approach is based on the assumption that any unknown sample spectrum is the sum of the products of the elemental amount and the library spectrum of each element for every channel. This sum is given by:

$$y_i = \sum_{j=1}^{m} x_j a_{ij} + e_i \qquad , \boldsymbol{i} = 1,2,3,...,\boldsymbol{n}$$

Where:

y_i - count rate in channel i for the unknown sample spectrum,

x_j - amount of component j in the unknown sample,

a_{ij} - count rate in channel i for component j (library spectrum of component j), and

e_i - random error in channel i due to statistical counting rate fluctuations.

A set of linear equations can be generated from Equation (5.1). The linear equations can be solved for x_j through minimizing the corresponding reduced Chi-square χ^2_υ, which is given by;

$$\chi_{\upsilon}^{2} = \sum_{i=1}^{n} \frac{e_i^2}{(n-m)\sigma_i^2}$$

Where:

(n-m) - number of degrees of freedom, and

σ_i^2 - variance of the random error in each channel.

The LLS approach has the advantage of using all of the available spectral data and being capable of analyzing spectra with unresolved peaks. However, in applying the LLS approach, the elemental library spectra, a_{ij} , must be available. These spectra will vary from one sample to the other due to the matrix effects, sample density, sample moisture, etc. Two approaches were introduced to overcome this problem;

1. Experimentally, the spiking technique, and
2. Simulation, The Monte Carlo Library Least-Squares (MCLLs) method.

The spiking approach is implemented by adding to the sample of interest known amounts of individual elements and then taking the difference of the measured total gamma-ray spectra with and without the spiked amount (Shyu 1991). The disadvantage of this approach is that it requires a large number of samples of known composition to obtain good results (Marshall and Zumberge, 1989). Each sample composition usually requires a separate experiment for each element. Therefore, it is a time-consuming and costly procedure.

The Monte Carlo Library Least-Squares (MCLLs) method (Shyu, 1991, Shyu, Gardner and Verghese, 1993, Gardner, 2000) is based on a Monte Carlo simulation to generate the elemental library spectra, thus avoiding most of experimental work. The MCLLS method is implemented through the following algorithm:

1. Use the Monte Carlo Code to generate the elemental library spectra for a known sample with assumed composition.

2. Use the linear library least-squares analysis method to obtain the elemental amounts in the unknown sample or samples for which the complete spectral response has been measured.

3. Compare the calculated elemental amounts for the unknown sample with those assumed for the Monte Carlo calculation. If they are close enough, this is the final result. Otherwise another iteration of these steps is required, starting with the sample composition estimated from the last iteration.

The CEARPGA code was originally developed to generate the elemental library spectra needed to implement the MCLLS method. The code incorporated a variety of variance reduction techniques to improve calculation efficiency such as forcing all prompt gamma rays to be emitted after a neutron interaction (stratified sampling), using the expected value splitting (EVS) technique to increase the score probability of each tracked gamma ray, using the correlated sampling method to deal with small variations of sample compositions, and using a detector response function to convert the incident gamma-ray spectra on the detector to pulse height spectra. While this code is efficient and accurate, it suffers from the big weight problem in which a few histories yield very large weights with very large variances. The big weight problem was found to be caused primarily by the expected value splitting technique used for tracking gamma rays (Shyu, 1991). Recently, (Zhang W., 2002) the Analog Linear Interpolation (ALI) approach was implemented in the CEARPGA code to overcome this big weight problem. The ALI approach and other improvements made to the CEARPGA code will be discussed in the following section.

5.2. The Analog Linear Interpolation (ALI) Approach:

The ALI approach (Zhang, 2002) is a combination of the analog Monte Carlo simulation method and a linear interpolation technique and is mainly employed to track prompt gamma rays emitted from neutron capture interactions in the sample. In this approach a set of *pseudo* gamma rays that represent the actual prompt gamma rays are first tracked by analog Monte Carlo to establish a set of energy-score tables. Later the linear interpolation approach is used to derive any incident prompt gamma-ray spectrum of interest, based on the energy-score tables. The procedure of implementing the ALI approach consists of the following steps:

1. Choosing the number and energy of the *pseudo* gamma rays

   Instead of tracking all prompt gamma rays emitted from the neutron capture interactions in the sample of interest, only a set of *pseudo* gamma rays are selected and tracked as representatives of all the prompt gamma rays. The *pseudo* gamma rays should cover the energy range of the actual prompt gamma rays so that interpolation can be used later. Currently, there are 24 pseudo gamma ray energies used, ranging from 0.5 to 12 MeV.

2. Determining the number of gamma rays to sample

   The number of gamma rays sampled for each energy is determined by trial and error to give optimum statistics.

3. Tracking pseudo gamma rays

Each *pseudo* gamma ray is tracked starting from the site of the current neutron radiative capture interaction by the analog Monte Carlo approach, except that the photoelectric absorption is sampled implicitly.

4. Tallying the scores of *pseudo* gamma rays

The magnitude of the score that a *pseudo* gamma ray has is the product of its weight accumulated along its track to the detector and detector efficiency. The scores of incident gamma rays are recorded to a set of energy-score tables based on both *pseudo* gamma-ray energy and the incident energy. The energy-score tables are of two dimensions, with one dimension representing the energy of incident gamma rays and the other representing the total scores of incident gamma rays in the previous histories. The score scheme for pair production annihilation photons takes into account the cases that both photons score simultaneously and each independently.

5. Calculating average neutron capture macroscopic cross sections

For each element in the sample, the average neutron capture macroscopic cross section needs to be calculated during the process of simulation and is used later to adjust its interpolated incident gamma-ray spectrum. For the i^{th} element in the sample region, the average cross section, $\mu^{i}_{(n,r)}$ is calculated according to the following formula:

$$\mu^{i}_{(n,r)} = \frac{\sum w^{i}_{j} \mu^{j}_{i}}{\sum_{j} w^{j}_{i}}$$

where μ_j^i is the neutron radiative capture macroscopic cross section of element i for the j^{th} neutron capture interaction in the sample, w_j^i is the weight factor of the neutron in the j^{th} neutron capture interaction .

6. Interpolating the spectra for all gamma rays of interest

   Incident spectra of gamma rays resulting from neutron capture interactions and radioisotope decays in the sample are obtained through linear interpolation at the end of the whole Monte Carlo simulation when a set of energy-score tables has been established. For the full energy channel of the gamma ray to be interpolated, the scores from the corresponding full energy channels of the pseudo gamma rays are used for interpolation. For other channels, the scores from the same channels are used.

In addition to the ALI approach, some other improvements to the CEARPGA code have been introduced, including (1) adopting the latest photon cross-section data, (2) using an improved detector response function, (3) adding the neutron activation backgrounds, (4) generating the individual natural background libraries, (5) adding the tracking of annihilation photons from pair production interactions outside of the detector, and (6) adopting a general geometry package.

5.3. Coincidence Counting Using the CEARPGA Code:

The ALI approach was implemented in calculating the coincidence spectra resulting from different elements. Thus, the latest version of the CEARPGA code, with a few additional calculations, was used for this purpose. The procedure for calculating the coincidence spectra consists of the following steps:

1. Interpolating the spectra for all gamma rays of interest ,

   After establishing the score tables of the pseudo gamma rays, we obtain the score tables of the gamma energies of interest by linear interpolation. These score tables are saved in separate files for further calculations.

2. Accounting for the coincidence schemes and geometry effects,

   The coincidence decay schemes and their probabilities for the element of interest are assumed and fed into a FORTRAN program. In the program, a scheme is chosen according to its probability. Once a scheme is chosen, the gamma rays are tracked according to their decay order. If two gamma rays are incident on the given detector geometries, their corresponding score is incremented. Cases where there is angular correlation between gamma rays can also be dealt with in this program.

3. Generating the coincidence spectrum;

   The coincidence spectrum is generated by multiplying the obtained gamma ray score from step 2 by the corresponding score table from step 1.

The previous procedure was implemented to obtain coincidence spectra. Unfortunately, it did not yield good results. To illustrate this, an experiment was conducted using a Co-60 source. The source was placed in a coal sample of similar dimensions as that used in the CEARPGA code to provide a scattering medium for the gamma rays. The NaI detectors were placed side by side with the coal sample above them.

The CEARPGA code was run for a coal sample and interpolation for the Co-60 1.173 and 1.3325 MeV was made. The simulated spectrum was calculated via the steps stated above. Figure (5.1) shows the results of the experimental and simulated spectra. Also included in the figure is the detector response to the individual Co-60 gamma rays.

Comparing the simulated spectrum with the experimental spectra, one finds that the current simulation methodology overestimates the coincident scattered gamma rays (coincident Compton continuum). This sort of behavior can have a large effect when more complicated coincidence decay schemes are involved. In general, one can summarize the reasons for the unsuccessful simulation results as follows;

1. The coincident Compton scattered gamma rays were incorrectly accounted for. This had a tremendous effect on more complicated decay schemes where there is a wide energy range. The effect of this is reflected on the energy range below the full energy peak. This can be verified by observing that the most intense coincidence region in the two dimensional spectra (Figure 4-11 and Figure 4-18) corresponds to low energies.
2. The "cross talk" between the detectors was not accounted for. This includes;
   a. Coincidences between the 0.511 MeV peak and the escape peaks;
   b. Coincidences between the backscatter peaks and the Compton edges; and
   c. General coincidences of a scattered gamma ray from one detector to the other.
3. Pulse pile up and true summing was not accounted for.

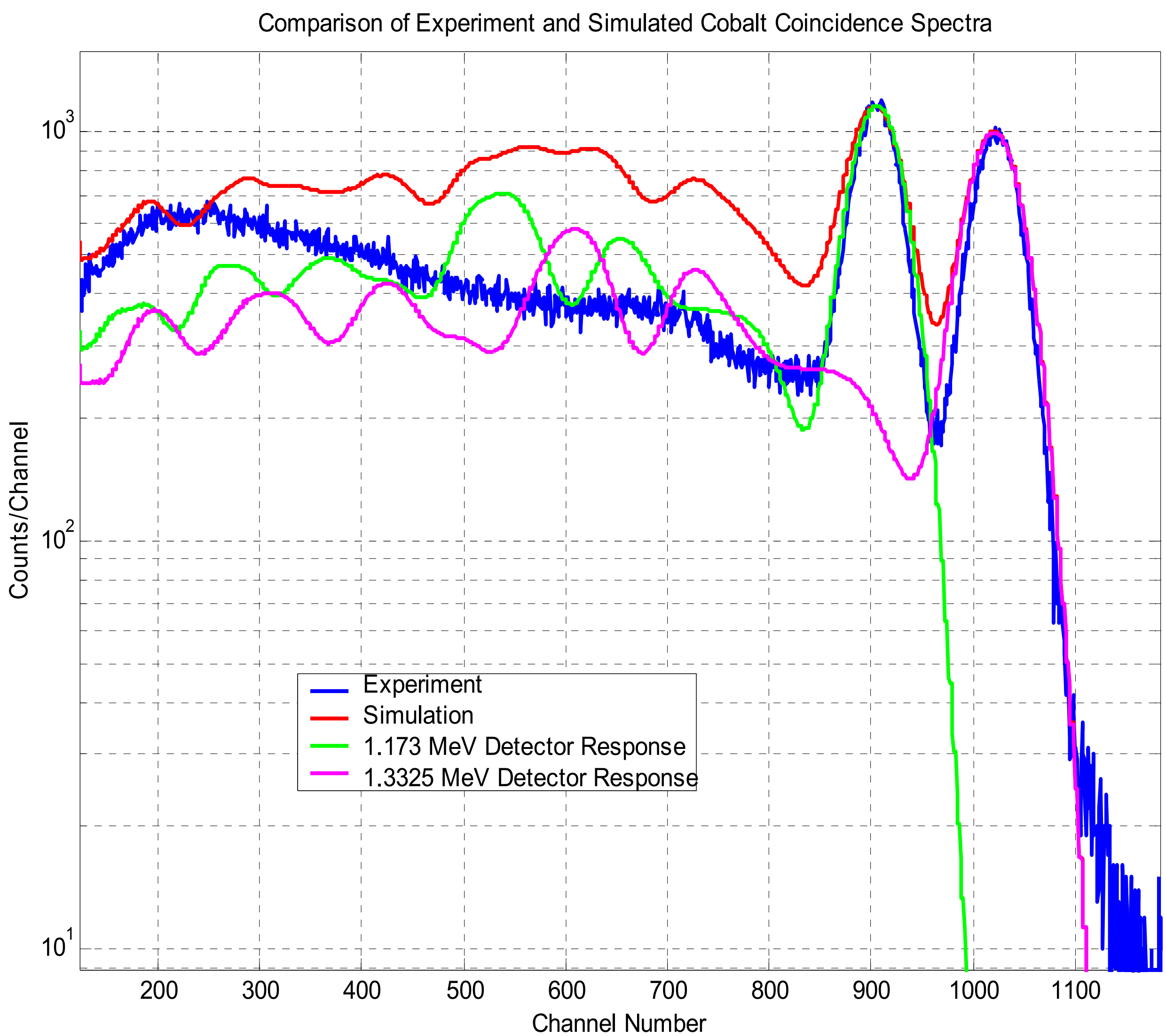

Figure 5-1: Comparison of Experiment and Simulated Co-60 Coincidence Spectra

We intend to continue pursuing the simulation of gamma-gamma coincidence spectra. The current CEARPGA code will still be used for this purpose, but without the ALI approach. This would require some modifications to the CEARPGA code, namely;

1. Adding another detector cell in the problem geometry;
2. Randomly choosing a decay scheme at the neutron interaction site and sampling all the gamma rays in that scheme;
3. Defining a coincidence event if there is energy deposited in both detectors; and
4. Accumulating a total and an elemental library spectrum.

Figure (5.2) shows a flowchart of the suggested modifications to the CEARPGA code. Note that this flow chart prevents sampling more than one gamma ray in a single detector. To take this into account, one would simply sample all the gammas in the scheme and, at the end of the simulation, observe if there were any gamma rays incident on both detectors. If so, the incident energies in the corresponding detectors would be recorded.

An efficient variance reduction technique that can be used in the simulation is Stratified Sampling. This would applied by sampling all the decay schemes at the interaction point, with the appropriate weight, instead of randomly choosing one scheme.

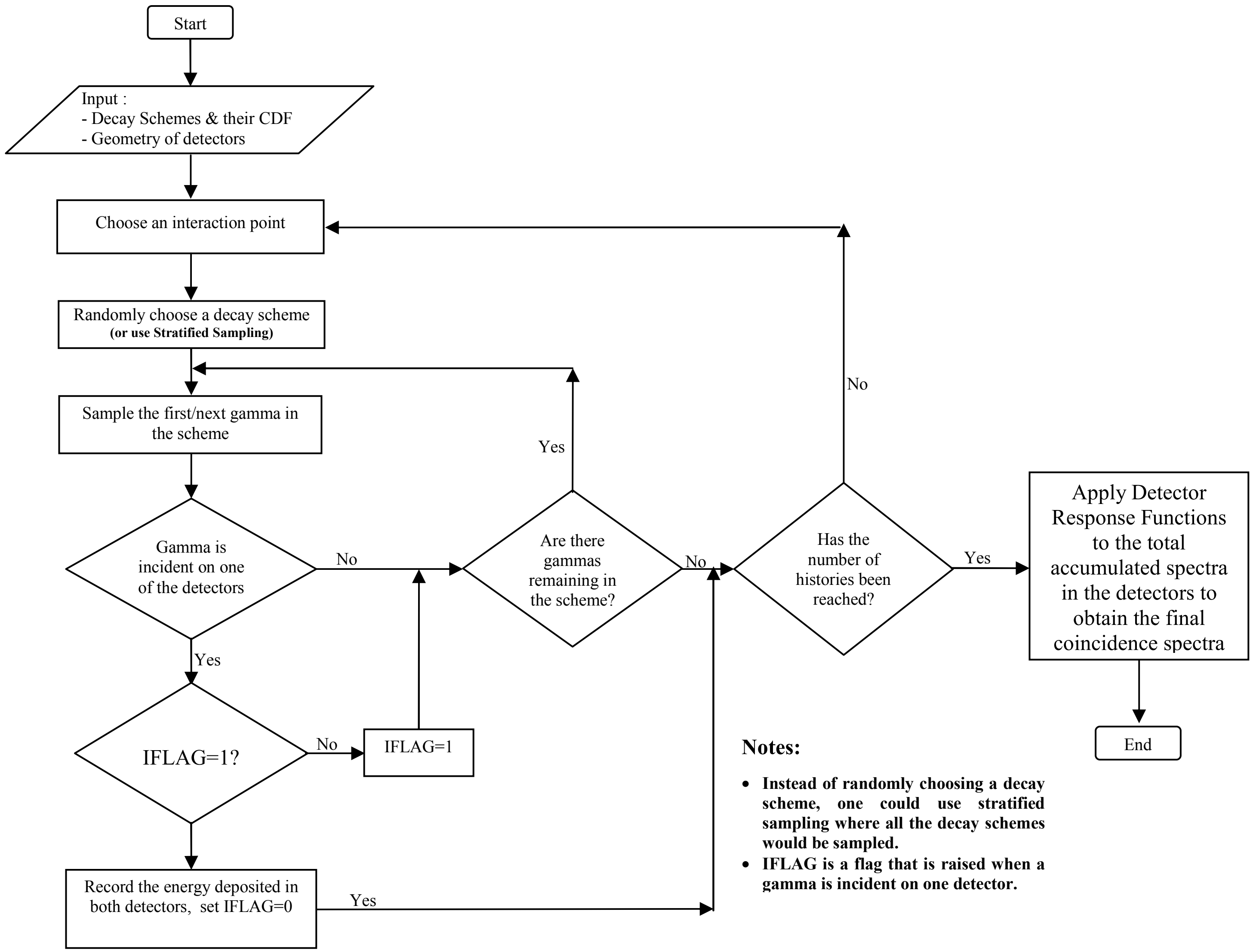

Figure 5-2: Flowchart of the Proposed Modifications to the CEARPGA Code

6. Discussion and Conclusions:

Initially, this work was intended to investigate the prompt gamma coincidence counting approach via experiments and simulations in a balanced manner. As time progressed, several new experimental applications of the coincidence counting approach were investigated. This forced us to devote more time to experimental applications than simulation. It is our intent to continue pursuing the coincidence simulation.

To start off, an introduction to the different electronic standards used in this work was given. It was shown that the old electronic system, based on NIM standards, provided us with acceptable results. In order to achieve better results, we configured a new electronic system based on NIM and CAMAC standards. Most importantly, the new electronic system allowed us to:

1. Obtain accurate timing information regarding coincident events; and
2. Perform multiparameter data acquisition.

Using the new electronic system, the initial observations were presented. These observations highlighted some of the advantages of using this system with the coincidence counting approach. Specifically, the following observations were presented;

1. Elimination of the hydrogen peak, and its Compton continuum;
2. Reduction of pulse pile up and summing effects;
3. Background elimination; and
4. Two dimensional spectra and some of the features in them.

Three practical applications of the coincidence counting approach were presented. The first application showed an example of how the approach can be used in elemental analysis using Library Least Squares (LLS). To demonstrate this, a system of three radioisotopes (Na-24, Co-60, and Cs-134) that emit coincident gamma rays was used. A known mixture of the three radioisotopes was used and data was deliberately collected at relatively high counting rates to determine the effect of pulse pile-up distortion. Compared to the normal results, the coincidence results were shown to give much better accuracy.

The second application was the two dimensional diagonal summing. The main advantages from this application are as follows:

1. Improved peak resolution; and
2. Very low background (Compton continuum).

In addition to these advantages, it was shown that different diagonal sums can be examined by use of the same set of data from the current electronic system (and software).

Two possible uses of the two dimensional diagonal summing were presented. The first was using this type of summing for identifying coincidence schemes and the second was for elemental analysis. The obtained spectra showed to be very promising and can be effectively used for these purposes.

The third practical application of coincidence counting approach was using the new NaI detector arrangement for oil well logging uses. The arrangement was designed to deal with the problem of the low detection probability of the high energy gamma rays of interest in the oil well logging industry. The arrangement consisted of two NaI detectors, one of which is a well type. The first detector is 1×5 inches and the second is a well type 5 inches long with a wall thickness of 0.35 inches, which gives a hole diameter of one inch.

Feasibility studies were performed with new NaI detector arrangement using a Na-24 radioactive source and also a natural sulfur sample (and a neutron source). It was shown that the escape peaks of the high energy gamma rays show up very clearly in the spectrum and there is a great enhancement in the Signal to Noise Ratio.

Finally, a Monte Carlo simulation attempt was made to try to predict the coincidence spectra. The attempt did not yield satisfactory results. It is our intent to continue pursuing coincidence simulation.

7. Future Work;

In general, the future work we intend to pursue is as follows:

1. Modifying the CEARPGA code to simulate gamma-gamma coincidence spectra.
2. Try the new NaI detector arrangement with a fast neutron source. This would allow us to measure the detection efficiency of the carbon and oxygen gamma rays and compare it to those using current detector setups.
3. Use the different projections of the two dimensional spectra to obtain coincidence schemes and angular correlation between gamma rays.
4. Use a Ge-NaI detector setup for coincidence measurements. By this we aim to take advantage of the high resolution of the Ge detectors and the high efficiency of the NaI detectors.

References

Alfassi, Z.B. and C. Chung (Ed.),"Prompt Gamma Neutron Activation Analysis", CRC Press, Boca Raton, 1995.

Bevington, P.R., "Data Reduction and Error Analysis for the Physical Sciences", McGraw-Hill, New York, 1969.

Demanins F. and F. Raicich, "Excited States in ^{93}Nb", Il Nuovo Cimento 105(1992) 245.

Demanins F. and F. Raicich, "Level and Decay Scheme of ^{141}Pr by means of the (n,n'γ) and (n,n' γ-γ) Reactions", Il Nuovo Cimento 107(1994) 2727.

Ehmann, William D. and Diane E. Vance, "Radiochemistry and Nuclear Methods of Analysis", Wiley-Interscience Publication, NY, 1991.

Ember P.P., T. Belgya, J.L. Weil, and G.L. Molnar, " A practical Test od a γ-γ Coincidence Measurement Setup for PGAA", Nuclear Instruments and Methods in Physics Research B, In Press.

Ember P.P., T. Belgya, and G.L. Molnar, "Improvement of the capabilities of PGAA by coincidence techniques", Applied Radiation and Isotopes 56 (2002) 535-541.

Falciglia F., F.R. LoSavio, M. LoSavio, M.E. Oliveri, and F. Patene, "Measure of the Speed of Gamma-rays as a Test of the Performance of a Fast Coincidence System", Nuclear Instruments and Methods in Physics Research A 355 (1995) 537-590.

Gardner R. P. and W. A. Metwally, "A New NaI Detector Arrangement for Efficient Detection of High Energy Gamma Rays" Applied Radiation and Radioisotopes, In Press.

Gardner R.P. and S.H. Lee, “Monte Carlo Simulation of Pulse Pile Up”, Denver X-Ray Conference, Advances in X-Ray Analysis [CD ROM], ICDD, Newtown Square, PA (1999), pp. 941-950.

Gardner R.P., A. Sood, Y.Y. Wang, L. Liu, P. Guo, and R.J. Gerhke, ”Single peak versus Library Least-Squares Analysis Methods for the PGNAA Analysis of Vitrified Waste”, Applied Radiation and Isotopes 48 (1997) 1331-1335.

Gardner R.P., C.W. Mayo, E.S. El-Sayed, W.A. Metwally, Y. Zheng, and M. Poezart, “A Feasibility Study of a Coincidence Counting Approach for PGNAA Applications”, Applied Radiation and Isotopes 53 (2000) 515-526.

Hatsukawa Y., M. Oshima, T. Hayakawa, Y. Toh, and N. Shinohara, “Application of Multiparameter Coincidence Spectrometry Using a Ge Detectors Array to Neutron Activation Analysis”, Nuclear Instruments and Methods in Physics Research A 482 (2002) 328-333.

Hoogenboom A.M., “A New Method In Gamma-Ray Spectroscopy: A two Crystal Scintillation Spectrometer With Improved Resolution”, Nuclear Instruments, 3(1985), pp. 57-68.

Jakubek J., P. Nuiten, J. Pluhar, S. Pospisil, M. Sinor, I. Stekl, S. Timoracky, and M. Vobecky, “Coincidence Gamma-Gamma Spectroscopy System for Instrumental Neutron Activation Analysis”, Nuclear Instruments and Methods in Physics Research A 414 (1998) 261-264.

Jungclaus A., R.F. Casten, R.L. Gill, and H.G. Borner,”Levels in ^{168}Er above 2 MeV and the onset of Chaos”, Physical Review C 49 (1994) 88.

Kim J.I. and J. Hoste, “Non-Destructive Neutron Activation Determination of Silver and Antimony in Bismuth by γ-γ Coincidence Spectrometry”, Analytica Chimica Acta 33 (1965) 449-458.

Kim J.I., A. Speecke and J. Hoste, “Neutron Activation Analysis of Copper in Bismuth by γ-γ Coincidence Measurement”, Analytica Chimica Acta 33 (1965) 123-130.

Knoll, Glenn F., “Radiation Detection and Measurement”, Third Edition, John Wiley and Sons, NY, 2000.

Koeberl Ch. And H. Huber, “Optimization of the Multiparameter γ-γ Coincidence Spectrometry for the Determination of Iridium in Geological Materials”, Journal of Radioanalytical and Nuclear Chemistry, Articles, 244(3) (2000) 655-660.

Marshall III, J.H., and J.F. Zumberge, “On-line Measurements of Bulk Coal Using Prompt Gamma Neutron Activation Analysis”. Nuclear Geophysics 3 (1989), 445.

McGarth C.A., P.E. Garrett, M.F. Villani, and S.W. Yates, “Gamma-Gamma Coincidence Measurements Following Inelastic Neutron Scattering”, Nuclear Instruments and Methods in Physics Research A 421 (1999) 458-463.

Medeiros J.A.G., C.B. Zamboni, A.L. Lapolli, G. Kenchian, and M.J.F. Da Cruz, “Decay of ^{72}Ga”, Applied Radiation and Isotopes 54 (2001) 245-259.

Metwally W.A., R.P. Gardner, and C.W. Mayo, “Elemental Analysis Using Library Least Squares (LLS) for γ-γ Coincidence Counting”, Nuclear Instruments and Methods in Physics Research B, In Press.

Meyer G., “Multiparameter Coincidence Spectrometry Applied to the Instrumental Activation Analysis of Rocks and Minerals”, Journal of Radioanalytical and Nuclear Chemistry, Articles, 114(2) (1987) 223-230.

Meyer G., D. Piccot, R. Rocchia, and J.P. Toutain, "Simultaneous Determination of Ir and Se in K-T Boundary Clays and Volcanic Sublimates", Journal of Radioanalytical and Nuclear Chemistry, Articles, 168(1) (1993) 125-131.

Moon C.B., S.J. Chae, J.H. Ha, T. Komatsubara, Y. Sasaki, T. Jumatsu, K. Yamada, K. Satou, and K. Furuno, "Level Structure of ^{120}Cs", Nuclear Physics A 696 (2001) 45-63.

Raman S., R.F. Carlton, and Wells J.C., "Thermal neutron Capture Gamma Rays from Sulfur Isotopes: Experimental and Theory", Physical Review C, 31(1) (1985), pp. 18-69.

Shyu, C.M., R.P. Gardner, and K. Verghese, "Development of the Monte Carlo – Library Least-Squares Method of Analysis for Neutron Capture Prompt Gamma-Ray Analyzers." Nuclear Geophysics, Vol. &, No.2 (1993), pp.241-268.

Shyu, Chaur-Ming, "Development of the Monte Carlo – Library Least-Squares Method of Analysis for Neutron Capture Prompt Gamma-Ray Analyzer". North Carolina State University, Ph.D Dissertation, 1991.

Sparrow Corporation (KMAX NT Software) http://www.sparrowcorp.com/ .

Thermal Neutron Capture Gamma-rays, Brookhaven National Laboratory, http://www.nndc.bnl.gov/wallet/tnc/capgam.shtml

Vobecky M., J. Jakubek, C. Granja Bustamante, J. Konicek, J. Pluhar, S. Pospisil, and L. Rubacek, "Multielement Instrumental Activation Analysis Based on Gamma-Gamma Coincidence Spectroscopy", Analytica Chimica Acta 386 (1999) 181-189.

Vobecky M., L. Pavlik, and J. Benes, "Non-Destructive Neutron Activation Assay of Submicrogram Quantities of Selenium", Radiochem. Radioanal. Letters 29(4) (1977) 159-164.

Wangen L.E., E.S. Gladney, and W.R. Hensley, "Determination of Selenium in Environmental Standard Reference Materials by a Gamma-Gamma Coincidence Method using Ge(Li) Detectors", Anal. Chem. 52(1980) 765-767.

Watson, Charles C., personal communication.

Zhang Wenchao and R.P. Gardner, "The Analog Linear Interpolation Approach for Monte Carlo Simulation of PGNAA: The CEARPGA Code", Nuclear Instruments and Methods in Physics Research B, In Press.

Zhang, Wenchao, "The Analog Linear Interpolation Approach for Monte Carlo Simulation of Prompt Gamma-Ray Neutron Activation Analysis", North Carolina State University, PhD Dissertation, 2002.